# Evaluation and Improvement of a Stochastic Parametric Tropical Cyclone Rainfall Model - for Flood Impact Assessment

A. Hasan


TU Delft

Deltares

# Evaluation and Improvement of a Stochastic Parametric Tropical Cyclone Rainfall Model - for Flood Impact Assessment

by

A. Hasan

to obtain the degree of Master of Science
at the Delft University of Technology,
to be defended publicly on Wednesday August 24, 2022. at 10:00 AM.

| | | |
|---|---|---|
| Student number: | 5359589 | |
| Project duration: | December 13, 2021 – August 24, 2022 | |
| Thesis committee: | Dr. Marc A. Schleiss, | TU Delft, Chair |
| | Dr. Franziska Glassmeier, | TU Delft |
| | Dr. ir. Ruud J. Van Der Ent, | TU Delft |
| | Ir. Tim W. B. Leijnse, | Deltares, Company Supervisor |
| | Dr. ir. Robert McCall, | Deltares |

*This thesis is confidential and cannot be made public until August 24, 2022.*



TU Delft Delft University of Technology

Deltares

# Preface

A child's enquiry and imagination knows no bounds. I clearly remember the day my mother and I were riding in the backseat of our car while my father was driving. I was probably around eight or ten years old. There were thick clouds and rain was imminent. "Do you know why it rains?" she asked. Why does the river flow? How are mountains formed? After few moments of an eight year old's contemplation, she helped me understand. That was the first spark that gradually became stronger and led me to pursue my career in the field of earth sciences.

Two years ago I arrived at TU-Delft, to learn and grow in the field of Geo-sciences and Remote Sensing. I learned about Deltares, a well known research institute for applied research in the field of water and subsurface soon after arriving in Delft. I was aware that this institute would help to acquire and further develop my research skills.

Looking back, I am beyond grateful for the opportunity to have worked on my thesis research with the company on tropical cyclones. But none of this would have been possible without the guidance and assistance of a few notable individuals.

First and foremost, I'd like to thank my supervisors, Marc Schleiss and Tim Leijnse. I want to acknowledge Marc for his time and effort in frequently provide me with excellent and critical feedback. I couldn't have adhered to my strict thesis schedule without our regular weekly meetings. Tim has taught me a great deal about this subject, has shown me how things work at Deltares, and most importantly, has always made me feel like I had someone to go to when I needed help. I am grateful for his continuous guidance and support. I also want to express my gratitude to Franziska Glassmeier and Ruud Van Der Ent for their time and feedback, which significantly improved the quality of my thesis. I would also like to thank Robert McCall for giving me the opportunity to conduct this study at Deltares and for always taking part in progress meetings. The Coastal Hazard team at Deltares has shown great interest in my work and I am grateful for their support.

This masters thesis concludes my time as a student here in Delft. I owe a debt of gratitude to my university friends for making Delft my home. I want to extend a special thanks to my family, especially my parents, for their confidence in me and for providing me with financial support. Last but not the least, I would like to thank my friends Adityam Rai, Antony Joseph Valiaveetil, Denzil Abraham Joy, and Musaab Elabbassi, for their grammatical expertise while writing my thesis and for their time in listening to technical/conceptual problems I was facing during my thesis. our Discussions helped me to clarify certain facts, and their inquiries frequently revealed flaws in my logic that allowed me come up with a better solution.

*A. Hasan*
*Delft, August 18, 2022*

# Summary

Torrential rain from Tropical Cyclones (TCs) can have a devastating impact, causing loss of life and damage to property. To better understand the risk faced by coastal communities, it is important to estimate how often a tropical cyclone could occur, how much rainfall it would produce and what the following impact would be. One way to do this is by analyzing past events and building parametric models to predict rainfall rates during tropical cyclone events. Parametric models are needed because methods like full physics meteorological models are too computationally expensive to deal with the large number of realisations needed for needed stochastic simulations. While many parametric precipitation models –such as the IPET, BaCla model, R-CLIPER exist, their accuracy remains limited and many challenges still need to be overcome. The most important challenges are output overestimation and a poor representation of rainfall over land, which results in poor skill when performing flood impact assessments. Therefore, this thesis aims to reduce these biases by answering the following research question:

**How can the spatio-temporal biases of the D.J.Bader & J.N. Claassen (BaCla) model be reduced, and how do they impact the parametric tropical cyclone precipitation model's ability to predict precipitation, associated flood hazards and damage?**

To answer this question, rainfall profiles were generated based on existing parametric models for case studies of Hurricanes Florence (2018), Matthew (2016) and Bonnie (2016) for the regions of Charleston (South Carolina, USA), Wilmington (North Carolina, USA) and selected area of North-South Carolina combined. The associated flooding scenario was calculated based on Super-Fast INundation of CoastS (SFINCS) model and damage is estimated by Flood Impact Assessment Tool (FIAT) model simulations. To check the accuracy of the modelled rainfall, values of the model were compared with actual observed Stage IV rainfall data collected by the American National Centers for Environmental Prediction (NCEP). Additionally, the damage related to the modelled and actual rainfall-based scenarios were compared. In these comparisons it is observed that Pressure deficit (pdef) based models are better suited for large rainfall rate and maximum sustained wind-speed (*Vmax*) based models shows better results for lower rainfall scenarios. Both these *Vmax* and *Pdef* based BaCla models produced better results compared to the benchmark IPET model.

The highest precipitation does not have a one-to-one relationship between the radius of maximum precipitation and the radius of maximum sustained wind speed, according to proposed alternative BaCla model that has been developed. Additionally, various adjustments were made to the fitting coefficients of the modified Holland wind profile fit, which is employed in the model to determine the azimuthal average of TC precipitation.This is done to overcome the BaCla model's overestimated and underestimated rainfall for hurricane Bonnie 2016 and Matthew 2016 respectively. Finally, the improved model is compared to the original BaCla and the benchmark IPET model. It is observed that the proposed model improves the spatial spread of rainfall as well as better estimates the cumulative rainfall. The improved model performed the best in the selected case study.

The new model ensures better rainfall representation over land. The overestimation and underestimation of precipitation is reduced, resulting in actual cumulative rainfall mostly lying within the 5th and 95th percentile of the model prediction. By correctly predicting cumulative rainfall for three additional hurricanes namely Alberto 2006, Charley 2004 and Hermine 2016, the model is expected to be applicable to area outside of the calibration data-set with more confidence. However, no definitive conclusion could be reached upon if the model is globally applicable as more case studies would be required in other oceanic basins. As a concluding remark, this research project highlights the importance of being able to generate accurate predictions to enhance the decision making and risk management of natural hazards: a model that accurately quantifies uncertainty and the impact associated with a tropical cyclone, representing a valuable tool for better understanding flood impact.

# List of Figures

# List of Tables

# Acronyms

**BaCla** D.J.Bader & J.N. Claassen

**BaClHa** D.J.Bader, J.N. Claassen & A. Hasan

**ConUS** contiguous United States

**CDF** Cumulative Distribution Functions

**DPR** Dual frequency Precipitation Radar

**EOL** Earth Observing Laboratory

**EORC** Earth Observation Research Center

**EBTRK** Extended Best Track Data-set

**FIAT** Flood Impact Assessment Tool

**GMI** GPM Microwave Imager

**GPM** Global Precipitation Mission

**IBTrACS** International Best Track Archive for Climate Stewardship

**IPET** Interagency Performance Evaluation Task Force

**JAXA** Japan Aerospace Exploration Agency

**MSR** Modified Smith for Rainfall

**MvCAT** Multivariate Copula Analysis Toolbox

**NASA** National Aeronautics and Space Administration

**NCEP** National Centers for Environmental Prediction

**PHRaM** Parametric Hurricane Rainfall Model

**PR** Precipitation Radar

**R-CLIPER** Rainfall- CLImatology and PERsistence

**RSMCs** Regional Specialized Meteorological Centers

**RFCs** River Forecast Centers

**SFINCS** Super-Fast INundation of CoastS

**SSHS** Saffir–Simpson hurricane scale

**SSHWS** Saffir–Simpson hurricane wind scale

**TC** Tropical Cyclone

**TCs** Tropical Cyclones

**TCWiSE** Tropical Cyclone Wind Statistical Estimation Tool

**TD** Tropical Depression

**TMI** TRMM Microwave Imager

**TRMM** Tropical Rainfall Measuring Mission

**TS** Tropical Storm

**VIRS** Visible and Infrared Radiometer System

**WES** Wind Enhanced Scheme

**WRF** Weather Research and Forecasting

# Symbols

| | |
|---|---|
| $\Delta p$ | Pressure Deficit [hPa] |
| $pdef$ | Pressure Deficit [hPa] |
| $vmax$ | Maximum Sustained Wind Speed [m/s] |
| $R$ | Radius (distance from eye) [km] |
| $pr(R)$ | Precipitation at a Distance R [km] |
| $\beta$ | azimuth [degree] |
| $R_{max}$ | Radius of Strongest winds [km] |
| $Rp_{max}$ | Radius of maximum precipitation [km] |
| $Rv_{max}$ | Radius of Maximum Sustained Wind Speed [km] |
| $\theta_{Di}$ | Angle [degree] |
| $\theta_{Ri}$ | Angle [rad] |
| $b_s$ | Fitting coefficient for adapted Holland wind profile |
| $x_n$ | Fitting coefficient for adapted Holland wind profile |

# Contents

# 1 Introduction

## 1.1. Context

Tropical Cyclones (TCs), also known as typhoons or hurricanes, are a low pressure system that forms over warm tropical waters, i.e., between 23.4°North and 23.4°South [17].TCs are known for their associated high wind speeds and heavy precipitation [19]. They have a closed wind circulation and a defined centre, known as the eye as could be seen in fig. 1.1. The eye of a TC on one hand is a circular area that has low pressure, warm temperature, and relatively calm weather. On the other hand, the eye wall, a ring of deep convective clouds around the eye, is usually the region where the highest winds and precipitation intensities are observed [35].

TCs are one of the major natural disasters that affect many countries around the world. Over the past two centuries, 1.9 million deaths have been attributed to hazards related to TCs, including strong wind, intense rainfall, and storm surge [51]. In China, between 1983 and 2006, seven tropical cyclones made landfall in the mainland, causing economic losses of 28.7 billion yuan (€4.06 billion) and killing 472 people on average each year [51]. Similarly, in the United States, Hurricane Harvey (2017) alone caused 106 deaths and an economic loss of $125 billion dollars (€118.16 billion) [49].

Rainfall rates and their locations are important factors that need to be considered for risk management. For resource planning, flooding, erosion, as well as structural risk assessments, even approximate estimates can be of great help. Hence, there is an ongoing search for adopting to accurate approaches for estimating rainfall rates and their distribution from the eye of the TC. Several dynamic weather models do exist like the Weather Research and Forecasting (WRF) model, which use physically-based equations to advance an atmospheric state forward through time, simulating the likely precipitation and other atmospheric parameters [22]. However, these dynamic models are computationally expensive [22], which is problematic because for risk assessments, lots of different scenarios need to be modelled due to the large uncertainties involved with TCs. Also, the dynamic models require multiple data inputs that are not that easily available globally. So, faster and less computationally intensive parametric models based on factors like storm motion, surface wind speeds, and atmospheric pressure were developed. A parametric rainfall model is considered to be good, if it is simple and needs as little information as possible to achieve reasonable predictive performance at a low computational cost.

Heavy precipitation events in both TCs and extra-tropical cyclones can contribute significantly to floods, which might intensify in the future [12]. Various driving processes might cause coastal flooding, for example (extreme) flooding is caused by the interplay of high sea levels, large river flows, and local precipitation [48]. Uncertainties surrounding various flooding mechanisms must be taken into account in order to accurately estimate the flood danger brought on by compound flooding [24].

To simulate compound floods, there are essentially three methods: simple, reduced-complexity, and full-physics process-based models [24]. All of these methods have a compromise between computing

demand and accuracy. This study has used the Deltares-developed reduced-complexity Super-Fast INundation of CoastS (SFINCS) model [24] to predict the flood hazard created by TC precipitation. The flood predictions made by SFINCS are used for planning long-term flood mitigation strategies and making Probabilistic Flood Risk Assessments [13]. A flexible suite of open source tools called Delft-Flood Impact Assessment Tool (FIAT), as developed by Deltares, is used to create and execute flood impact models that use the unit-loss approach. Delft-FIAT is a simplified damage assessment tool for estimating direct losses to buildings, contents, and roadways as well as expenditures associated with business disruption and road closures. It can execute a significant number of damage calculations automatically and is designed to be quick, adaptable and connect to any hydrodynamic model [14]. This is necessary in order to compare an average expected sum to the initial capital expenditure and ongoing operating expenses of mitigation infrastructure and strategy investments and also to make appropriate policy recommendations [29].

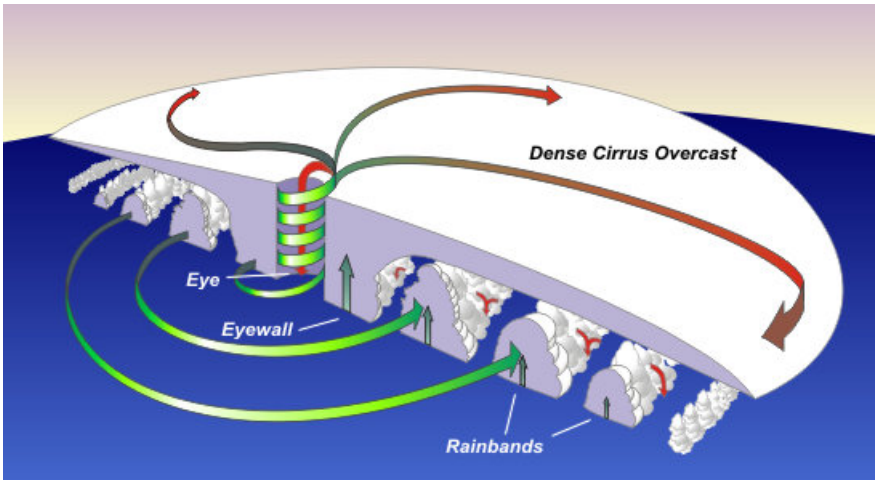


Figure 1.1: Cross section of a typical hurricane [19]

This thesis was born from a collaboration between TU Delft and Deltares- a leading institute for applied research on water and the subsurface. Deltares is performing ongoing research in tackling these issues in order to improve the accuracy of the input to their highly developed flood models. Deltares provides TC risk assessment for the present and the future based on their synthetic cyclone simulator known as Tropical Cyclone Wind Statistical Estimation Tool (TCWiSE) [31], [25].

## 1.2. Research Objective and Question

The main objective of the research is to reduce the biases in Deltares's currently used BaCla model and improve the accuracy of rainfall profiles in TCs and along with that provide the associated risk assessment. Hence, to achieve that goal the following research question is formulated:

**How can the spatio-temporal biases of the BaCla model be reduced, and how do they impact the parametric tropical cyclone precipitation model's ability to predict precipitation, associated flood hazards and damage?**

The main research question will be answered through the use of the following sub-questions:

1. How well does the present BaCla model predict rainfall associated with TCs and what are the main biases?
2. How can the spatio-temporal biases of the BaCla parametric models in the precipitation prediction be reduced?
3. How good is the improved model in predicting rainfall as compared to IPET, the current practice?
4. How do different parametric tropical cyclone precipitation distributions affect the associated flooding and flood damage?

## 1.3. Challenges

Several parametric models do exist but each come with their own limitations. Some underestimate the rainfall like the Rainfall- CLImatology and PERsistence (R-CLIPER) model and Parametric Hurricane Rainfall Model (PHRaM) [28], whereas other models like IPET [6] and Modified Smith for Rainfall (MSR) [18] model overestimate the rainfall. Calculating flood damages is the main goal of this thesis. Accurate prediction of rainfall rates and spatial or temporal patterns in tropical cyclones over land is a crucial component to realise this goal. Accurate prediction of rainfall rate and its spatial and temporal pattern will be achieved by reducing the bias and uncertainty in the currently used acBaCla model, keeping in mind the computational efficiency. This study will also focus on finding out the spatial distribution of rainfall associated with tropical cyclones at various distances from the eye with respect to the direction of movement of TC.

The focus of this work is on estimating flood damages. A key factor in this is the accurate representation of rainfall rates and rainfall spatial or temporal structure in TCs.

## 1.4. Outline

To address the research questions above, the remainder of this report has been divided in six chapters. Chapter 2, the literature review, conceptualizes tropical cyclone fundamental processes, followed by a compilation of existing and currently used parametric models. Chapter 3 serves as an overview of all data sources used. Chapter 4 describes the methods to conduct the research. This includes the general approach, working of SFINCS and FIAT model, and an overview of case studies considered. Chapter 5, the results and discussion, presents the performance of BaCla in case studies of Hurricane Florence, Matthew and Bonnie which hit the US in 2018, 2016 and 2016 respectively. The flood risk assessment based on SFINCS and FIAT model is also presented. It is followed by an interpretation of different model variations along with highlighting what could be going wrong. Then, the proposed improvised model is further tested here and the model is evaluated for its performance over land. Finally, the new model is compared with the original BaCla model to assess whether the goal of the research has been met. The work is concluded in chapter 6, providing the key findings, limitations and future recommendations.

# 2

# Literature Review

## 2.1. Tropical cyclone fundamentals

Tropical Cyclone motion is a very complex atmospheric system consisting of multi-scale and non-linear system interaction. Some of the well-known factors that affect TC dynamics are vertical wind shear, warm eddy core interactions, eddy angular flow convergence, dry air intrusions, eye wall cycles, low-level temperature advection, ocean currents, etc. In the case of near land cyclonic flow, some other factors like coastline shape, topography, soil moisture do play an important role, particularly during the land-falling stages

TCs are one of the major cause of coastal flooding. Storm surge due to intense winds over ocean and high sustained precipitation over land are considered to be the primary divers. Extreme precipitation over land causes in-land flooding along with supporting immediate coastal flooding due to storm surge. In some regions of the world, this can contribute to 15-17% of the total annual rainfall, where many TCs are responsible for the highest rainfall accumulation on an hourly and daily time scale [41]

TC precipitation can be categorized into two main types, convective and stratiform. Convective precipitation is caused by the rising hydrometeors that grow with altitude until they fall down. Stratiform precipitation, on the other hand, is caused by weak vertical air motion and drifts down over a larger area of the weak updraft and grows slowly due to aggregation and deposition [41]. Convective precipitation can mostly be found in the inner eye wall, where there are high wind speeds, and stratiform precipitation forms further away from the eye. To understand and distinguish between different tropical cyclones Saffir–Simpson hurricane wind scale (SSHWS), formerly the Saffir–Simpson hurricane scale (SSHS), is used. It classifies hurricanes that exceed the intensities of Tropical Depression (TD) and Tropical Storm (TS) into five categories based on intensities of their sustained winds. A TD forms when a low pressure area is accompanied by thunderstorms that produce a circular wind flow with maximum sustained winds below 62 km/h. An upgrade to a TS occurs when cyclonic circulation becomes more organized and maximum sustained winds gust between 63 km/r and 118 km/h. SSHS classification can be refereed in the table 2.1.

Table 2.1: Saffir–Simpson hurricane scale (SSHS) classification along with TS and TD

| **Category** | **Wind Speeds (for 1-minute maximum sustained winds)** | | | |
|---|---|---|---|---|
| | **m/s** | **knots(kn)** | **mph** | **km/h** |
| **Five (major)** | ≥70 | ≥137 | ≥157 | ≥252 |
| **Four (major)** | 58-70 | 113-136 | 130-156 | 209-251 |
| **Three (major)** | 50-58 | 96-112 | 111-129 | 178-208 |
| **Two** | 43-49 | 83-95 | 96-110 | 178-208 |
| **One** | 33-42 | 64-82 | 74-95 | 119-153 |
| **Tropical Storm** | 18-32 | 34-63 | 39-73 | 63-118 |
| **Tropical Depression** | ≤17 | ≤33 | ≤38 | ≤62 |

Lonfat, Marks Jr, and Chen [27] after studying azimuthal rainfall rate of 260 TCs in all basins between 1998 and 2000, where TS are categorised by winds <33 m/s, CAT12 are hurricane of category 1-2 and CAT35 are hurricanes of category 3-5, found intense rainfall in within 100 km of the eye and intensity of rainfall increases with the increase in wind-speed fig. 2.1 .

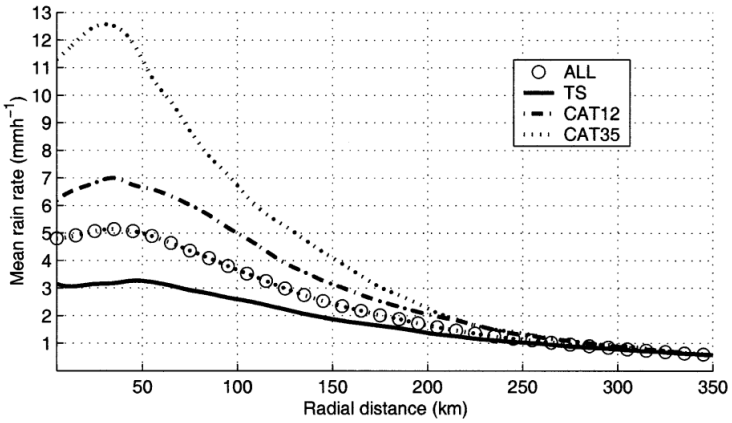


Figure 2.1: Azimuthal mean rain rate for different strengths in the TRMM data [27]

Furthermore, Jiang, Halverson, and Simpson [21] tested the relationship between maximum sustained wind-speed and rainfall over land and over ocean. It was concluded that the correlation between maximum wind-speed and maximum precipitation is more over the ocean as compared to land as can be seen in fig 2.2. Therefore, there maybe a reduced model performance of parametric precipitation model based on wind-speed over land [21]. It might also be concluded that if the model is trained and evaluated separately for over-ocean and over-land evaluated in the same way the prediction accuracy might increase.

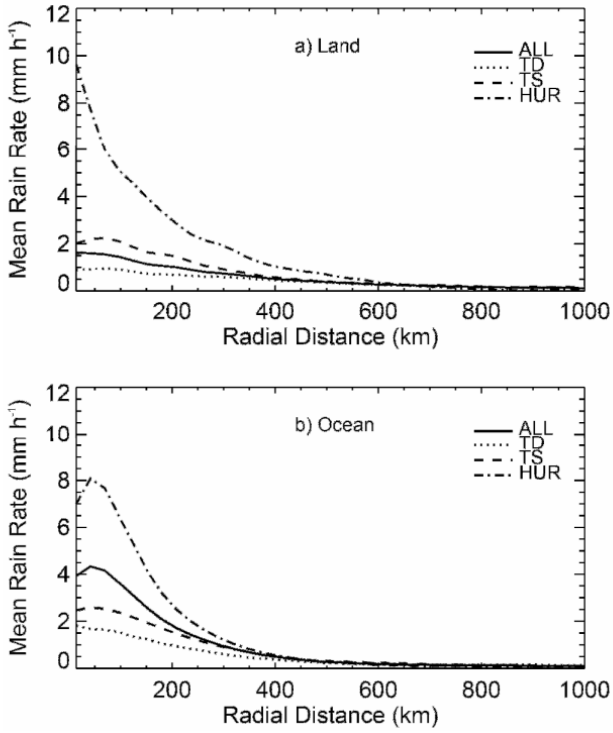


Figure 2.2: Azimuthal mean rain rate for different strengths: land vs. ocean [21]

## 2.2. Parametric precipitation models

Conventionally, rainfall is one of the most difficult variables to model within an atmospheric system. The variation of the rainfall amount at a different distance from the eye of cyclones is a result of simultaneously interacting numerous nonlinear processes. Even the most comprehensive modelling systems, with very detailed physics, and numerical algorithms assimilating observational data, have limited success in estimating the rainfall intensity and location associated with the hurricane [16]. Apart from that most of the physics based models require a lot of data that is needed to run the model which is generally not available globally [22]. This guides us towards parametric models that makes use of combined statistical methods and physically-relevant environmental conditions that governs formation, movement , and intensity of TC and is much less computationally intensive. [22] A parametric precipitation model predicts precipitation based on TC parameters, such as storm motion, surface wind speeds, atmospheric pressure etc. A good parametric rainfall model should be simple and require as little information as possible to achieve reasonable predictive performance at a low computational cost.

Several parametric models do exist but most of them come with some limitations. R-CLIPER model [47] and the PHRaM model [27] clearly showed a strong correlation to the amount of rainfall with maximum horizontal wind speed Vmax. In contrast, the IPET model (US Army Corps of Engineers) [6] did suggest the pressure deficit Δp from the eye at a certain radius R has a linear relation with precipitation. In a 2021 TU Delft thesis written by J.N. Claassen [11], in collaboration with Deltares, titled "Parametric Precipitation Model for Tropical Cyclone Radial Rainfall Profiles: Reducing the biases in the Bader model [2] for the North Atlantic" a "best-fit" Frank copula approach is tested for both maximum sustained wind speed [m/s] (*vmax*), and the pressure deficit [hPa] (Δp). While this method has been able to provide an estimate of the rainfall intensity, several improvements are still required in order to provide sufficient accuracy for the forecast.

### 2.2.1. IPET Model

IPET was introduced by the US Army Crops of Engineers to better evaluate hurricane protection systems. The model was based on work of Lonfat, Marks Jr, and Chen [27] and Chen, Knaff, and Marks Jr [9]. The model computes mean rainfall intensity $p_r(R)$ with distance R (in km) from the hurricane center to the point of interest and azimuth $\beta$ (in degrees) relative to the direction of motion. The symmetric component is estimated by assuming linear dependence of mean rainfall intensity at $R_{max}$ on the central pressure deficit $\Delta P$ and fitting an exponential decay function with distance.

$$pr(R) = \begin{cases} 1.14 + 0.12\Delta P & r \leq R_{max} \\ (1.14 + 0.12\Delta P)e^{-0.3\left(\frac{r-R_{max}}{R_{max}}\right)} & r > R_{max} \end{cases} \tag{2.1}$$

Where *pr(R)* is in millimeter per hour and $\Delta P$ in millibars. This model's inputs include the storm's position in terms of latitude and longitude, time, the radius of its strongest winds $R_{max}$, and the central pressure deficit ($\Delta P$). The asymmetric component is computed by multiplying the symmetric mean rainfall values by a factor of 1.5 for storm passing to the left of the sub-basin centroid (i.e. 50% more rain on the right hand side of the storm).[6] It is important to notice that IPET based results do not have a probabilistic estimate component.

### 2.2.2. BaCla Model

BaCla model is an improvement to IPET model as it does contain probabilistic estimate components. In BaCla model $p_{max}$ is estimated based on copula and adapted Holland wind profiles are used to calculated 1D rain profile. Asymmetry may or may not be added to make a 2D rain profile. The details of the model have been discussed below.[11]

#### Blending of satellite and Stage IV data

As observed by Claassen [11] the spatio-temporal variation of Tropical Rainfall Measuring Mission (TRMM) and Global Precipitation Mission (GPM) data can vary significantly. This results in limited capture of most of the tropical cyclones. Apart from that, for some time steps TC are captured partially because the area satellite captures does not overlap with the area affected by TC.Therefore, the difference between two data frames captured the TC can of several days. To overcome this downside data from both passive microwave sensor (TRMM Microwave Imager (TMI)/GPM Microwave Imager (GMI))

and radar (Precipitation Radar (PR)/Dual frequency Precipitation Radar (DPR)) are used. While passive microwave sensors have a larger spatial coverage the data obtained from the radar is more reliable. Apart from that, both TRMM as well as GPM are not available or become less reliable above land, and TRMM is limited to the tropics. To overcome these limitations and recompile more reliable and frequent precipitation data over land, the satellite data is blended with the Stage IV product.

An overview of the procedure followed by Claassen [11] to merge the satellite data with Stage IV is provided in section 2.3. In order to combine the different data sources, Claassen [11] blended data within a 550 km radius of the TCs eye, as this is approximately the radius of a TC. International Best Track Archive for Climate Stewardship (IBTrACS) best track data is used to determine the maximum sustained wind speed pressure deficit for longitude and latitude of the eye at each time step. Linear interpolation was used to estimate the track at the time of interest as the best track data is 6 hourly.

From the longitude ($x_{eye}$) and latitude ($y_{eye}$) of the eye, points have been generated every $\frac{1}{360}$ degrees ($\theta_{Di}$) and radians ($\theta_{Ri}$) and every 10 Km in radius (R) outwards. the longitude and latitude of each point has been calculated as follows:

$$\theta_{Ri} = \frac{\theta_{Di}\pi}{180} \tag{2.2}$$

$$Lon_{i,j} = x_{eye} + \frac{1}{\sqrt{2}}(cos(\theta_{Ri})r_j - sin(\theta_{Ri})r_j) \tag{2.3}$$

$$Lat_{i,j} = x_{eye} + \frac{1}{\sqrt{2}}(cos(\theta_{Ri})r_j + sin(\theta_{Ri})r_j) \tag{2.4}$$

Where $Lon_{1,1} = x_{eye}$ and $Lat_{1,1} = y_{eye}$

For each longitude $Lon_{i,j}$ latitude point $Lat_{i,j}$ associated precipitation value is calculated for both data types of TRMM/GPM and Stage IV separately by linear interpolation. Next, each point is labelled as above land or above the ocean by testing whether it falls within the coastline polygon provided by MATLAB (coast.mat). Following this, the rainfall at point is selected based on the scheme in 2.3 where $p_{i,j}$ is precipitation at $Lon_{i,j}$ and $Lat_{i,j}$

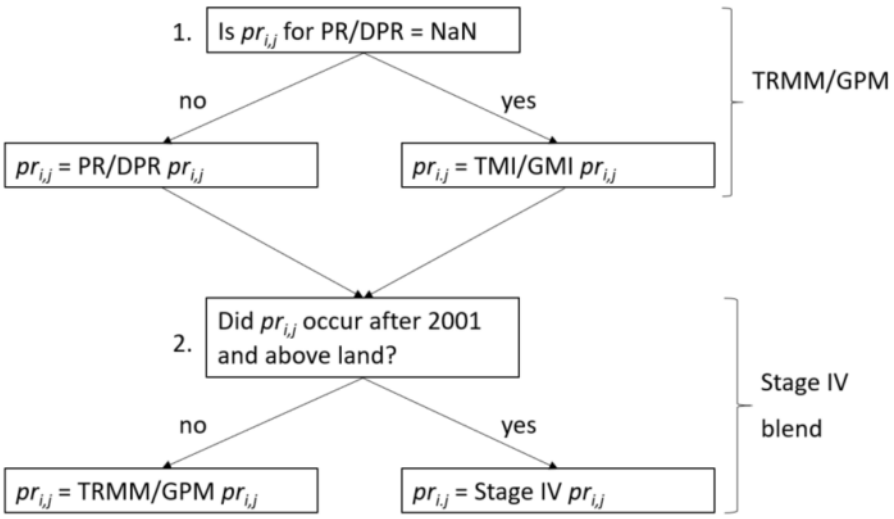


Figure 2.3: Data blending selection schema [11]

In step 1, the PR/DPR data is favored over TMI/GMI. If PR/DPR is not available. TMI/GMI is used. The combination of the PR/DPR and TMI/GMI precipitation will be known as the TRMM/GPM data. A second data set is produced by blending the TRMM/GPM data with the available stage IV data. Stage IV data is available hourly, therefore, the precipitation is averaged according to the nearest hour. Above land the Stage IV data is favored over the TRMM/GPM.

### Estimation of radial profiles

The azimuthally averaged rainfall rate is the mean precipitation at different radii. During the blending process, the precipitation is already calculated at 10 km increments away from the eye for every degree, resulting in 360 vectors. These vectors have been averaged, excluding NaN values, to obtain the mean rainfall every 10 km. These increments have been considered as a proper resolution for the study, ensuring computational efficiency.

Additionally, for each 10 km increment, the number of non missing values are noted, as often not the entire TC is captured. To illustrate this consider the following examples: there are 360 data points for every distance, hence if exactly half of the TC is being captured, this means that 180 out of 360 data points are present at every distance. If on the other hand, 30% of the TC is captured, no points are being captured close to the eye. As this is likely the area where the highest precipitation is expected, it is possible that the true maximum was not captured. Consequently, taking note of the ratio of present and missing data provides an indication of its reliability.

### Parametric precipitation model

A copula is a joint multivariate distribution used to model dependence structure of two (or more) random variables. In BaCla model Multivariate Copula Analysis Toolbox (MvCAT), a copula toolbox developed in MATLAB is utilised to get the most appropriate copula among 26 set of copula families that describes the best dependence structure of two variables based on performance matrix. Once the most favorable copula is identified, the corresponding variable marginal distribution are used to sample values of $p_{max}$.

BaCla model finds out the relation between $p_{max}$ and the maximum sustained wind-speed as well as the pressure deficit separately. Adapted Holland wind-profile is used to identify the azimuthal average of TC precipitation using formula:

$$pr(R) = \left( \frac{p_{max} * R_p^{b_s}}{exp(R_p^{b_s})} \right)^{x_n} \tag{2.5}$$

Here, $R_p = \frac{Rp_{max}}{R} = \frac{Rv_{max}}{R}$ assuming $Rp_{max} = Rv_{max}$. The fitting coefficients $b_s$ and $x_n$ has been identified using 4 different methods named and explained in alphabetical bullet points [11].

(A) Least square fitting method is used for each of the two data sets separately.

(B) Least square fitting method for $p_{max}$ below and above 5mm/h separately for each data sets.

(C) $x_n$ is calculated such that the sampled $p_{max}$ is the curve $p_{max}$ by making $x_n = \frac{log(p_{max})}{log(\frac{p_{max}}{exp(1)})}$, $b_s$ is determined using least square method.

(D) $x_n$ is identified such that the samples $p_{max}$ is the curve $p_{max}$ by making $x_n = \frac{log(p_{max})}{log(\frac{p_{max}}{exp(1)})}$. $b_s$ is identified as the best fit of the area under the graph where $b_s$ is tested for a variety of samples between 0 and 2 to find the optimal fit.

The fig 2.4 shows the performance for each fit for different precipitation strength.

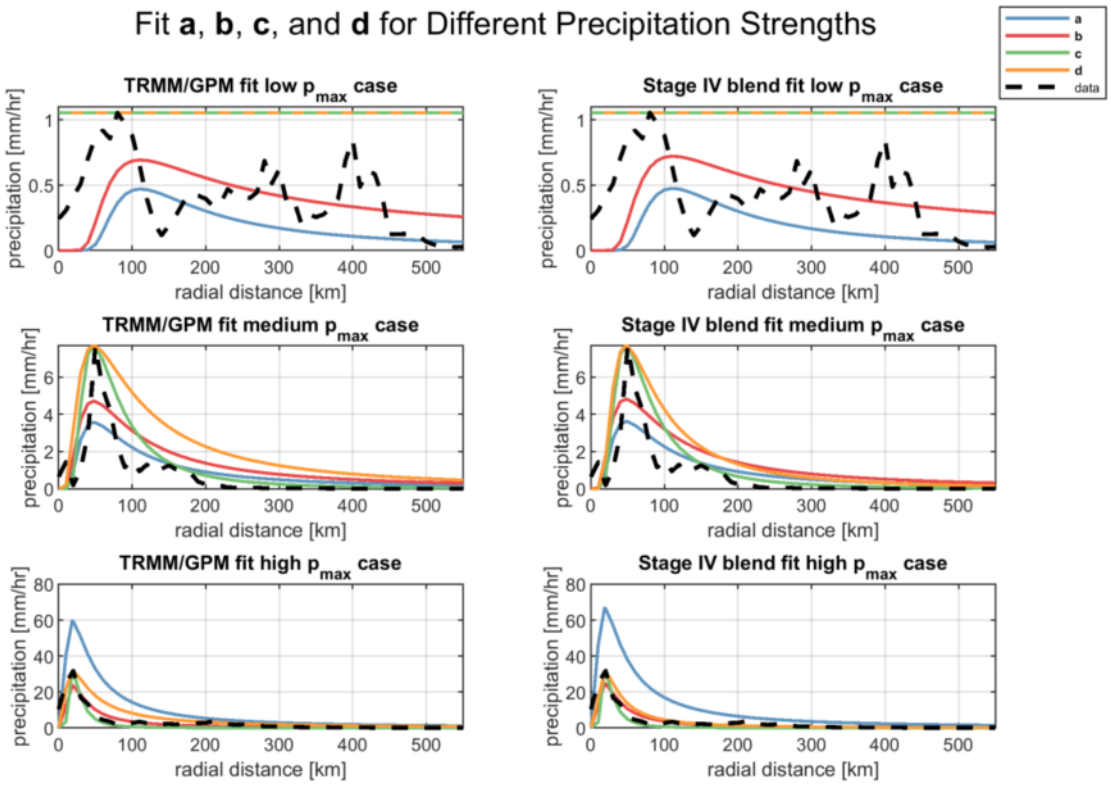


Figure 2.4: The fit from eq. 2.5 using method **a**, **b**, **c** and **d** to determine the coefficients for different precipitation magnitude. [11]

Each of the four methods for fitting coefficients $b_s$ and $x_n$ has some limitations discussed below alphabetically corresponding to method.

(A) The best fit for $b_s$ and $x_n$ appears to be a good fit for low $p_{max}$ values but is not a good fit for samples where $p_{max}$ >15mm/h.

(B) It makes a distinction between $p_{max}$ above and below 5mm/h. This performs significantly better for higher $p_{max}$ but still not the best fit.

(C) It was unsuitable for $p_{max}$ values under 2.8mm/h as low values of $b_s$ and $x_n$ would result in an error resulting in extreme values of precipitation. So, an alternative radial fit was introduced for values below 2.8mm/h, where precipitation is same pr(R) = $p_{max}$, low quantity, at all radii. **c** performs well at larger radii and fit reaches the true $p_{max}$.

(D) It results in higher precipitation values for larger radii leading to overestimation of the total rainfall. It also follows the same rainfall distribution method for rainfall less than 2.8mm/h as in **c**.

In Holland parameter, the coefficients of $x_n$ determines the $p_{max}$ of the curve, the $b_s$ coefficients controls the slope at which the curve descends after reaching the fit's $p_{max}$.

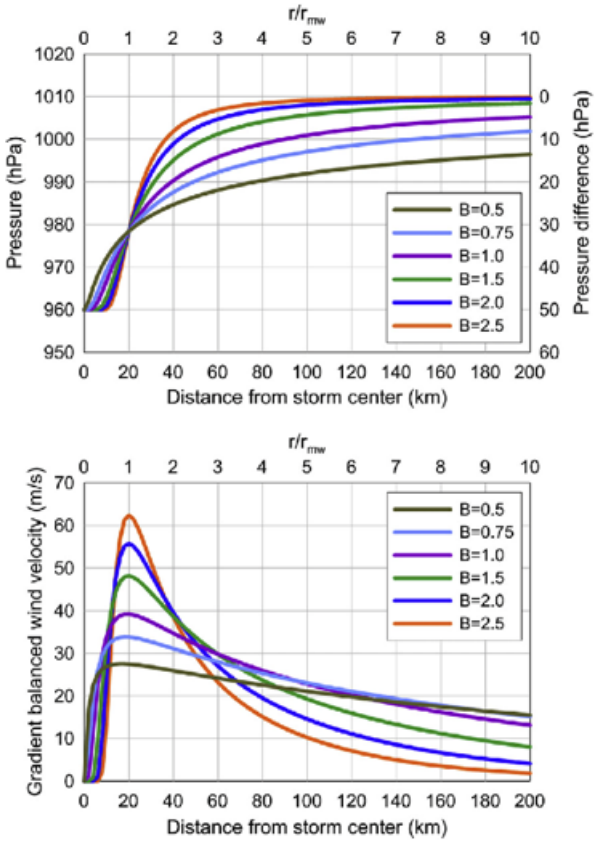


Figure 2.5: Pressure profiles and gradient balanced wind velocity profiles for different values of Holland parameter B (bs) [10]

The model is finally tested with $b_s$ and $x_n$ calculated using method **d**, for its potential to reproduce the precipitation of hurricane Florence 2018.It was observed that the $\Delta P$ based model performs best in the particular case of Florence 2018. [11].

# 3

# Data

The data utilized in the study are presented in this chapter. Precipitation and best track are the two key categories of data. To get the maximum resolution and the finest depiction above land and ocean, many data sources for precipitation were gathered by Claassen [11], almost the same has been used in this study except IBTrACS data. Claassen [11] used Extended Best Track Data-set (EBTRK) with a temporal resolution of 6 hours where as in this study IBTrACS data with a temporal resolution of 3 hrs are used. An overview of the data used along with their resolution is provided in Table 3.1. The input parameters and data for SFINCS and FIAT models have been discussed in section 4.4 & 4.5 respectively.

## 3.1. TRMM

The TRMM was a joint mission by the U.S. National Aeronautics and Space Administration (NASA) and the Japan Aerospace Exploration Agency (JAXA)[27]. The satellite acquired data for 17 years in orbit from November 1997 till June 2015. This mission was specifically designed to gather tropical precipitation data between 35°north and south latitude [11].

The main sensors onboard TRMM are a microwave imager TMI, PR and a Visible and Infrared Radiometer System (VIRS) to quantify the precipitation [27]. The 2A12 “TMI Profiling”, contains surface rainfall as well as vertical hydrometeor profiles on a pixel by pixel basis from the TMI instrument data using the Goddard Profiling algorithm GPROF2010. Surface rain is represented as the liquid portion of precipitation and are in mm/hr. The spatial resolution is approximately 5.1 x 5.1 km, except for the data originated before August 2001, whose resolution is 4.4 x 4.4 km due to a shift in the orbit.The 2A12 data has been acquired from the JAXA/ Earth Observation Research Center (EORC) TC database [11].

Table 3.1: Overview of the different data types and sources used in this research [11]

| Product | Product type | Years active | Instrument | Spatial resolution | Temporal resolution | Source |
|---|---|---|---|---|---|---|
| TRMM | 2A12:TMI | 1997-2015 | Microwave imager | 5.1 x 5.1 km | varies | JAXA/EORC TC online databa |
| TRMM | 2A25:PR | 1997-2015 | Precipitation radar | 4 x 4 km | varies | Nasa Earth Data online database |
| GPM | 2AGROFGMI | 2015-present | Microwave imager | 13 x 13 km | varies | JAXA/EORC TC online database |
| GPM | 2ADPR | 1997-2015 | Precipitation radar | 5 x 5 km | varies | Nasa Earth Data online database |
| STAGE IV | STAGE IV Hourly | 2002-present | Radar, gauge | 4 x4 km | varies | EOL online database |
| IBTrACS | Global | 1840-present | - | - | 3-hourly | NCEI NOAA online database |

The vertical rainfall rate profiles are estimated by 2A25 “PR Profile”. Surface rain is represented as the liquid portion of precipitation and are in mm/hr. The spatial resolution is 4 x 4 km.The 2A25 data has been provided by the NASA Earth database [11].

## 3.2. GPM

The GPM is the advance successor of TRMM. GPM only has two instruments on board, namely the DPR and the GMI, with the capabilities of sensing light rain and falling snow [44]. The most significant upgrade from TRMM to GPM is its capability for a more global coverage. It was launched in February 2014 and operates in a non-sun-synchronous orbit with an inclination of 65°north and south latitude reach. It can capture precipitation across all hours of the day from the tropics to the Arctic and Antarctic circle along with observing hurricanes and typhoons [44].

The 2AGPROFGMI generates surface rainfall and vertical hydrometeor profiles on a pixel by pixel basis similar to 2A12, . However, it uses an updated version of GPROF2010, called GPROF2014. Surface rain is represented as the liquid portion of precipitation and is also in mm/hr. It has a spatial resolution 13 x 13 km. The 2AGPROFGMI data has been acquired from the JAXA/EORC TC database as well [11].

The 2ADPR data originates from the GPM on board DPR. Same as 2AGPROFGMI, the surface rain is represented in mm/hr and has a resolution of 5 x 5 km.The 2ADPR data is provided by NASA Earth database [11].

## 3.3. Stage IV

Stage IV is a product of the American National Centers for Environmental Prediction (NCEP). Stage IV is available from late 2001 on-wards. The stage-IV data-set is a mosaic of 12 contiguous United States (ConUS) River Forecast Centers (RFCs) regionally analysed and produced. The regional analysis completed at the RFCs uses an advanced multi-sensor analysis algorithm, and are subjected to the gauge correction and quality control.[4]

Stage IV has a 4 x 4 km spatial and hourly temporal resolution, merging data from 140 radars and approximately 5500 gauges over the ConUS. The data has been retrieved through the Earth Observing Laboratory (EOL) online database [4].

## 3.4. IBTrACS

The IBTrACS provides location and intensity for global tropical cyclones. The aim of the IBTrACS project is to collect the historical tropical cyclone best-track data from all available Regional Specialized Meteorological Centers (RSMCs) and other agencies, combine different data sets into one product, and distribute the data in formats used by the tropical cyclone community. Each RSMC forecasts and monitors storms for a specific region and annually archives best-track data, which consist of information on a storm’s position, intensity, and other related parameters. Files are available subset by Basin or time period generally at an interval of 3hrs from the 1840s to present day [23].

# 4

# Methods

The method section is divided into five parts. Section 4.1 provides an overview of the approach used. Section 4.2 and 4.3 outlines the case study and the validation case studies, talking about the area of interest, the TC considered and their characteristics. Section 4.4 describes the SFINCS model in details, including the factors that it takes into account for water level estimation. Section 4.5 explains the working principle of the FIAT model and how it assesses the flood risk.

## 4.1. General approach

The primary research objective of this thesis is to evaluate the effectiveness of rainfall and flood risk prediction for different parametric models (i.e. BaCla and IPET model). The selected parametric models will be making use of parameters associated with TCs like central pressure deficit, radius of maximum wind-speed and radius of maximum precipitation as discussed in detail in section 2.2.2.

Before selecting the cyclone for the study, the area of the study must be selected. In this study, a selected area of North-South Carolina and Georgia is considered to be a suitable fit as there is ground data available for rainfall, high quality data for flood risk calculation and most importantly the region gets affected by a lot by TCs. Three TCs are taken into consideration, each with very distinct characteristics in terms of wind and rainfall rates: Matthew (2016), Bonnie (2016), and Florence (2018). The track information like time, location and intensity for the TC is obtained from IBTrACS data. After obtaining the track, parametric model of Holland, Belanger, and Fritz [18] is used to calculate spatially varying wind fields with the help of Wind Enhanced Scheme (WES). Nederhoff et al. [30] relationships are employed either to determine the most likely TC geometry or to consider geometry as a stochastic variable [31]. Both general correlations and calibrations for various basins are available to the user. As a result, azimuthal wind speeds are reliable. Based on Schwerdt, Ho, and Watkins [43], TC asymmetry is taken into account and a constant inflow angle of 22°is assumed [50].

Once the research location has been chosen and the TCs parameters have been obtained the models and the testing parameters are selected. In the current work, IPET and the BaCla model are used to generate rainfall, and the outcomes will be verified using high resolution stage IV data. For *pdef* and *vmax* BaCla model both symmetric and asymmetric rainfall distribution will be analyzed. The different percentiles for rainfall variations will be evaluated as well. After the rainfall has been modelled, the SFINCS and FIAT models are used to asses the flooding and flood damage respectively. The working of SFINCS and FIAT are discussed in subsequent sections. The basic workflow chart (Fig. 4.1) attached below, shows the flow diagram of the methodology followed from selection of area of interest and TC to running different models.

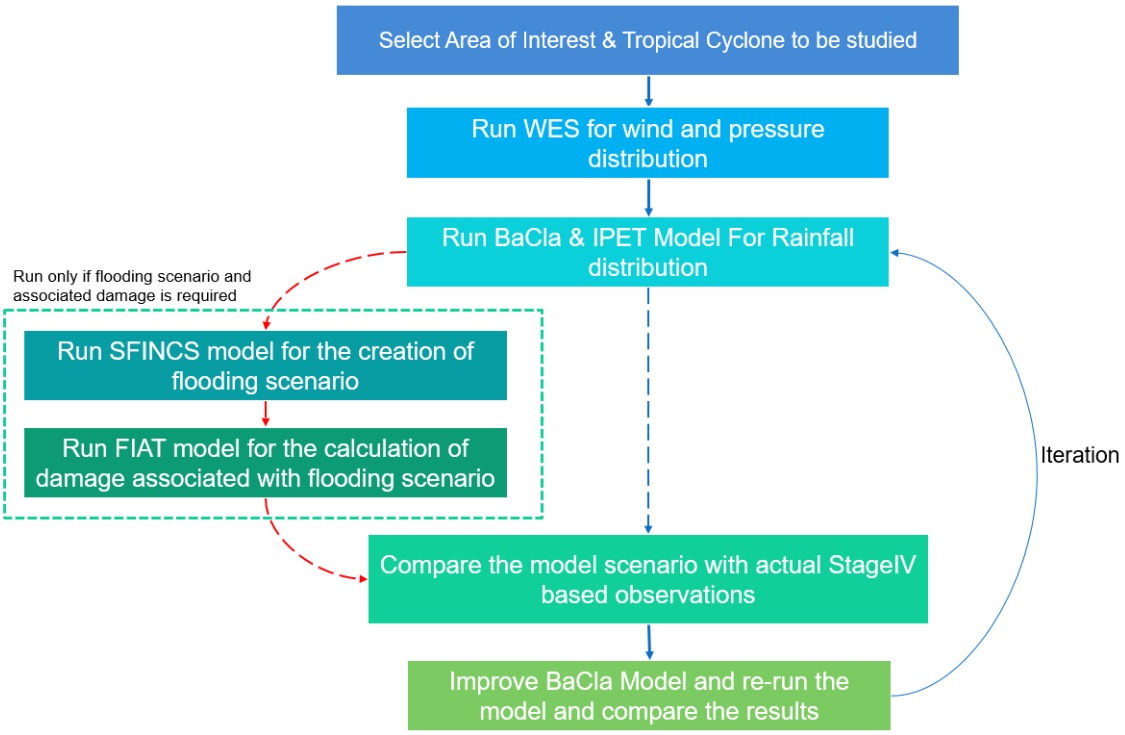


Figure 4.1: A schematic workflow diagram of methodology used

Finally, the sum of total rainfall over the selected region of North Carolina, South Carolina and Georgia (Which is referred as N-S Carolina at most places in this thesis) fig 4.2 is investigated along with Charleston and Wilmington.The obtained results are then evaluated for its effectiveness in representing the real scenario, which in this case is based on calculations made using Stage IV data. The discrepancies in the model are then corrected and the above mentioned steps are repeated to check the quality of improvement.

## 4.2. Overview of calibration case studies

Three tropical cyclones are considered: Florence 2018, Matthew 2016 and Bonnie 2016.

Once the tropical cyclone and its year of occurrence is selected, by making use of IBTrACS data information like pmax, vmax and Δ P are extracted. They are used as an input to run BaCla and IPET model. For all the time steps the modeled rainfall data are calculated for different percentiles and compared to actual stage IV data.To define the occurrence of rainfall, BaCla model uses a percentile-based threshold since that describes rare events in the tail of statistical distribution [52]. A percentile is a measurement that tells us what percent of the total frequency of rainfall data set that was at or below that measure. By increasing the percentile threshold, extremes can be more clearly identified, but it implies lower sample sizes and less reliable results [20]. For comparing the modeled and actual amount of rainfall over-land, three locations: Charleston (South Carolina, USA), Wilmington (North Carolina, USA) and selected region of North-South Carolina (USA) were selected as the selected TCs pass either through or nearby these locations fig 4.2. The two smaller regions around Charleston and Wilmington are used to study the performance of the models close to and farther away from the eye of the storms while the bigger domain around them is useful to get a sense of the overall situation. The smaller region are also useful in estimation of damages associated to flooding because of TCs. To understand the actual rainfall variation to that of the modeled one we selected a large portion of North and South Carolina as well. For Charleston and Wilmington SFINCS model and FIAT models are further used for flooding and associated damage values.

To gain a deeper understanding of the model's performance above land, the model has been tested by attempting to reproduce the rainfall that precipitated during hurricane Florence 2018, Matthew 2016 and Bonnie 2016. All the three tropical cyclones are different in terms of wind speed, tracks and precipitation values. The direction of motion, area of interest considered in study and type of cyclone can

be seen in fig. 4.2.

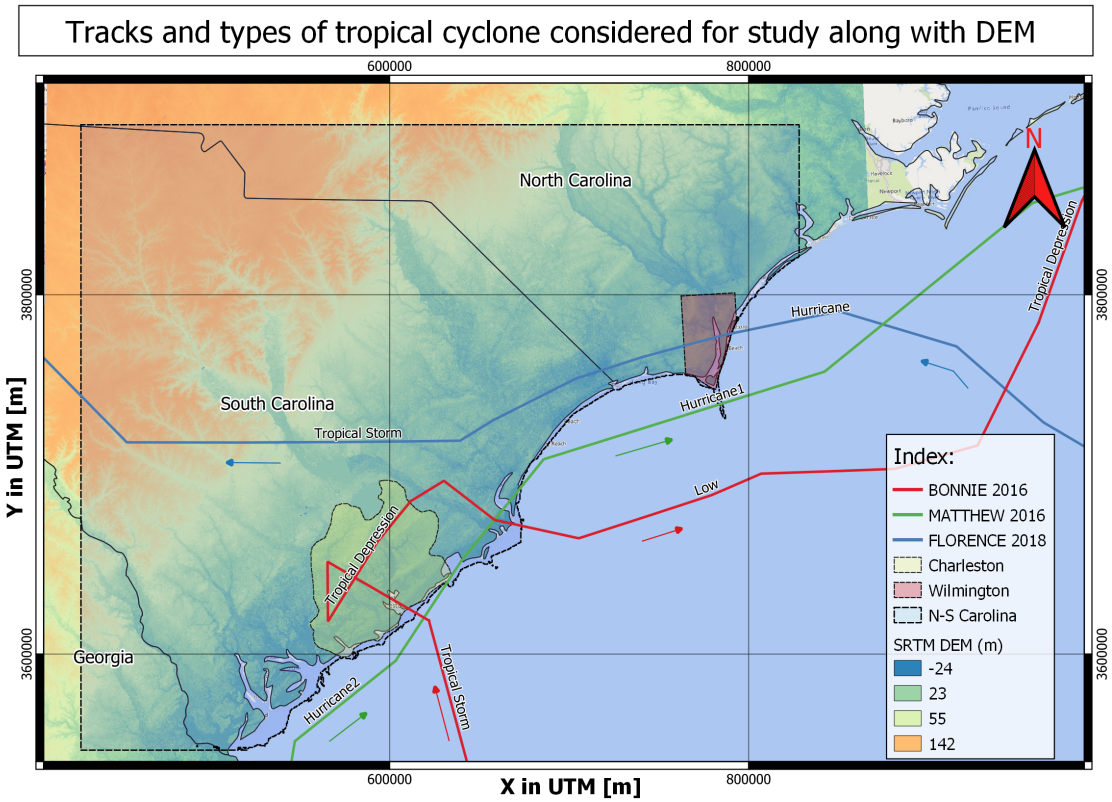


Figure 4.2: Different tropical cyclones selected in the area of interest

### 4.2.1. Florence 2018

Florence was a relatively large and slow moving TC that originated from a convectively active tropical wave, which was accompanied by a broad low pressure system that moved off the west coast of Africa on 30 August 2018 [34]. It made landfall as a category 1 hurricane [46] on the 14th of September at Wrightsville Beach, North Carolina, with a sustained maximum wind speed of 145 km/hr. After landfall, Florence's winds steadily weakened as it moved inland, however, torrential rain continued to fall for days. The storm produced record breaking precipitation across North and South Carolina, exceeding the highest single storm precipitation observed in this part of the country (above 20 inches/ 508mm at some location) [46]. As a result, nine river gauges exceeded their 1 in 500 years expected floods and USGS reported several dams breached [34]. The flooding significantly damaged homes and other infrastructure, resulting in an estimated $16.7 billion in damages. As Florence produced relatively large amount of rain without being a major hurricane, and continued to produce large amount of precipitation as it traveled inland, it serves as an interesting and challenging case for testing the accuracy of the parametric rainfall model.

### 4.2.2. Matthew 2016

Matthew was a category five hurricane with wind speed of around 160 mph or 71.52m/s on 29th September 2016, in the Caribbean sea. It reduced to category one hurricane with 75 mph or 33.5 m/s winds near McClellanville, South Carolina on 8th October, 2016. It resulted in exceptionally heavy rainfall amounting between 10(254mm) to 18(406.4mm) inches at large regions of North and South Carolina. As soils were heavily saturated with the rain in the previous month because of hurricane Hermine, deadly flash flooding immediately resulted. Matthew unfortunately resulted in billions of dollars of damage and 32 fatalities across eastern Carolina. Matthew's storm surge was around 6 feet(1.82m).[33]. Due to all of these factors, including the fact that it was affecting North and South Carolina, it was chosen as the second storm to examine.

Table 4.1: Overview of the different Tropical Cyclones considered

| Tropical Cyclone | Severity | | RVmax [km] | Cum. Precip. N-S Carolina $[mm/m^2]$ | Cum. Precip. Charleston $[mm/m^2]$ |
|---|---|---|---|---|---|
| | Before landfall | After landfall | | | |
| Florence 2018 | Category 2 | Cat1/TS/TD | 55-101 | 197.74 | 24.73 |
| Matthew 2016 | Category 2/1 | Category 1 | 120-82 | 197.32 | 235.29 |
| Bonnie 2016 | TS | TD | 50-80 | 50.04 | 56.26 |

### 4.2.3. Bonnie 2016

Bonnie was an yearly out-of-season tropical storm that developed along the south east coast of USA in May 2016. It became a tropical storm on May 28th while approaching the Gulf Stream east of Jacksonville, Florida. The storm reduced to a tropical depression before moving ashore at Isle of Palms, South Carolina, but regained tropical characteristics near Cape Lookout, North Carolina as it moved back to sea. It lead to heavy rain of around 5 inches (12.7cm) in Carolina's and was having its track crossing Charleston. So, it was also selected to test our model [33].

The table 4.1 provides a summary of three calibration TC that were taken into consideration.

## 4.3. Overview of validation case studies

To validate the effectiveness of the improved model three new tropical cyclones Alberto 2006, Hermine 2016 and Charley 2004 are selected. They have different characteristics and pass through the same area of interest are selected. The following discussion includes a brief explanation of each of them and the track they followed.

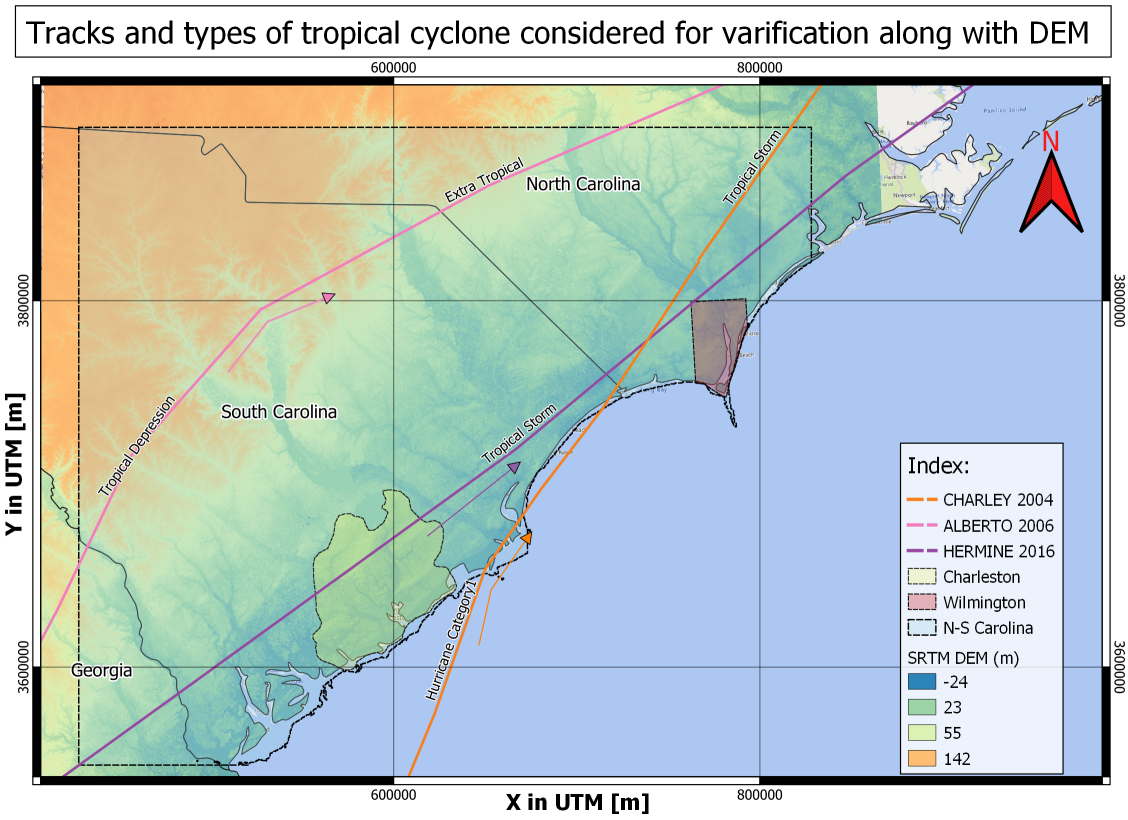


Figure 4.3: Different new tropical cyclones selected in the area of interest

Table 4.2: Overview of the different Tropical Cyclones considered for verification of improved model

| Tropical Cyclone | Severity | | RVmax [km] | Cum. Precip. N-S Carolina $[mm/m^2]$ | Cum. Precip. Charleston $[mm/m^2]$ |
|---|---|---|---|---|---|
| | Before landfall | After landfall | | | |
| Alberto 2006 | NA | TD/ET | 31-60 | 60.22 | 47.35 |
| Charley 2004 | Category 1 | Cat 1/TS | 100-40 | 16.73 | 14.03 |
| Hermine 2016 | NA | TS | <20 | 117.71 | 86.76 |

### 4.3.1. Alberto 2006

Disturbed weather over Central America and the northwestern Caribbean Sea led to the formation of Tropical storm Alberto 2006 and it produced torrential rainfall.At 0000 UTC on June 13, the cyclone grew stronger and peaked at 60 kt, with a minimum pressure of 995 mb, about 100 n miles south of Apalachicola, Florida. After then, the storm started to lose strength as it approached the coast, and at around 16:30 UTC on June 13, Alberto made landfall with winds of 40 knots close to Adams Beach, Florida. Alberto weakened as it moved deeper inland and towards the northeast. At 1200 UTC on June 14, it started to lose its tropical features over South Carolina and became extra-tropical. After moving back over the Atlantic, it intensified into a strong extra-tropical storm about south of Nova Scotia [5].

### 4.3.2. Hermine 2016

Hermine 2016, a category 1 hurricane (according to the Saffir-Simpson Hurricane Wind Scale), made landfall just east of St. Marks in Florida. Hermine had maximum sustained winds of 50 kt as it proceeded northeastward just inland across Georgia, South Carolina, and North Carolina's coasts on September 2 and early September 3. Deep-layer southwesterly shear increased dramatically during that time, and Hermine gradually started to display non-tropical characteristics with the formation of frontal boundaries, resulting in an increase in the asymmetry of the convective structure. Hermine, around 1200 UTC on September 3, became extra-tropical, near Oregon Inlet, North Carolina [1].

### 4.3.3. Charley 2004

Hurricane Charley 2004 swiftly grew stronger, before making landfall on Florida's southwest coast as a Category 4 storm on the Saffir-Simpson Hurricane Scale. Despite its tiny size, Storm Charley inflicted significant wind damage on Charlotte County, Florida, making it the fiercest hurricane to strike the United States since Andrew in 1992. Over the Florida peninsula, there was significant damage that was well inland. At around 1400 UTC on August 14, as a weakening hurricane with top winds of about 70 kt, Charley made landfall once more close to Cape Romain, South Carolina. Over southeastern North Carolina, Charley quickly fell to a tropical storm [39]. The table 4.2 provides a summary of three validation TC that were taken into consideration.

## 4.4. The SFINCS model

In order to get flooding scenario, several factors needs to be taken into account along with rain, such as fluvial, wind-driven surge, tidal and waves. To take these factors into account Deltares developed SFINCS model. SFINCS (Super-Fast INundation of CoastS) is based on the equations of Bates, Horritt, and Fewtrell [3] in which several terms in the Saint-Venant equations are simplified and neglected [24]. SFINCS is the first reduced-complexity models to include all the processes that are deemed relevant for the computation of coastal compound flooding (i.e. fluvial, pluvial, tidal, wind-driven surge and waves).

The SFINCS model is developed to efficiently simulate compound flooding events at limited computational cost and good accuracy. SFINCS solves the Simplified Shallow Water Equations (SSWE) and thus includes advection in the momentum equation. However, it can also run using the LIE (Local Inertial Equations) without advection. Processes such as spatially varying friction, infiltration and precipitation are included. Moreover, SFINCS includes wind-driven shear and an absorbing-generating weakly-reflective boundary is considered which are not included in other reduced-physics models. Wave-driven flooding has so far only been modelled in those models by adding over-topping volume sources terms from another wave model, rather than actually solving for the waves itself (e.g. Brown et al. [7]).

SFINCS uses a text-based input file that contains relevant information regarding the model grid (grid

spacing, and number of cells in both directions), simulation times, and various physical and numerical input parameters. Additionally, a depth file (containing the vertical elevation of each cell) and a mask file need to be provided. The mask file indicates which cells are active, inactive or boundary cell. Inactive cells are the one which are located below or above certain threshold elevation. Time series for water level boundary conditions are provided at one or more boundary points along the coast. The model computes the water level at each boundary grid cell as the weighted average of the provided water levels at the two nearest boundary points. This research analyzes SFINCS with both a static offshore water level and a variable water level.

Other input files for SFINCS include those with the location and time-series of point discharges, and spatially-varying roughness and infiltration rates. Meteorological forcing (i.e. winds and precipitation) can be provided as spatially-uniform time-series, or in a gridded or spiderweb format, whereby the forcing variables are provided as a function of space and time.

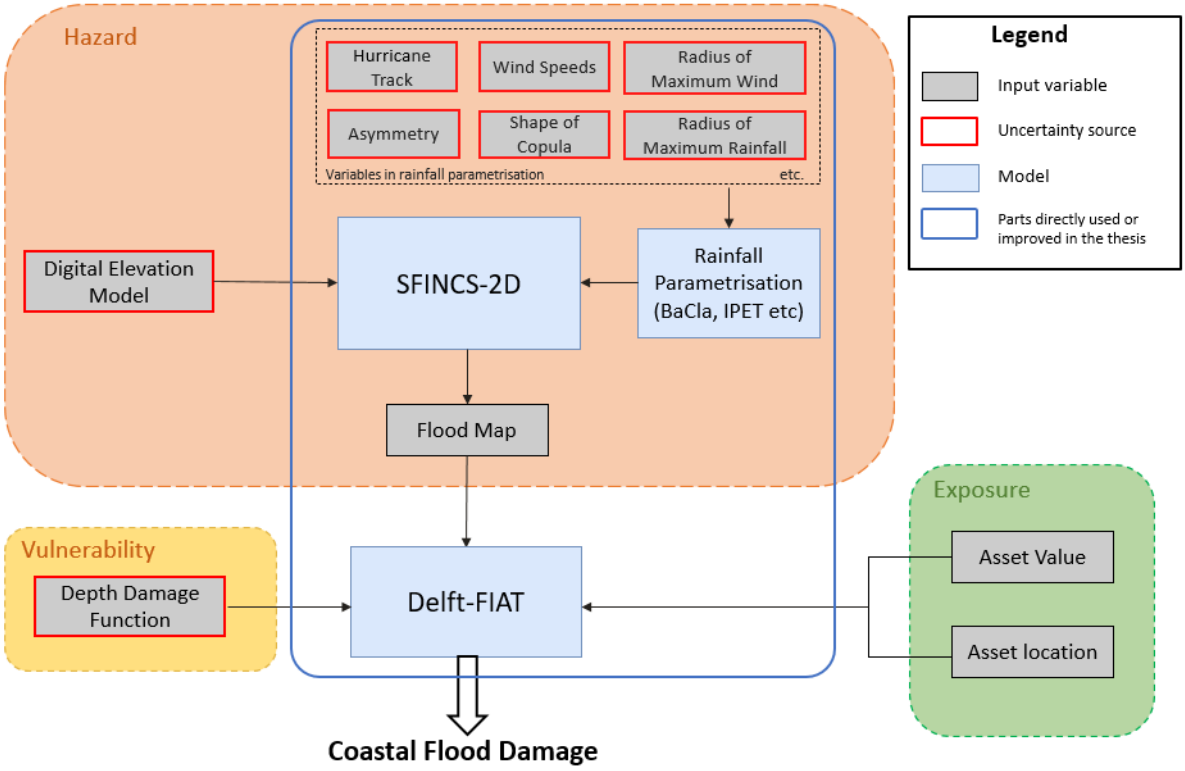


Figure 4.4: Schematic representation of the modelling chain used to calculate damage assessment along with different source of uncertainty [37]. The two blue boxes are the one relevant to this thesis.

In this thesis the parameters that were controlled or changed while running SFINCS model are: grid sizes, date and time, location of observation station for calculation of rainfall variation over time, a mask file to crop the area of interest and tidal effects while calculating the flooding. For Charleston, a grid size of 200 by 200 meters is used whereas for Wilmington, 100 by 100 meters is used. Different grid sizes were employed to calculate flooding scenarios more quickly, and this little adjustment in grid size had little impact on creating flooding scenarios or calculating damage. For the reasons described in the section 5.5, both flooding scenarios—one taking into account tidal effects and the other without, are taken into consideration.

## 4.5. The FIAT model

The Flood Impact Assessment Tool, or FIAT, is used to calculate and show the economic consequences due to flooding [29]. FIAT is a flexible open-source tool-set, where direct damages are estimated at the unit level (e.g. a single building or piece of infrastructure).It incorporates information about the exposed

assets, depth damage functions, and flood inundation maps together with absolute occurrence rates and anticipated damages from single events [38].

FIAT takes into account the probability of forcing events on a yearly basis, ranging from high or low input amounts which occur once in a century, to replicate levels which correspond to the mean input every year [13]. The flood inundation maps with absolute occurrence rates are overlaid with a polygon file showing the built environment of the study area through the spatial positions of building footprints. The polygon file roughly describes each and every building within an urban area, its use, condition, and number of people living there. Based on the provided data, damage is calculated per raster cell comparing the number of buildings affected to the maximum damage that can occur. Damage raster maps for each probability are combined statistically into an expected annual damage report by overlaying the individual raster file while taking their probability in relation to one another in account [29]. A schematic representation of the modelling chain is used to calculate damage assessment along with different sources of uncertainty as shown in fig 4.4.

The FIAT model also takes into account the shared socioeconomic pathways (SSPs) for predicting the future scenario in order to calculate the damage. In this study SSP2 (i.e., the middle of the road scenario) has been considered [15]. The associated damage has been estimated in US dollar ($). Building data of 2012 and population data of 2019 has been used for calculations. Fig 4.5 shows diagram of different SSP scenarios and what they stand for along with the workflow diagram of Delft-FIAT model. Delft-FIAT is used in this study because it does an exposure assessment in addition to the hydrodynamic analysis. Hazard data (from the SFINCS model) may be translated into monetary and social values using this tool. This conversion may be completed in a matter of minutes and is a useful tool for decision- and policy-makers [2].

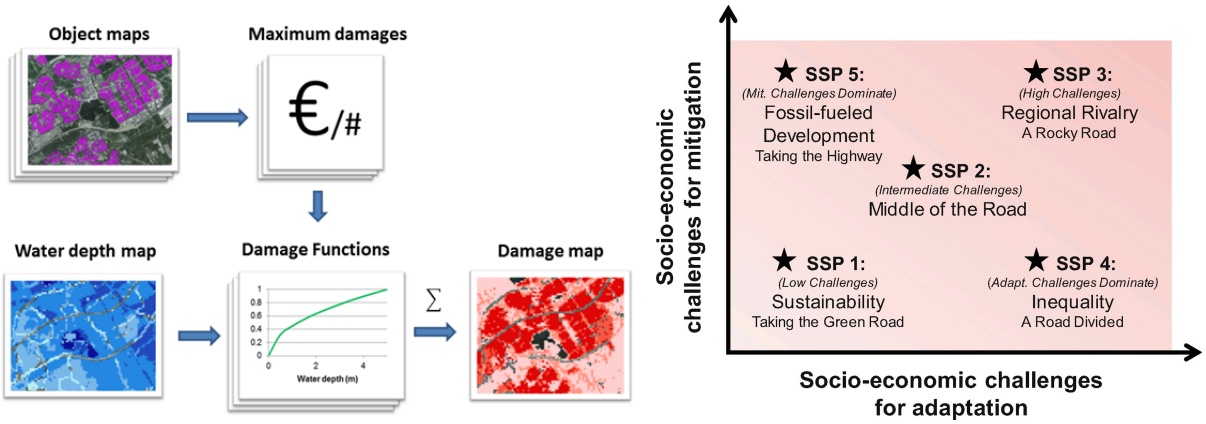


Figure 4.5: Workflow of Delft-FIAT model[14] along with the different SSPs options[36] it provides.

# 5

# Results and Discussion

This study will be looking at the amount of rainfall that BaCla Model suggest for $pdef$ and $vmax$ based inputs for symmetrical and asymmetrical scenarios. The results will be compared with IPET and the actually observed rainfall measured by gauges of Stage IV data to come to a conclusion for the effectiveness of the model. This chapter will suggest possible improvements in the BaCla model and will also look into how the improved model performs after the suggested improvements are implemented. The improved model will be called as D.J.Bader, J.N. Claassen & A. Hasan (BaClHa) model. The flooding scenarios using the SFINCS model and the accompanying damage using the FIAT model will both be evaluated in relation to the amount of precipitation.

## 5.1. Calibration case studies

Understanding what each graph represents is crucial before looking at the case studies. In almost each of the case studies, the cumulative precipitation map for selected area of interest will be investigated (e.g. fig. 5.1), which will help in better understanding the spatial rainfall distribution. Difference between modeled and observed (stageIV) based results will be compared. The spatial cumulative rainfall distribution map of just pressure deficit based symmetrical model is shown in the report. To get the idea on how the pressure deficit ($pdef$) based symmetrical/asymmetrical cases and maximum sustained windspeed ($vmax$) symmetrical/ asymmetrical model perform for different percentile (in our case 5, 50 and 95) are performing there are bar graphs plots (e.g. fig 5.2) are plotted. The bar graphs reflect the cumulative amount of precipitation that occurred per unit area because of a particular TC. The bar graphs only reflects the values for selected location and number of days for which the eye of TC was close to the area of interest. For some of the cases there are Cumulative Distribution Functions (CDF) are also plotted showing Pdef and Vmax symmetric and asymmetric case along with IPET, observed(Stage IV) and 100 runs of pdef symmetric and asymmetric model with random percentile fig. 5.2.

### 5.1.1. Florence 2018

After following the steps as discussed in the Methodology section, at first, the cumulative rainfall over the selected region of north south Carolina and Georgia (fig 5.1) is investigated. As discussed in section 4.2 Florence was a relatively large and slow moving tropical cyclone that made a landfall as category 1 hurricane and produced record breaking rainfall in North and South Carolina. The percentile of *pdef* that captures the similar amount of cumulative rainfall per unit area as the observed (Stage IV) data is considered. Looking at the rainfall distribution of *BaCla Pdef* $50^{th}$ *percentile* model and StageIV results in the fig 5.1, we see that the BaCla model provides higher amount of rainfall for all percentiles at a location which is at larger distance from the eye. The fig 5.1 & 5.2 shows that the model is able to capture cumulative rainfall for the selected area of interest, but not the spread and peak amount of rainfall. This suggests that the model needs to be improved for limiting high amount of rainfall at larger distances from eye of TC as there is less or no rainfall at those distances in reality.

The fig. 5.2 shows that the cumulative rainfall prediction per unit area of the BaCla model broadly agrees with the observations in the sense they lie between $30^{th}$ and $65^{th}$ percentile. However, on average, fig (5.2), all the models, including IPET, over-estimate the rainfall. Fig 5.2 shows that as the

percentile values increases i.e a score at or below which a given percentage of rainfall data falls, the amount of rainfall increases. As expected, the rainfall amount increases with the increase in percentile. This applies to both *pdef* based or *vmax* based model. The asymmetric case shows slightly higher amount of rainfall as compared to the symmetric one. This is due to the fact that we are only examining specific spiderweb segments that are located inside the region of interest. When the cumulative rainfall of spiderweb is evaluated, both symmetrical and asymmetrical situations exhibit comparable values. Overall, it looks like the BaCla model over-estimates rainfall at large distances from the region where the storm makes landfall, as well as far away from the eye (around 300 km away). To further investigate the location and area based applicability of the BaCla model, the two smaller regions in Wilmington (where Florence made landfall) and Charleston (approx 300 km away) are analyzed.

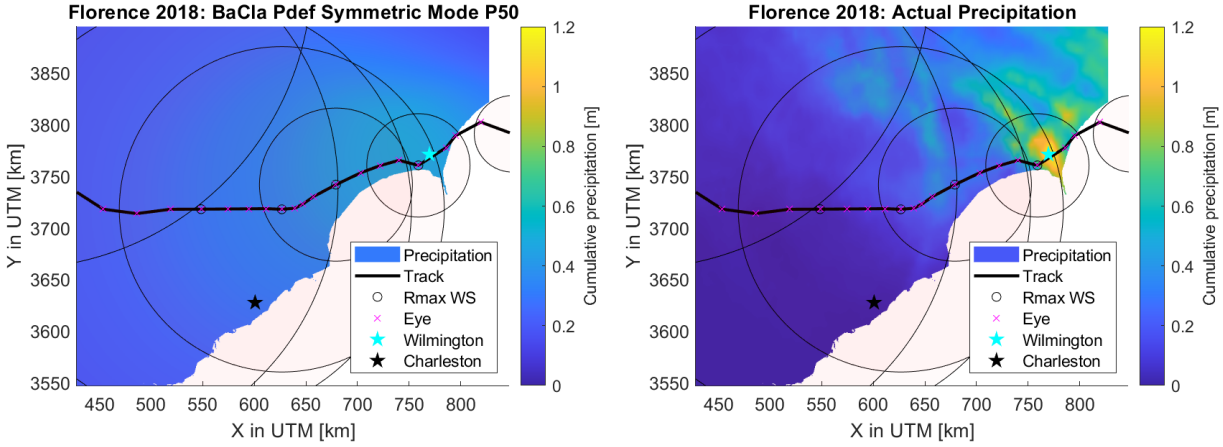


Figure 5.1: Florence 2018: N-S Carolina $50^{th}$ percentiles Pdef BaCla model vs observed (stage IV) cumulative precipitation. The black line shows the track of TC, red crosses are the location of eye at different time interval, the circles represent the radius of maximum wind-speed and the stars location of ground station at Charleston and Wilmington.

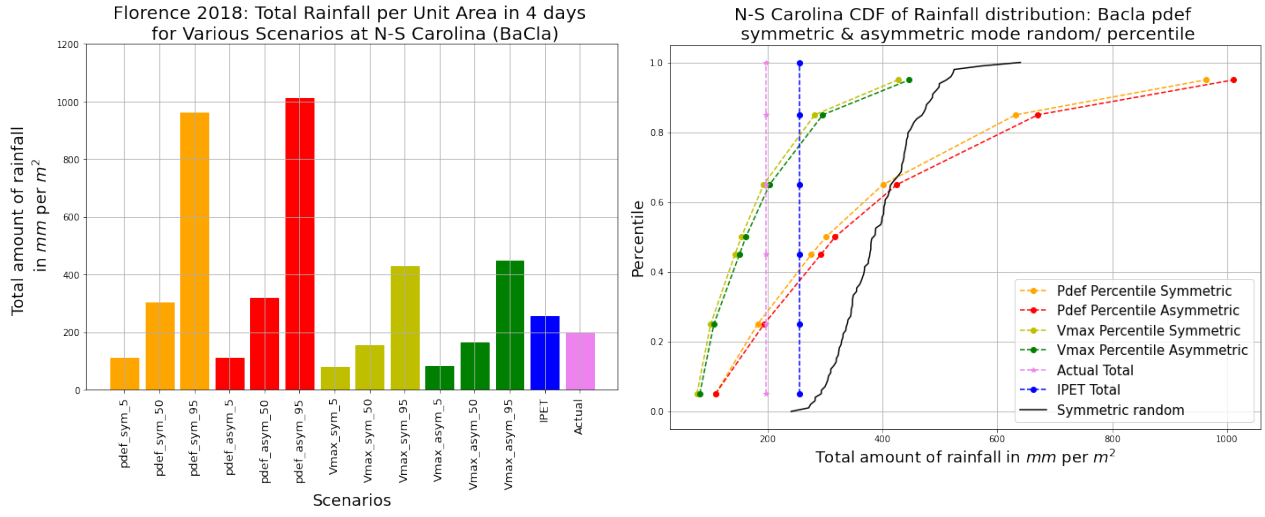


Figure 5.2: Florence 2018: N-S Carolina cumulative precipitation plot for different percentile and models along with its CDF. The blue color stands for IPET model, pink for observed stage IV data, orange for $pdef$ symmetric, red for $pdef$ symmetric, light green for $vmax$ symmetric and dark green for $vmax$ asymmetric model. The black and grey color are for $pdef$ symmetric and asymmetric random percentile model respectively.

When fig 5.3, $75^{th}$ percentile of pressure deficit *pdef* based precipitation at Wilmington, is compared with stageIV based observations, it shows that the BaCla model based precipitation variation is smooth and gradually reducing. For stageIV based data fig 5.3, there is more rainfall in the south eastern region or near the selected station at Wilmington as compared to the other parts. Before looking into the cumulative rainfall variation per unit area it is interesting to look how the rainfall at a particular

station actually varied over a span of 4 days between $14^{th}$ of September 2018 to $17^{th}$ of September 2018. This was the time when the tropical cyclone was near the coast and moved inland. The fig 5.4, suggests that even the $95^{th}$ percentile pdef based model is not able to capture the peak amount of rainfall. This might be because our model considers the radial mean values of rainfall whereas in this case we are comparing it with actual rainfall at that particular location suggested by stageIV data. IPET model based results is not able to capture any of the peaks. Random percentile pdef symmetrical model shows variation in rainfall but still fails to capture peak. This might not be the perfect way of comparison but will surely give an idea about the variation.

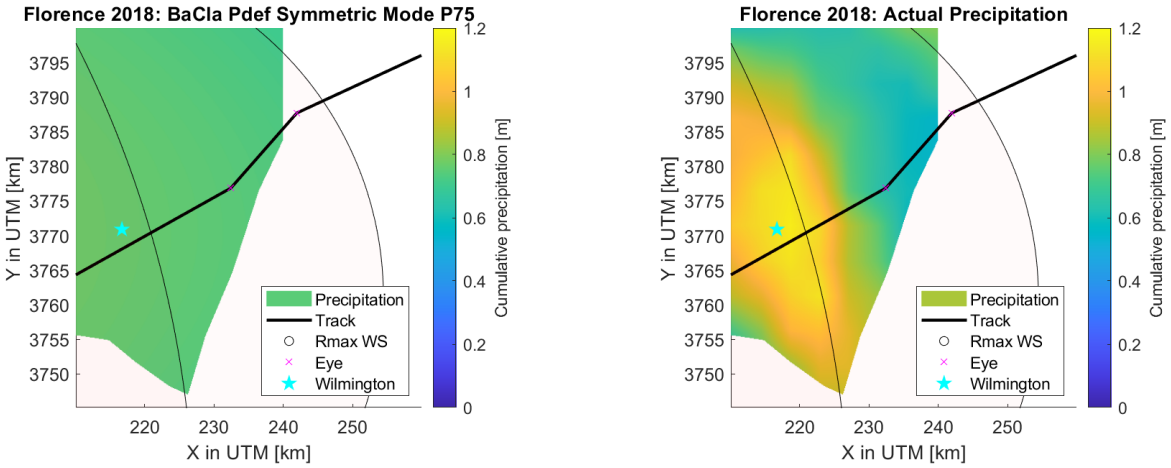


Figure 5.3: Florence 2018: Wilmington 75 percentiles Pdef BaCla model vs observed (stage IV) cumulative precipitation

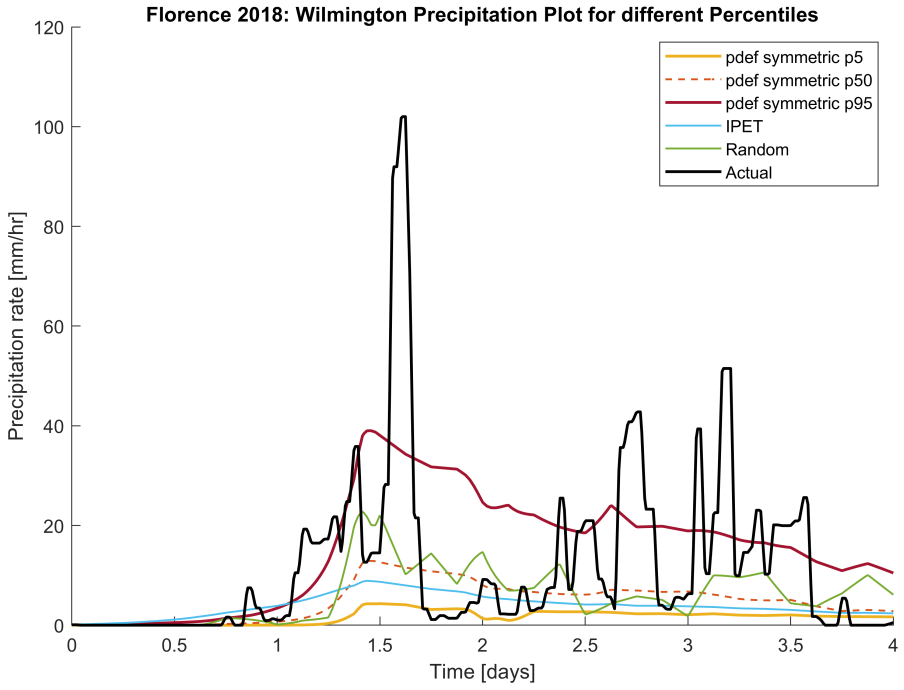


Figure 5.4: Florence 2018: Wilmington precipitation plot for a particular station. The yellow, dotted red and red line shows rainfall variation based on BaCla model, cyan represents IPET, green represents random percentile, and the black line shows the Stage IV data over the span of 4 days.

Fig. 5.4 is the result of multiple adapted Holland wind profile, it shows that the pressure deficit *pdef* based model displays gradual rainfall reduction once the peak amount of rainfall is achieved,

which results in over estimation of rainfall for higher percentile based pdef models as shown in fig 5.5. Maximum velocity *vmax* based models shows slightly lower amount of rainfall in general because $vmax$ has slightly stronger relation with $pmax$. The $pdef$ based model have higher uncertainty range as a result shows higher amount of rainfall and may act advantageous for extreme rainfall prediction [11]. IPET underestimates rainfall quite significantly, depicting almost half of the actual amount of rainfall that occurred. Looking at the cumulative distribution function fig. 5.5 which also includes the results of randomly selected 100 pdef symmetric and asymmetric model. The CDF shows that around $80^{th}$ percentile pdef model captures the actual amount of rainfall at Wilmington. The random percentile based results generally lie between $40^{th}$ to $65^{th}$ percentile of pdef based results.

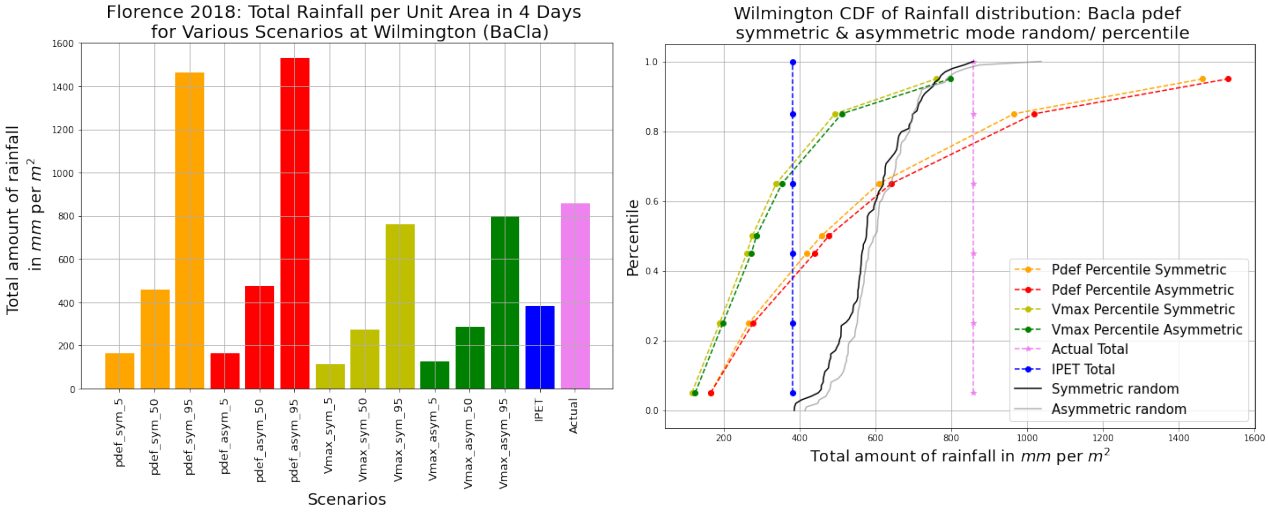


Figure 5.5: Florence 2018: Wilmington cumulative precipitation plot for different percentile and models along with its CDF. The blue color stands for IPET model, pink for observed stage IV data, orange for $pdef$ symmetric, red for $pdef$ symmetric, light green for $vmax$ symmetric and dark green for $vmax$ asymmetric model. The black and grey color are for $pdef$ symmetric and asymmetric random percentile model respectively.

Now, let's observe how effective the model is at Charleston which is at a distance of around 300 km from the eye of TC, Florence 2018. The fig. 5.8 shows that if the same $75^{th}$ percentile based pdef symmetrical model overestimate rainfall by quite a lot. So, $5^{th}$ percentile based results are compared. The fig 5.6 shows that the model is providing high amount of rainfall at locations where there is less or no amount of rainfall. It means that the model is not good at estimating the rainfall at large distance from the eye of TC. To correct that a threshold must be introduced for distance up-to which the model is applicable and after which it over-estimates rainfall or the variable of copula needs to corrected so it can effectively capture the distant locations rainfall as well.

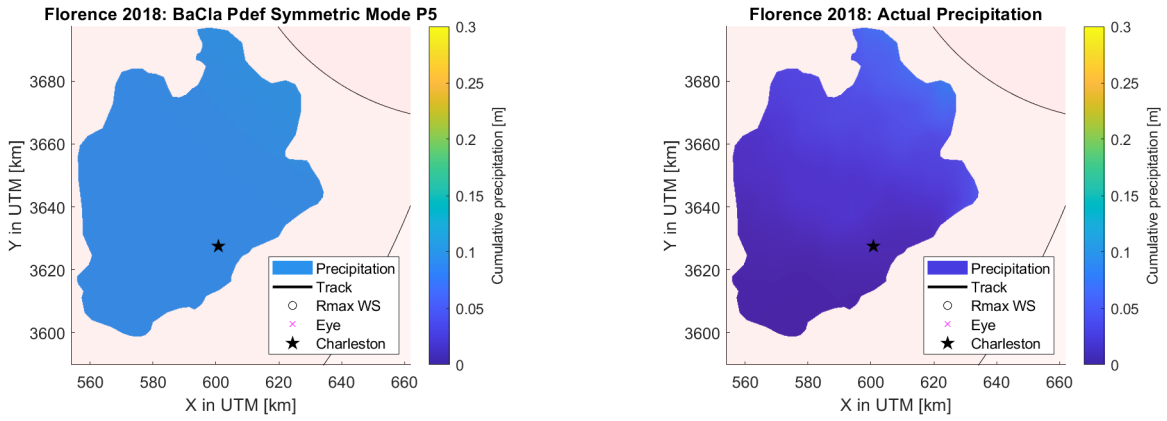


Figure 5.6: Florence 2018: Charleston 5 percentiles Pdef BaCla model vs observed (stage IV) cumulative precipitation

Fig. 5.7 shows rainfall variability over the span of 4 days based on different models and stageIV

data at Charleston because of Florence 2018. Fig 5.8 shows the model strongly over-estimates the total amount of precipitation in the area. This is because the peak amount of rainfall rate is less than 2.8mm/h, which causes the BaCla model to predict the same amount of rainfall across all radii as explained in section 2.2.2.The model provides same low quantity precipitation at all radii but they accumulate over time and space, which makes the predicted cumulative rainfall per unit area to be too large as fig 5.8 justifies. Similar results are observed for *IPET* or BaCla *pdef* based and *vmax* models. Fig 5.8 shows the CDF of symmetrically or asymmetrically selected random percentile values in 100 runs lies between the $40^{th}$ to $90^{th}$ percentile of percentile based observations.

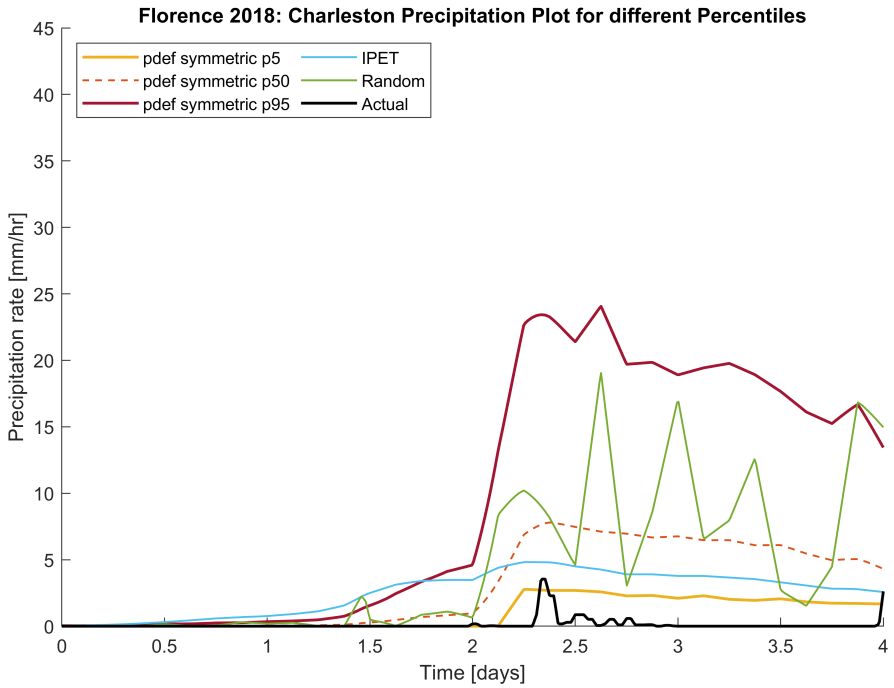


Figure 5.7: Florence 2018: Charleston precipitation plot for a particular station

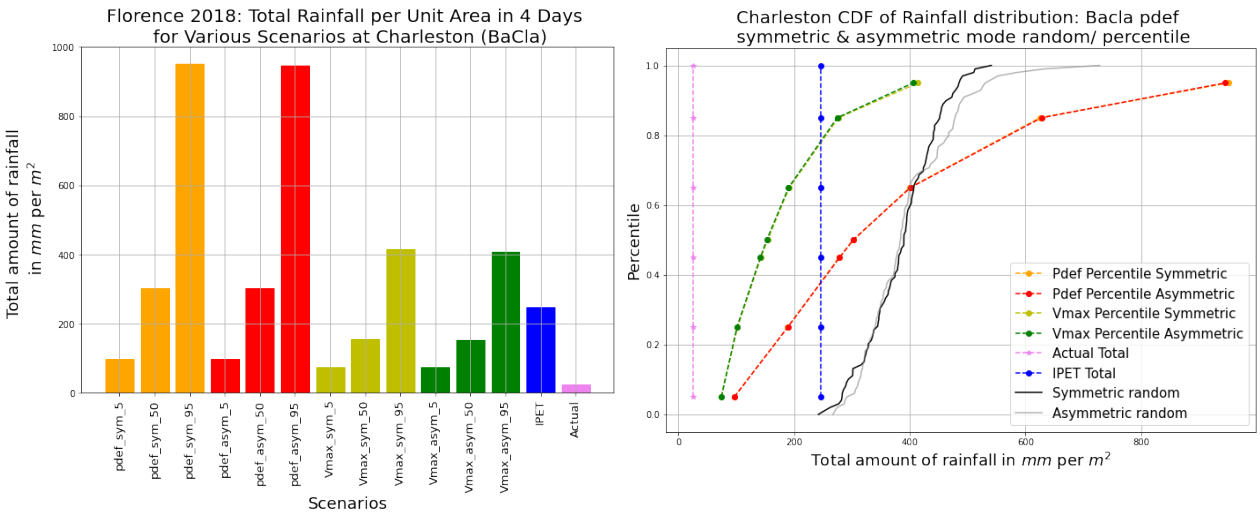


Figure 5.8: Florence 2018: Charleston cumulative precipitation plot for different percentile and models along with its CDF

Overall the insights on model performance based on Florence 2018 case study are as follows:

1. Model over-estimates rainfall at larger distance from eye of TC.

2. When the peak amount of rainfall is less than 2.8 mm/hr, it provides equal high amount of rainfall at all radii.

3. Peak amount of rainfall is not captured by the model and after reaching the peak value of rainfall it shows a gradual fall.

4. IPET as currently used standard method is not good enough for smaller areas of interest, as it highly over estimates rain at Charleston and underestimates in Wilmington. For larger area like that of North and South Carolina is can provide rainfall near by the actual one.

5. 100 randomly selected percentile based rainfall model is neither able to capture Charleston nor Wilmington.

### 5.1.2. Matthew 2016

Moving forward, for Matthew as well, the first thing investigated is rainfall distribution over the selected region of North Carolina, South Carolina and Georgia. As discussed in section 4.2 Matthew was a category five hurricane that reduces to category one hurricane with wind-speed of around 33.5 m/s near south Carolina and results in exceptionally heavy rainfall. Fig 5.9 shows that the maximum amount of rainfall is concentrated from coast to more in-land based on observed stageIV data . When it is compared with the model based results, fig 5.9 shows that even for $95^{th}$ percentile pdef based model the maximum amount of rainfall is concentrated more within or nearby the radius of maximum wind speed and not moving more into in-land. Even the amount of rainfall that the model estimates it quite less than what actually occurred based on gauges of stageIV data. Fig. 5.9 shows that the model based precipitation variation is smooth and gradually reduces which is not the case with stageIV based observation. StageIV based data suggests two separated regions of intense rainfall. This kind of performance might be because of assumption in adapted Holland wind-profile [equation 2.5], that maximum amounts of precipitation occurs at radius of maximum wind speed or radius of maximum pressure deficit. It is also assumed that radius of maximum wind speed is equal to the radius of maximum precipitation. This suggests that the assumption of radius of maximum wind speed is equal to radius of maximum precipitation must be re-investigated. It is also possible that the higher amount of rainfall, more in-land is because of other factors like land surface friction that were not taken into account.

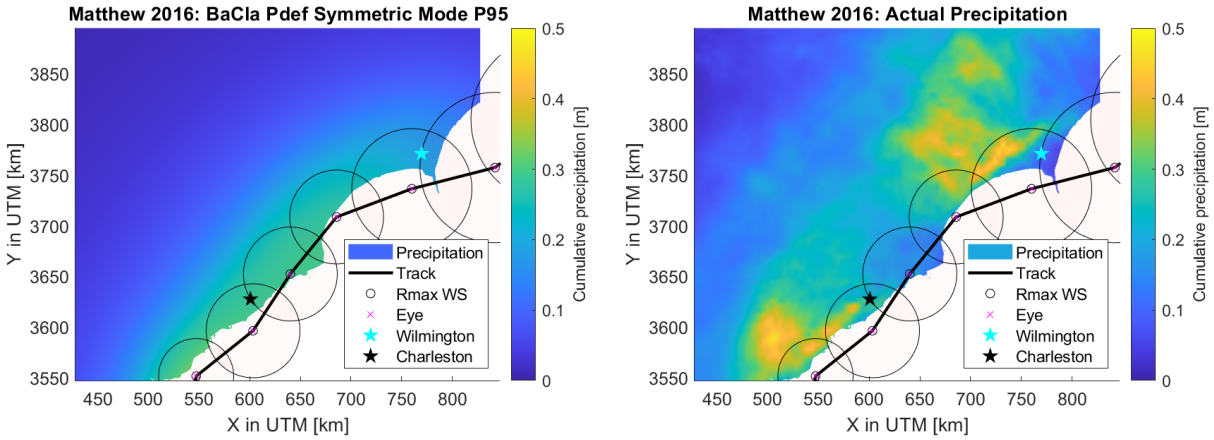


Figure 5.9: Matthew 2016: N-S Carolina $95^{th}$ percentiles Pdef BaCla model vs observed (stage IV) cumulative precipitation. The black line shows the track of TC, red crosses are the location of eye at different time interval, the circles represent the radius of maximum wind-speed and the stars location of ground station at Charleston and Wilmington.

When the cumulative rainfall per unit area (fig 5.10) is observed, the model predictions does not agree with the Stage IV observations, as the stageIV result is far more than even the $95^{th}$ percentile based calculation of the BaCla model. Even IPET model highly underestimates the rainfall as compared to actual stageIV based observations. As expected when the percentile values increases the rainfall increases but that still remains highly under actual values, this might be because BaCla model is not able to capture the rainfall more in-land. The BaCla model considers the radius of maximum wind-speed to be the radius of maximum precipitation which might not be true in all cases. Random percentile

based results still lies between $40^{th}$ and $65^{th}$ percentile of percentile based model runs (fig 5.10). To investigate the applicability of the BaCla model for a smaller area of study, Charleston is selected. It is nearby the coast from where the track of Matthew 2016 crosses.

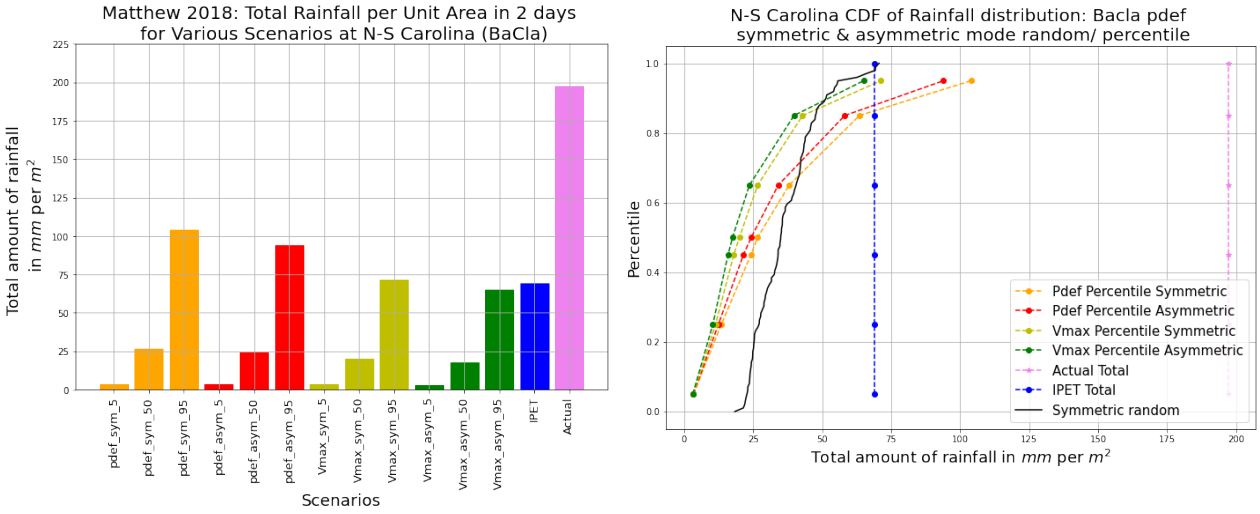


Figure 5.10: Matthew 2016: N-S Carolina cumulative precipitation plot for different percentile and models along with its CDF. The blue color stands for IPET model, pink for observed stage IV data, orange for $pdef$ symmetric, red for $pdef$ symmetric, light green for $vmax$ symmetric and dark green for $vmax$ asymmetric model. The black color is for $pdef$ symmetric random percentile model.

When fig. 5.11, $95^{th}$ percentile of pdef based precipitation at Charleston is compared with actual stageIV based results, it is observed that for stageIV based results, the rainfall is heavily concentrated in a smaller south-western region whereas the model based results. BaCla shows a gradual reduction in rainfall from the coast to more inland.

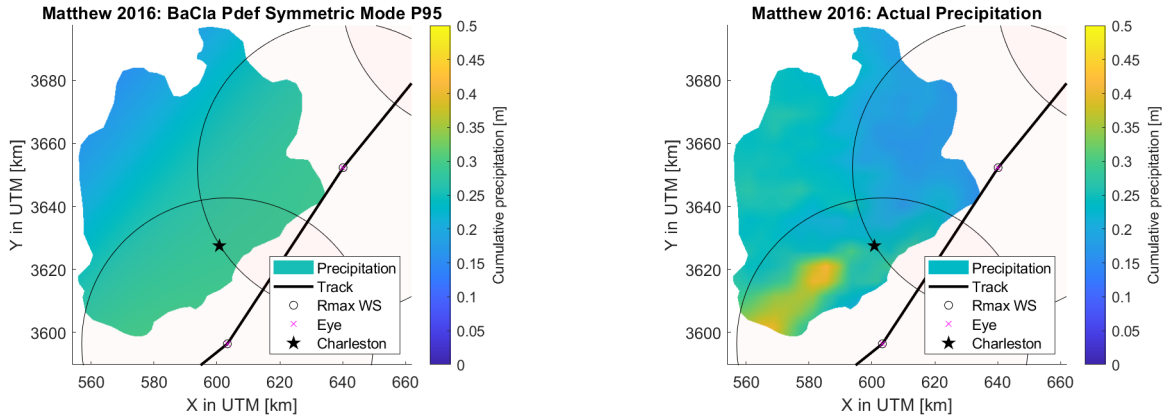


Figure 5.11: Matthew 2016: Charleston $95^{th}$ percentiles Pdef BaCla model vs observed (stage IV) cumulative precipitation

Looking at the fig 5.12 that shows the variation of rainfall at a particular station in Charleston over the span of 2 days and 6 hours when the TC is nearby, it is detected that the parametric models merge the three peaks of stageIV based observation into one for almost all the cases but the rise and fall of peaks are gradual and spread contrary to actual rainfall.This suggests that the models are good at capturing the highest peak amount of rainfall but not as effective in detecting all the peaks. This might be because of adapted Holland wind profiles being used.

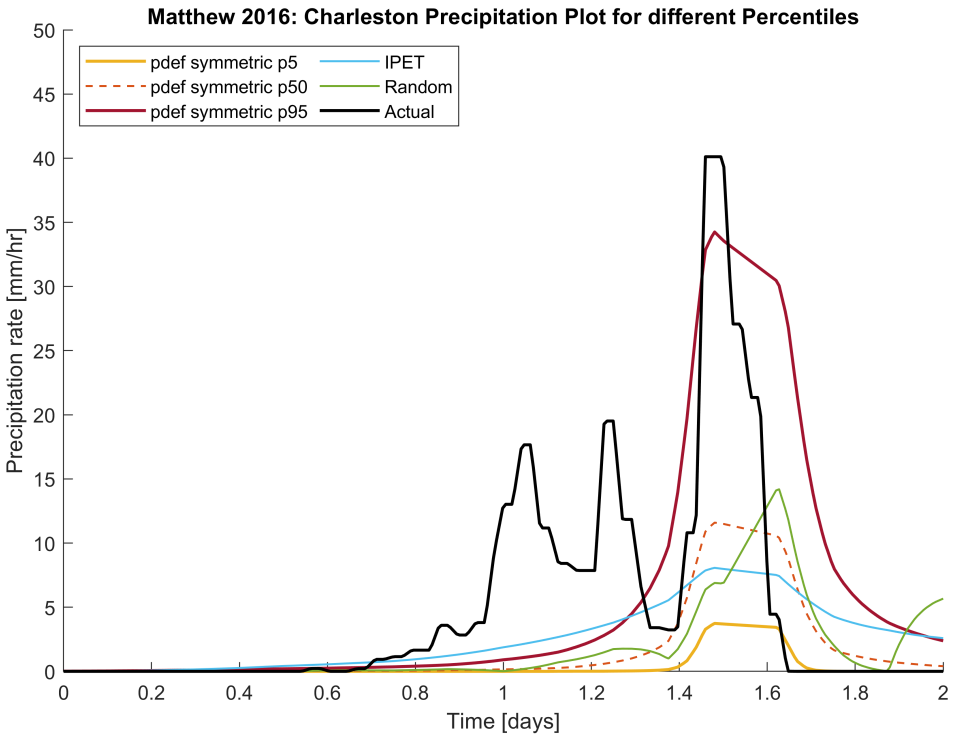


Figure 5.12: Matthew 2016: Charleston precipitation plot for a particular station. The yellow, dotted red and red line shows rainfall variation based on BaCla model, cyan represents IPET, green represents random percentile, and the black line shows the Stage IV data over the span of 2 days.

Fig. 5.13 shows the cumulative rainfall variability over the span of 2 days and 6 hours because of Matthew 2016 at Charleston. The model generally underestimates the cumulative rainfall per unit area. This might be because of capturing just one peak amount of rainfall by the model as it is based on adapted Holland wind profile or because of the radius of maximum wind speed is considered to be same as radius of maximum precipitation which is limiting the amount of rainfall more in-land. IPET still underestimates the rainfall by almost half of the actual one. The CDF of randomly selected percentile values in 100 runs for $pdef$ symmetric model lies between 25 to 90 percentile of percentile based observations fig 5.13.

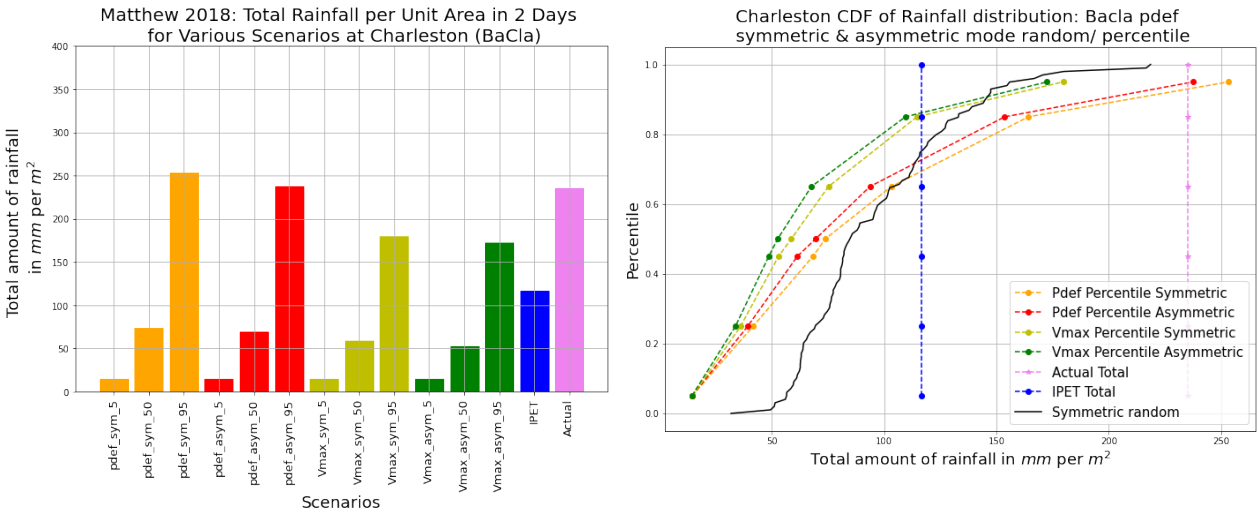


Figure 5.13: Matthew 2016: Charleston cumulative precipitation plot for different percentile and models along with its CDF.

Over-all the insights on model performance based on Matthew 2016 case study are as follows:

1. Model under-estimates rainfall at larger distance from eye of TC. Perhaps assuming that the radius of maximum wind speed and radius of maximum precipitation are the same might not always be true.

2. The model just tries to capture one peak amount of rainfall and after reaching the peak value of rainfall it shows a gradual fall.

3. IPET always underestimates the amount of rainfall.

4. 100 randomly selected percentile based rainfall model is neither able to capture N-S Carolina nor Charleston.

### 5.1.3. Bonnie 2016

Finally, for Bonnie 2016, the rainfall variation was investigated for selected regions of North Carolina, South Carolina and Georgia (fig 5.14). As discussed in section 4.2 Bonnie was a slow moving TC that became tropical storm and then tropical depression while it was near the coast. It resulted in light and spread rainfall based on stageIV observations (fig 5.14) but as discussed earlier, when the amount of rainfall is less than 2.8 mm/hr, the model provides max of lower amount of rainfall spread over the radii. Therefore, even 5 percentile $pdef$ symmetric BaCla model shows higher cumulative rainfall evenly spread over the region. So, it becomes a must to correct the amount of rainfall that the BaCla model predicts for the scenarios where the highest amount of rainfall is less than 2.8mm/h .

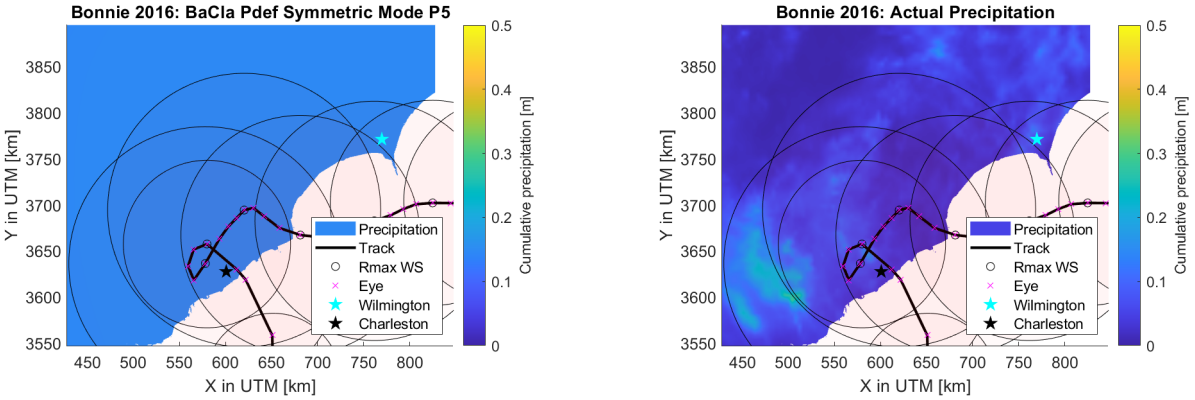


Figure 5.14: Bonnie 2016: N-S Carolina 5 percentiles Pdef BaCla model vs observed (stage IV) cumulative precipitation. The black line shows the track of TC, red crosses are the location of eye at different time interval, the circles represent the radius of maximum wind-speed and the stars location of ground station at Charleston and Wilmington.

Looking at the cumulative rainfall 5.15, as expected most of the model based results overestimates the amount of rainfall than the actual one, except the 5 percentile based results of maximum velocity *vmax* based model. The CDF shows an interesting effect of cumulative precipitation when the peak amount of rainfall is less than 2.8mm/h. The $65^{th}$ percentile maximum velocity *vmax* based BaCla model shows higher cumulative rainfall than the 85 or $95^{th}$ percentile case. This is because of the cumulative effects of less that 2.8mm/hr of peak rainfall. Similar is the case with $pdef$ based 5 and 25 percentile based observations. To investigate the applicability of the BaCla model for a smaller area of study, Charleston is selected. It is nearby the coast from where the track of Bonnie 2016 crosses.

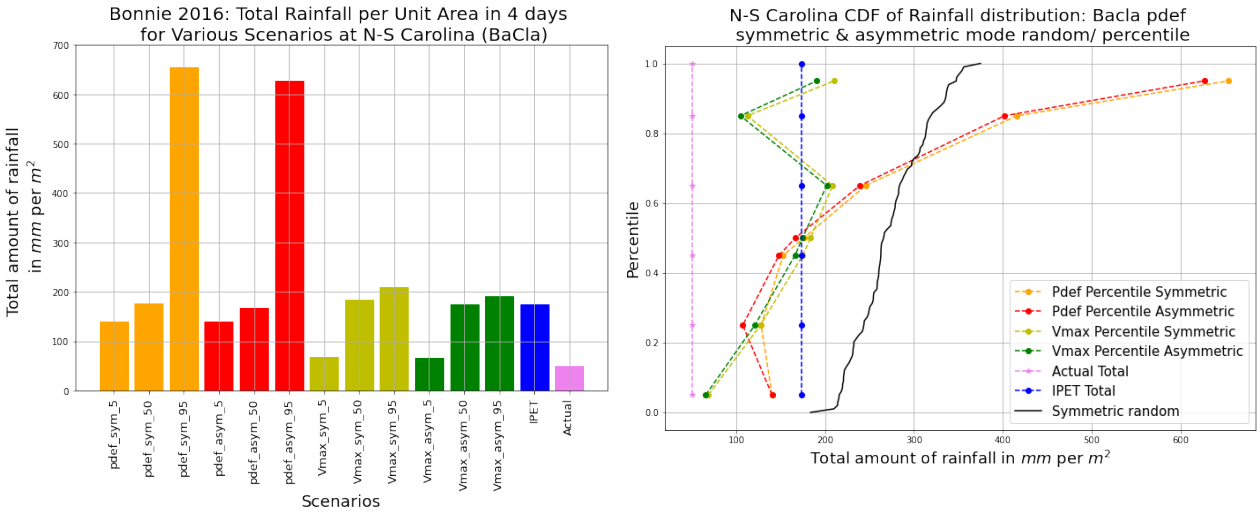


Figure 5.15: Bonnie 2016: N-S Carolina cumulative precipitation plot for different percentile and models along with its CDF. The blue color stands for IPET model, pink for observed stage IV data, orange for $pdef$ symmetric, red for $pdef$ symmetric, light green for $vmax$ symmetric and dark green for $vmax$ asymmetric model. The black color is for $pdef$ symmetric random percentile model.

When fig. 5.16, $50^{th}$ percentile of symmetric $pdef$ based precipitation at Charleston is compared with Stage IV based results, the figures suggest high amount of gradually reducing rainfall predicted by the model. Looking at fig. 5.17 that shows the variation of rainfall at a particular station in Charleston over the span of 4 days between $29^{th}$ May and $2^{nd}$ June 2016 when the TC is nearby, it is detected that the parametric models fails to capture the peaks of stageIV based observation and shows continuous high amount of rainfall in almost all the cases. This suggests that the models is not good at capturing the highest peak amount of rainfall when the peak amount of rainfall is low. So it must be looked at if 2.8 mm/h threshold is the right value above which adapted Holland wind profile works fine or the value needs to be changed. As the model is based on adapted Holland wind profile it shows one peak and then gradual reduction in rainfall. The random case as expected remains random and can show random distribution for different runs.

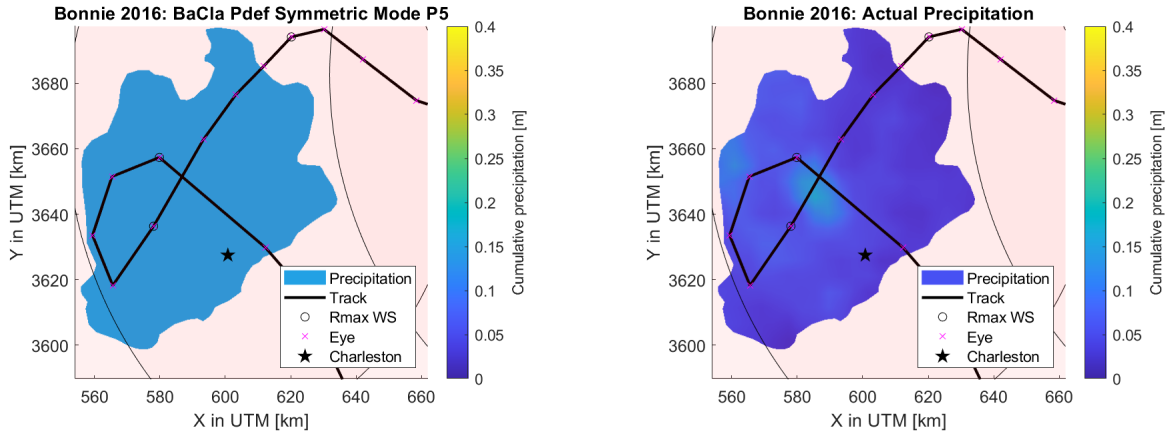


Figure 5.16: Bonnie 2016: Charleston 5 percentiles Pdef BaCla model vs observed (stage IV) cumulative precipitation

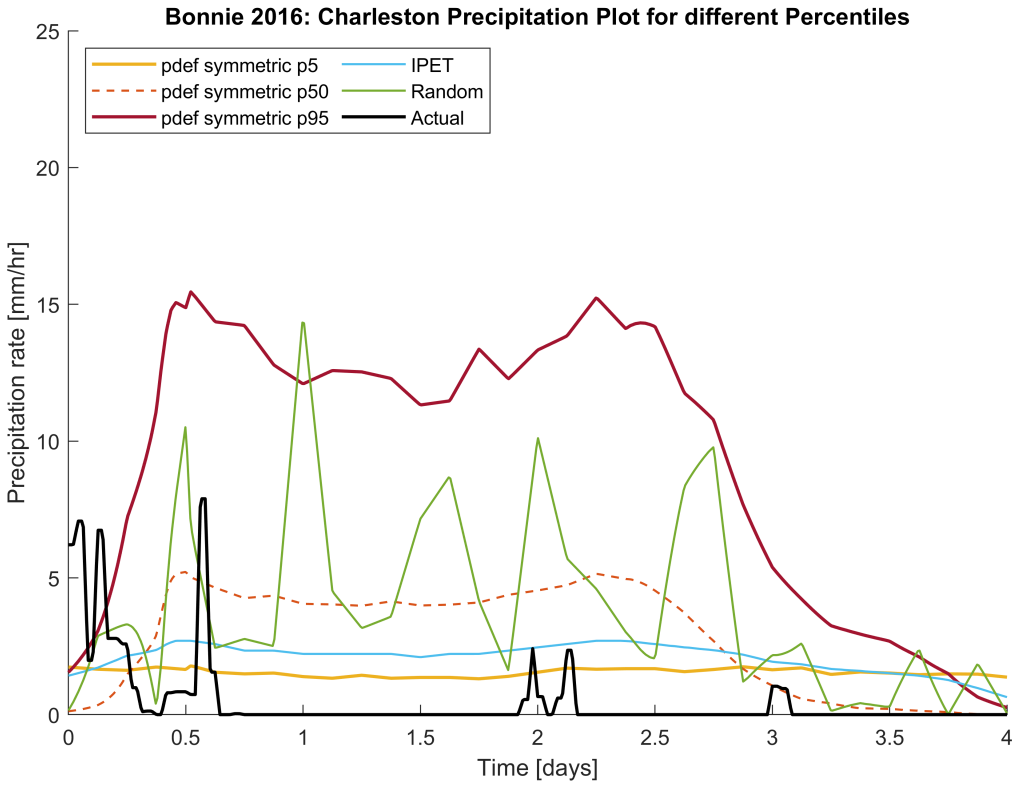


Figure 5.17: Bonnie 2016: Charleston precipitation plot for a particular station. The yellow, dotted red and red line shows rainfall variation based on BaCla model, cyan represents IPET, green represents random percentile, and the black line shows the Stage IV data over the span of 4 days.

Fig. 5.18 shows the cumulative rainfall variability over the span of 4 days because of Bonnie 2016 at Charleston. The model strongly overestimates the cumulative rainfall in the area. This might be because of the constant high amount of rainfall distribution assumption of BaCla model for lower peak amount of rainfall. IPET also overestimates the rainfall by almost 10 times of the actual one. The CDF of randomly selected percentile values in 100 runs for $pdef$ symmetric model lies between $30^{th}$ to $90^{th}$ percentile of percentile based observations.

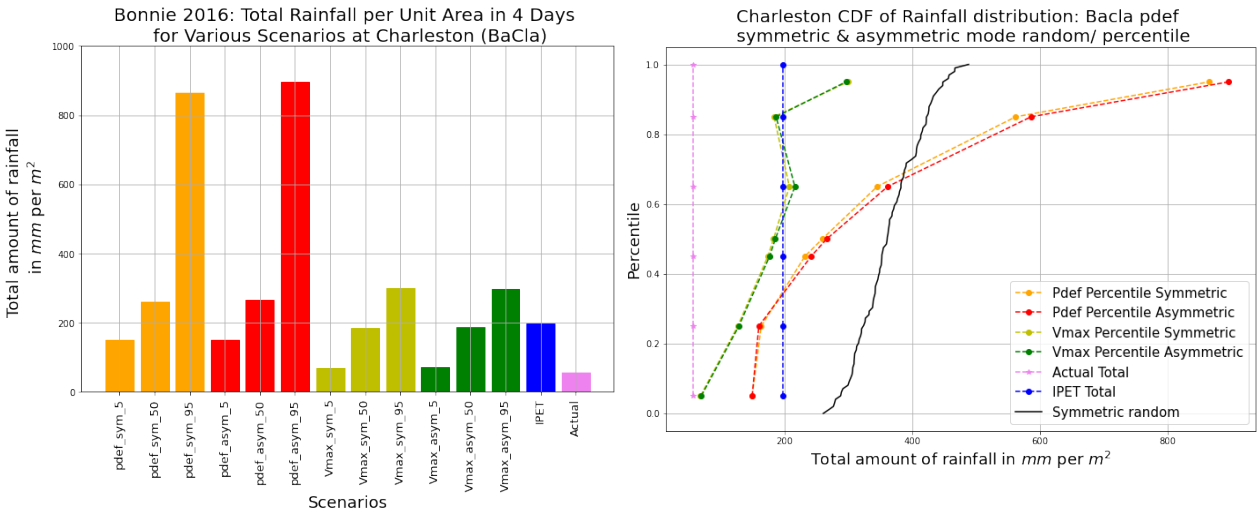


Figure 5.18: Bonnie 2016: Charleston cumulative precipitation plot for different percentile and models along with its CDF

Over-all the insights on model performance based on Bonnie 2016 case study are as follows:

1. Model over-estimates rainfall even at location near to the eye of TC.
2. When the peak amount of rainfall is less than 2.8 mm/h it provides equal high amount of rainfall at all radii.
3. Peak amount of rainfall is not captured by the model and after reaching the peak value of rainfall it shows a gradual fall.
4. IPET always overestimates the amount of rainfall.
5. 100 randomly selected percentile based rainfall model is neither able to capture N-S Carolina nor Charleston.

### 5.1.4. Overall rainfall prediction

To summarize the insights over the 3 hurricanes together:

- BaCla model overestimates the amount of rainfall in cases where the peak amount of rainfall is less than 2.8mm/h because of uniform rainfall assumption.
- The appropriate threshold for using method D (best fit area under the total rainfall curve method) to get fitting coefficients may not be 2.8 mm/hr (section 2.2.2).
- Radius of maximum wind-speed not necessarily always equal to radius of maximum precipitation.
- Peak amount of rainfall not necessarily always captured by the model.
- Based on the location and scenarios the models over or underestimates the amount of cumulative rainfall.
- For tropical cyclones of category 1 or above the model underestimates the cumulative amount of rainfall whereas for low wind-speed Tropical storms and tropical depressions it overestimates the amount of rainfall based on current study.
- In general, randomly selected percentile based rainfall model is neither suitable to capture rainfall for smaller region nor for larger area of interest.

## 5.2. Improved Model

Based on the insights obtained by studying three different case studies, three major factors that are decided to be targeted for improvement of the model are:

1. The validity of the assumption that the radius of maximum wind speed is equal to the radius of maximum precipitation based on available data.
2. BaCla model's consideration for providing equal high value for amount of rainfall for the cases when the peak amount of rainfall is less than 2.8mm/h, which might be leading to a too high cumulative amount of rainfall.
3. The appropriate threshold for using method D (best fit area under the total rainfall curve method) to get fitting coefficients may not be 2.8 mm/hr (section 2.2.2).

### 5.2.1. Relation between radius of maximum wind-speed and radius of maximum precipitation

The average radius of maximum precipitation based on blended data are plotted with the radius of maximum wind-speed based on available IBTrACS data for 53 separate tropical storms (fig. 5.19).For the selected tropical there were 220 time steps with the radius of maximum wind-speed and stageIV based the radius of maximum precipitation. Out of those observation 170 time steps were selected for which the radius of maximum precipitation was less than 300 km from the eye based on the study of Lonfat et al. [28], Jiang, Halverson, and Simpson [21] as well as Bader [2]. The above mentioned

studies suggested that maximum amount of precipitation generally occurs within 300 km from the eye of tropical cyclones fig. 2.1, 2.2. So, the cases where the maximum amount of precipitation is farther than 300 km are removed and a linear curve was fit along with polynomial fit of order 2, 3 and 4 for the values fig. 5.19(Appendix A). The equation 5.1 of the linear fit obtained is mentioned below. In equation y is radius of maximum precipitation and x is the radius of maximum wind-speed. The equation suggests that when the radius of maximum wind-speed is zero the radius of maximum precipitation is 34.7867km. Which is almost equal to the upper limit of the radius of the eye of most of the Tropical Cyclone (Average radius of eye is in range of 16.1 to 32.2 km) [32]. The equation also suggests what when the radius of maximum wind speed is around 96km then it is equal to radius of maximum precipitation. Above this value the peak amount of rainfall occurs inside the radius of maximum precipitation based on the simple linear equation considered. In extremely powerful storms, the inner eye-wall dissolves and is replaced by the outer eye-wall during an eye-wall replacement cycle. When this occurs, the intensity of a hurricane may momentarily decrease before temporarily regaining power when the new outer eye-wall's diameter reaches the size of the old eye-wall [45].The reason for higher amount of rainfall inside or outside of the eye for a TC having radius less or more than 96 km, could be attributed to the dissipation of inner eye-wall resulting in outer eye-wall circling the eye as occurred in case of super Typhoon Winnie 1997 [40]. There is less evidence available to support high rainfall inside the eye of TC due to a lack of literature available on the rainfall distribution pattern during an eye-wall replacement cycle. Rainfall distribution pattern during an Eye-wall replacement cycle based on few literature studies can be found in appendix D.

$$y = 0.6383x + 34.7867 \tag{5.1}$$

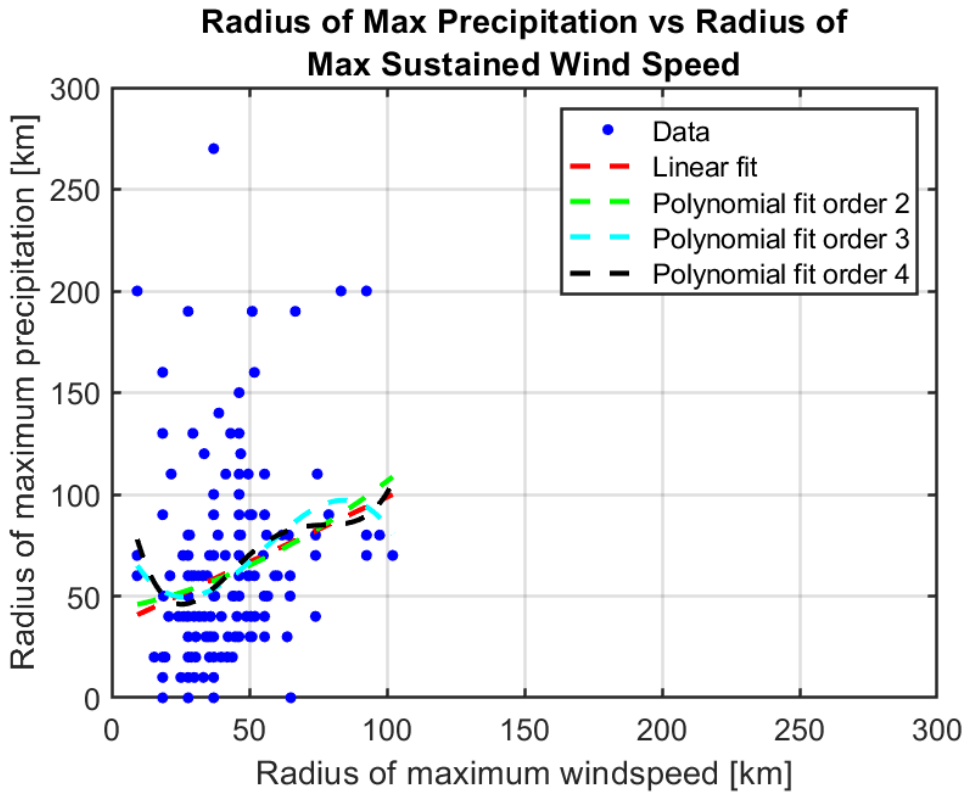


Figure 5.19: Radius of maximum sustained wind-speed vs radius of maximum precipitation

The Gaussian Model probability PDF is presented for the given data since the $R^2$ values are relatively low (fig. 5.20). The Gaussian model is considered as that is the most common distribution in climatology (Central Limit Theorem).The linear fit is drawn in magenta, and each point for the radius of maximum wind-speed with the highest chance of occurrence for the radius of maximum precipitation is plotted in red. The graph 5.20 suggest the linear fit, and the points of highest probability runs almost

with same slope and different Y intercept. The Y intercept value for linear fit it 34.7 km whereas for the Gaussian model it is 18.1 km. After the point where the radius of maximum wind-speed is greater than 60 km the probability curve behaves differently. This might be because of less availability of data for the extreme values. But this method appears to be a promising option with more data.

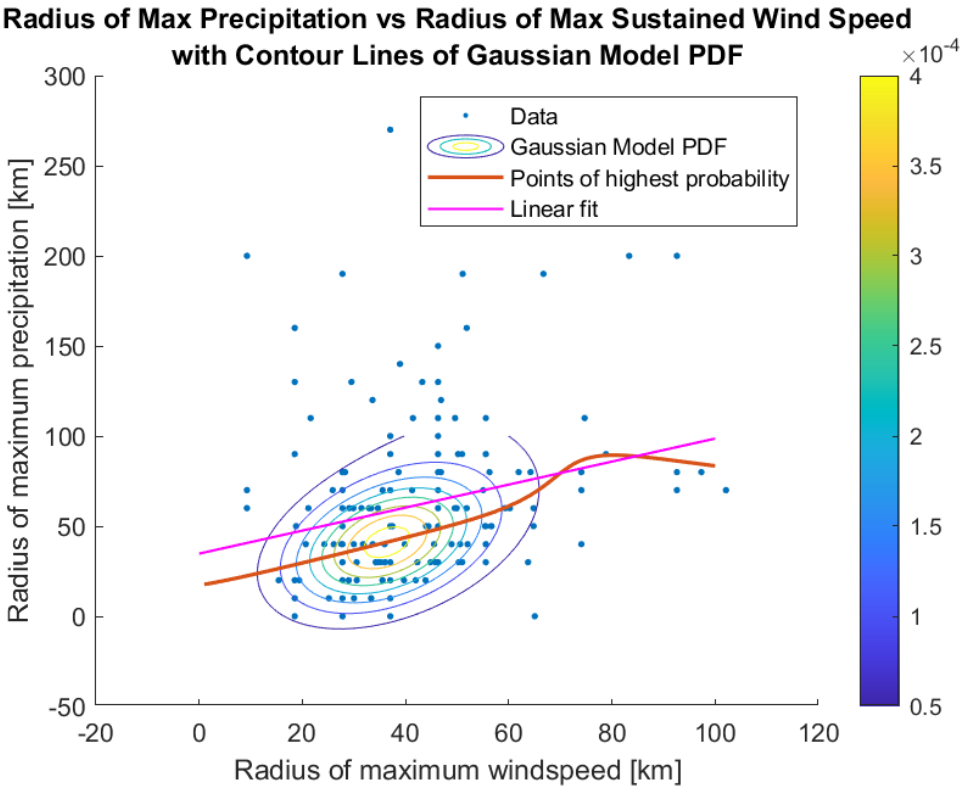


Figure 5.20: Radius of maximum sustained wind-speed vs radius of maximum precipitation with contour lines of Gaussian model PDF

In this study linear fit is considered to keep model simple. As there was less data available for radius of maximum wind-speed greater than 80km. So, linear fit appeared to be a less biased fit.

Based on the equation 5.1 the relation between radius of maximum wind-speed and radius of maximum precipitation, the BaCla Model was tested again for Matthew as it was the case where it was observed that most of the precipitation was extending quite in land whereas the model based precipitation was concentrated over the coast. The changes in Rmax values for precipitation increased the spread of rainfall and that almost compensated for the cumulative amount of rainfall as well (fig. 5.21d and table 5.5). The relation resulted in reduction in spread of rainfall when the radius of maximum wind-speed is more than 96 km which is visible in few time steps of Florence 2018 (fig. 5.21b and Bonnie 2016 table 5.4& 5.1). For Florence where the radius of maximum wind-speed is almost near to 100km the results are almost similar to that of BaCla model results (fig. 5.21a and table 5.6).

### 5.2.2. Fitting coefficient for cases where peak amount of rainfall is less than 2.8mm/hr

The case studies also suggested that when peak amount of rainfall is less than 2.8mm/hr, the BaCla model providing equal high amount of rainfall for all area inside the spiderweb is not suitable (fig. 5.21c and table 5.3).This was resulting in a very high amount of rainfall (table 5.3). So, method A (least square fitting section 2.2.2) of curve (fitting fig. 2.4) is tried for capturing peak amount of rainfall below 2.8mm/hr and the performance of the model is tested. The changes resulted in better capturing cumulative rainfall as visible in fig. 5.21c and table 5.3. These two changes in the parent BaCla model helped to improved the model a lot but still there were cases where the amount of rainfall was just a bit higher than 2.8mm/h and method D for curve fitting was implemented in adapted Holland wind profile resulting in high amount of cumulative precipitation specifically for low wind speed TC, for example in

case of Bonnie 2016 (fig. 5.21f table 5.1).

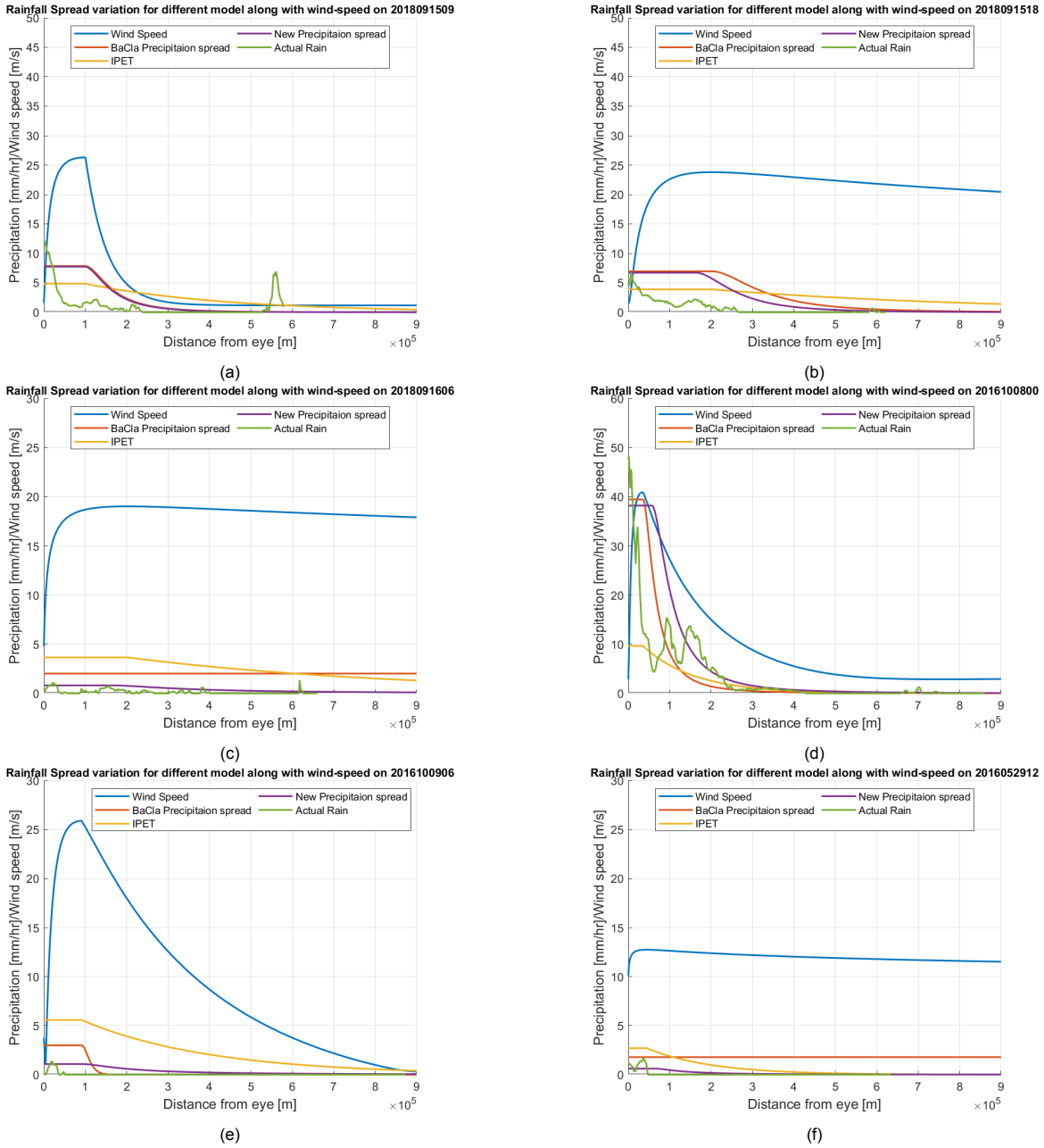


Figure 5.21: Radial Rainfall and wind-speed variation of different TCs for different percentile based on different models. **(a)** Florence 2018: Radial Rainfall and wind-speed variation for $50^{th}$ percentile **(b)** Florence 2018: Radial Rainfall and wind-speed variation for $50^{th}$ percentile **(c)** Florence 2018: Radial Rainfall and wind-speed variation for 5 percentile **(d)** Matthew 2016: Radial Rainfall and wind-speed variation for $95^{th}$ percentile **(e)** Matthew 2016: Radial Rainfall and wind-speed variation for 5 percentile **(f)** Bonnie 2016: Radial Rainfall and wind-speed variation for 5 percentile

### 5.2.3. Threshold 2.8mm/hr vs 5mm/hr

To prevent the high amount of rainfall for cases where peak amount of rainfall is just above 2.8 mm/hr, it is tested that if a threshold of 5mm/hr performs better than of 2.8mm/hr peak amount of rainfall as considered in case of method B (separate least square fitting for rainfall above and below 5mm/hr) but with method A(least square fitting). This was done instead of just following method B, as method A shows less or no rainfall for larger distances for low $pmax$ values contrary to B that shows higher amount of rainfall for larger distances (fitting fig. 2.4). This is one of the problem that this thesis is trying to address.

Table 5.1: An overview of the various modifications made to the BaCla model for Bonnie 2016 (Charleston)

| Bonnie 2016 (Charleston) | | | | | | | |
|---|---|---|---|---|---|---|---|
| Different model improvements | Symmetric pressure deficit model-based cumulative rainfall for different percentile per unit area ($mm/m^2$) | | | | | IPET ($mm/m^2$) | Actual ($mm/m^2$) |
| | 5% | 25% | 50% | 75% | 95% | | |
| Only precipitation Rmax changed | 148.47 | 153.40 | 254.12 | 428.35 | 863.19 | 198.08 | 56.26 |
| Instead of const. using method A fit for peak rainfall | 45.10 | 93.29 | 256.29 | 429.15 | 861.32 | | |
| Using method A fit for peak rainfall below 5mm/hr | 44.83 | 78.19 | 148.80 | 430.22 | 866.49 | | |
| All three changes together | 44.68 | 78.62 | 149.19 | 428.54 | 868.31 | | |
| Previous BaCla model | 149.31 | 163.54 | 259.36 | 429.03 | 865.53 | | |

Table 5.2: An overview of the various modifications made to the BaCla model for Matthew 2016 (Charleston)

| Matthew 2016 (Charleston) | | | | | | | |
|---|---|---|---|---|---|---|---|
| Different model improvements | Symmetric pressure deficit model-based cumulative rainfall for different percentile per unit area ($mm/m^2$) | | | | | IPET ($mm/m^2$) | Actual ($mm/m^2$) |
| | 5% | 25% | 50% | 75% | 95% | | |
| Only precipitation Rmax changed | 27.17 | 67.11 | 118.67 | 196.94 | 395.59 | 116.49 | 235.29 |
| Instead of const. using method A fit for peak rainfall | 16.29 | 44.01 | 74.69 | 126.58 | 260.12 | | |
| Using method A fit for peak rainfall below 5mm/hr | 15.88 | 41.12 | 74.27 | 126.43 | 259.43 | | |
| All three changes together | 24.05 | 69.23 | 119.18 | 190.94 | 392.84 | | |
| Previous BaCla model | 14.55 | 41.76 | 73.82 | 126.37 | 253.32 | | |

Table 5.3: An overview of the various modifications made to the BaCla model for Florence 2018 (Charleston)

| Florence 2018 (Charleston) | | | | | | | |
|---|---|---|---|---|---|---|---|
| Different model improvements | Symmetric pressure deficit model-based cumulative rainfall for different percentile per unit area ($mm/m^2$) | | | | | IPET ($mm/m^2$) | Actual ($mm/m^2$) |
| | 5% | 25% | 50% | 75% | 95% | | |
| Only precipitation Rmax changed | 97.34 | 186.41 | 316.73 | 510.63 | 1010.92 | 246.15 | 24.73 |
| Instead of const. using method A fit for peak rainfall | 39.05 | 188.41 | 305.18 | 487.88 | 966.36 | | |
| Using method A fit for peak rainfall below 5mm/hr | 45.62 | 95.84 | 304.12 | 485.38 | 942.67 | | |
| All three changes together | 49.90 | 106.28 | 312.34 | 513.55 | 992.97 | | |
| Previous BaCla model | 96.29 | 188.84 | 302.77 | 490.31 | 951.64 | | |

Table 5.4: An overview of the various modifications made to the BaCla model for Bonnie 2016 (N-S Carolina)

| Bonnie 2016 (N-S Carolina) | | | | | | | |
|---|---|---|---|---|---|---|---|
| Different model improvements | Symmetric pressure deficit model-based cumulative rainfall for different percentile per unit area ($mm/m^2$) | | | | | IPET ($mm/m^2$) | Actual ($mm/m^2$) |
| | 5% | 25% | 50% | 75% | 95% | | |
| Only precipitation Rmax changed | 139.49 | 116.08 | 153.68 | 286.40 | 608.58 | 173.76 | 50.04 |
| Instead of const. using method A fit for peak rainfall | 34.57 | 55.07 | 173.76 | 311.39 | 648.24 | | |
| Using method A fit for peak rainfall below 5mm/hr | 34.41 | 65.32 | 117.50 | 313.31 | 655.99 | | |
| All three changes together | 33.28 | 63.84 | 109.32 | 286.63 | 613.20 | | |
| Previous BaCla model | 140.26 | 127.99 | 176.09 | 311.50 | 654.18 | | |

Table 5.5: An overview of the various modifications made to the BaCla model for Matthew 2016 (N-S Carolina)

| Matthew 2016 (N-S Carolina) | | | | | | | |
|---|---|---|---|---|---|---|---|
| Different model improvements | Symmetric pressure deficit model-based cumulative rainfall for different percentile per unit area ($mm/m^2$) | | | | | IPET ($mm/m^2$) | Actual ($mm/m^2$) |
| | 5% | 25% | 50% | 75% | 95% | | |
| Only precipitation Rmax changed | 7.61 | 26.11 | 50.46 | 87.80 | 184.04 | 68.96 | 197.32 |
| Instead of const. using method A fit for peak rainfall | 3.90 | 13.92 | 27.22 | 48.06 | 102.71 | | |
| Using method A fit for peak rainfall below 5mm/hr | 8.76 | 13.29 | 26.94 | 48.38 | 102.23 | | |
| All three changes together | 14.47 | 26.66 | 50.05 | 84.84 | 182.64 | | |
| Previous BaCla model | 3.39 | 13.46 | 26.63 | 48.45 | 103.99 | | |

Table 5.6: An overview of the various modifications made to the BaCla model for Florence 2018 (N-S Carolina)

| Florence 2018 (N-S Carolina) | | | | | | | |
|---|---|---|---|---|---|---|---|
| Different model improvements | Symmetric pressure deficit model-based cumulative rainfall for different percentile per unit area ($mm/m^2$) | | | | | IPET ($mm/m^2$) | Actual ($mm/m^2$) |
| | 5% | 25% | 50% | 75% | 95% | | |
| Only precipitation Rmax changed | 115.26 | 183.33 | 315.02 | 513.50 | 1020.39 | 255.61 | 197.74 |
| Instead of const. using method A fit for peak rainfall | 45.82 | 183.57 | 304.39 | 490.43 | 978.10 | | |
| Using method A fit for peak rainfall below 5mm/hr | 49.69 | 101.22 | 303.11 | 488.37 | 953.91 | | |
| All three changes together | 54.11 | 115.75 | 311.36 | 515.43 | 1003.30 | | |
| Previous BaCla model | 109.58 | 183.06 | 302.13 | 492.30 | 963.08 | | |

Making change in threshold from 2.8mm/h to 5mm/h resulted in better capturing of cumulative rainfall for Bonnie 2016 (fig. 5.21f) and Matthew 2016 (fig.5.21e, table 5.1 & 5.2). Combining these three changes together is expected to result in an improved model that should be able to capture the cumulative amount of rainfall for all three previously consider case studies along with three new randomly selected TCs. The results of these three changes together and individually are discussed in the tables below along with old BaCla model, IPET and observed (StageIV) results for calibration TCs.

## 5.3. Validation: Previously considered TC

After making the above mentioned three changes we obtain a new improved model. The new model will be refereed as BaClHa in the coming sections. In this section, the BaClHa model's performance is compared to the BaCla model.

### 5.3.1. Florence 2018

#### N-S Carolina

For Florence 2018 as in the BaCla model, the BaClHa model is able to capture cumulative precipitation (fig.5.23) but now the spread of precipitation is better captured (fig.5.22). For N-S Carolina the BaCla $pdef$ symmetric mode model predicts 183.06 $mm/m^2$ and 302.13 $mm/m^2$ of precipitation for $25^{th}$ and $50^{th}$ percentile. The BaClHa $pdef$ symmetric mode model on the other hand predicts 115.75 $mm/m^2$ and 303.11 $mm/m^2$ of precipitation for $25^{th}$ and $50^{th}$ percentile (table:5.6). The actual amount of precipitation based on StageIV data is 197.74 $mm/m^2$. So, both model are able to capture cumulative rainfall but the spread in range of rainfall is larger in BaClHa. This is because the BaClHa model has reduced the high amount of precipitation that BaCla showed larger distance from the eye of TC. The fig. 5.23 shows that the $95^{th}$ percentile cumulative rainfall per unit area in BaClHa model is slightly higher as compared to BaCla. This might-be because of increase in spread of rainfall for the cases where the radius of maximum wind-speed is less than 96km/hr as discussed in section 5.2.

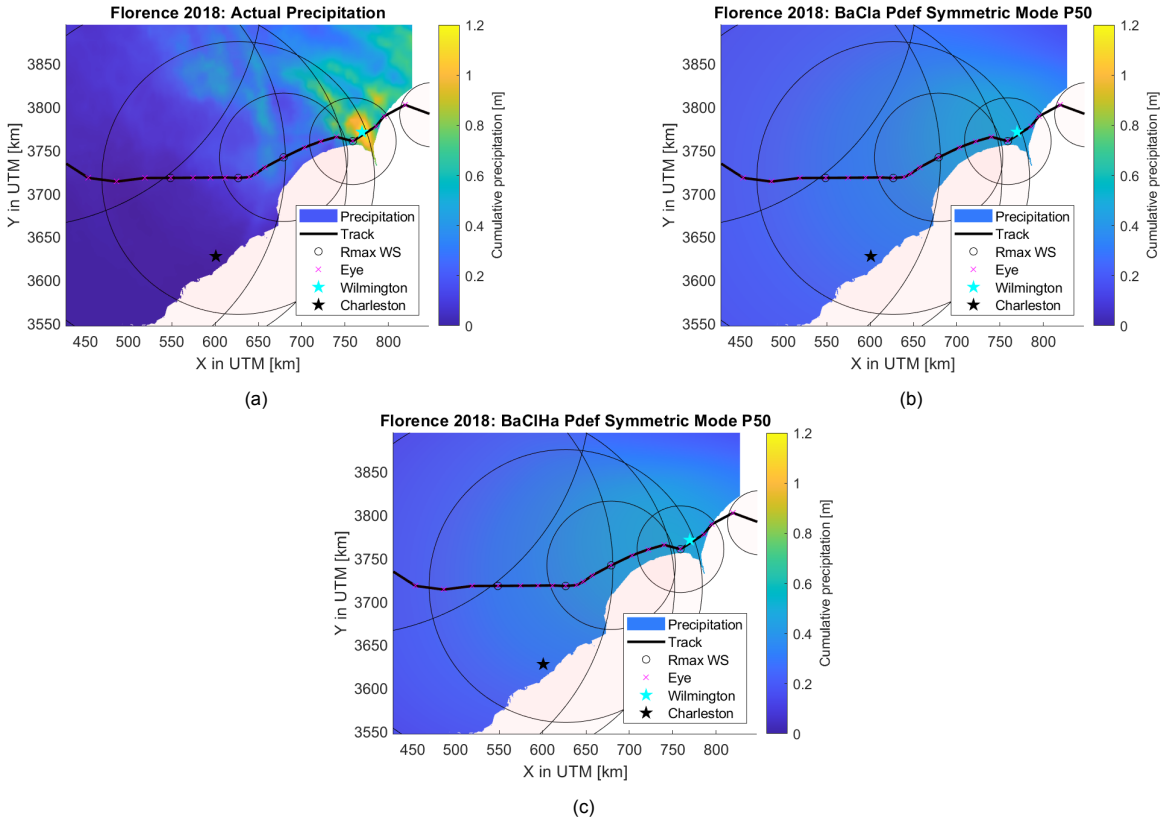


Figure 5.22: Florence 2018: Cumulative precipitation at selected regions of North South Carolina **(a)** Observed (Stage IV) cumulative precipitation **(b)** BaCla model cumulative precipitation for $50^{th}$ percentile **(c)** Improved model (BaClHa) cumulative precipitation for $50^{th}$ percentile

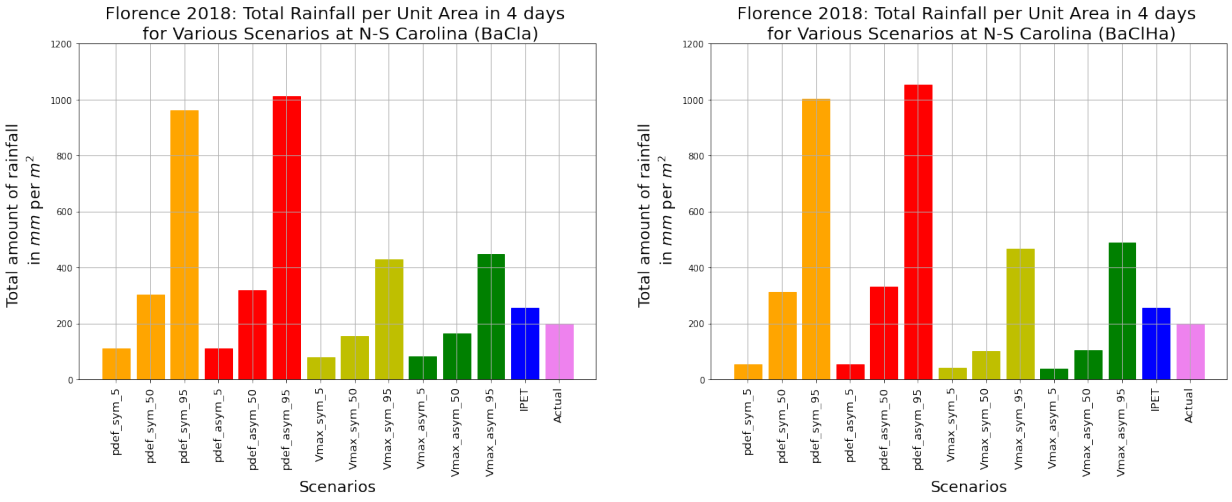


Figure 5.23: Florence 2018: Cumulative precipitation for different model at selected regions of N-S Carolina **(a)** BaCla model results **(b)** Improved model (BaClHa) results

## Charleston

The figure 5.24 shows the BaClHa model does help in capturing the spread of rainfall but the reduction is still gradual not as sharp as it is in StageIV based observations. The BaClHa model is not able to effectively capture the cumulative amount of rainfall at Charleston (fig. 5.25) but has improved the values as compared to BaCla. The BaCla $pdef$ symmetric mode model predicts 96.29 $mm/m^2$ of precipitation whereas the BaClHa model suggest 49.90 $mm/m^2$ of precipitation for 5 percentile (table:5.3).The actual amount of precipitation based on StageIV data is 24.73 $mm/m^2$.

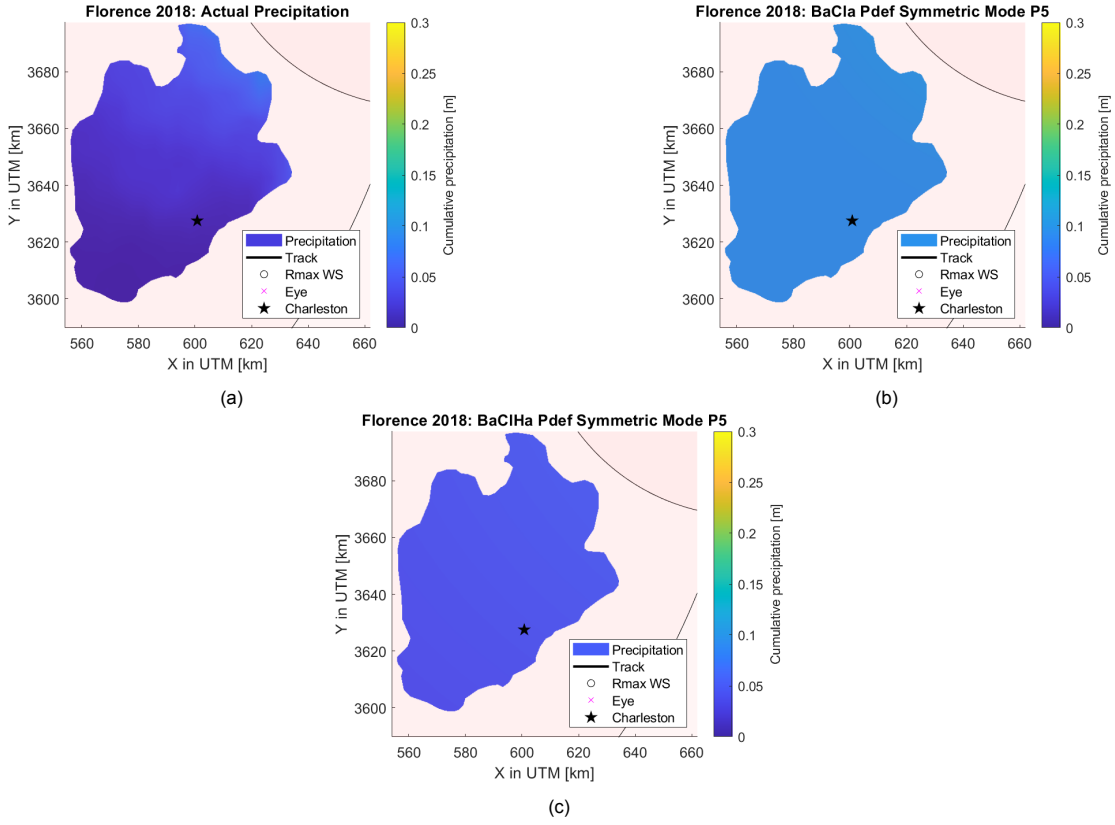


Figure 5.24: Florence 2018: Cumulative precipitation at Charleston **(a)** Observed (Stage IV) cumulative precipitation **(b)** BaCla model cumulative precipitation for 5 percentile **(c)** Improved model (BaClHa) cumulative precipitation for 5 percentile

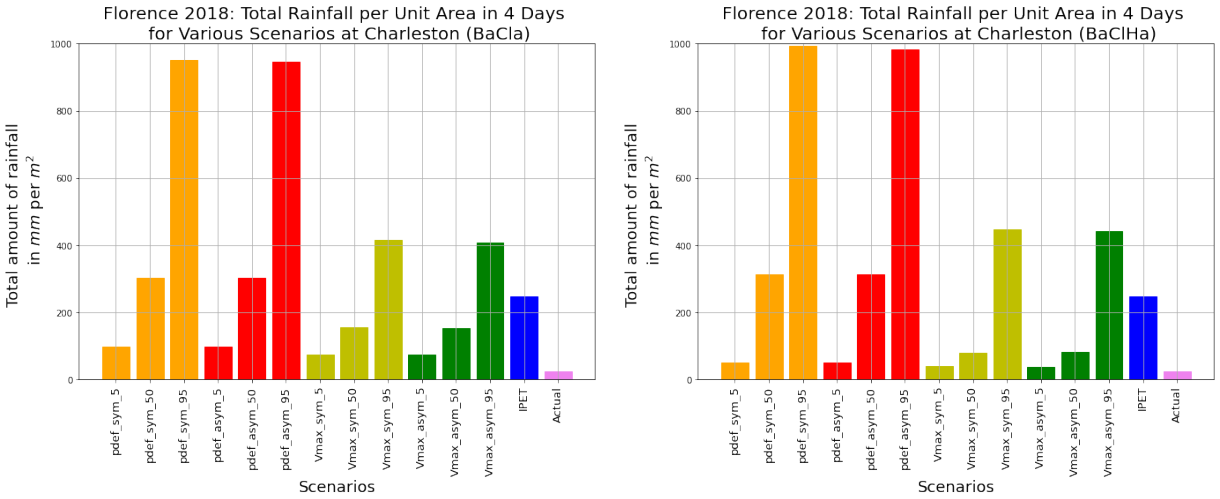


Figure 5.25: Florence 2018: Cumulative precipitation for different model at Charleston Carolina **(a)** BaCla model results **(b)** Improved model (BaClHa) results

## Wilmington

The BaClHa model is able to completely capture the cumulative amount of rainfall at Wilmington (fig. 5.27) but has slightly improved the results as compared to BaCla. The BaClHa model predicts sightly higher amount of rainfall per unit area $mm/m^2$ due to which $vmax$ based models are able to capture the actual cumulative rainfall. The figure 5.26 shows the BaClHa model is not that effective in capturing the peak amount of rainfall and exact spatial distribution of rainfall as observed based on StageIV data. This is because the symmetric model is being considered and the model considers the radial mean amount of rainfall to capture the peak amount of rainfall as discussed in earlier.

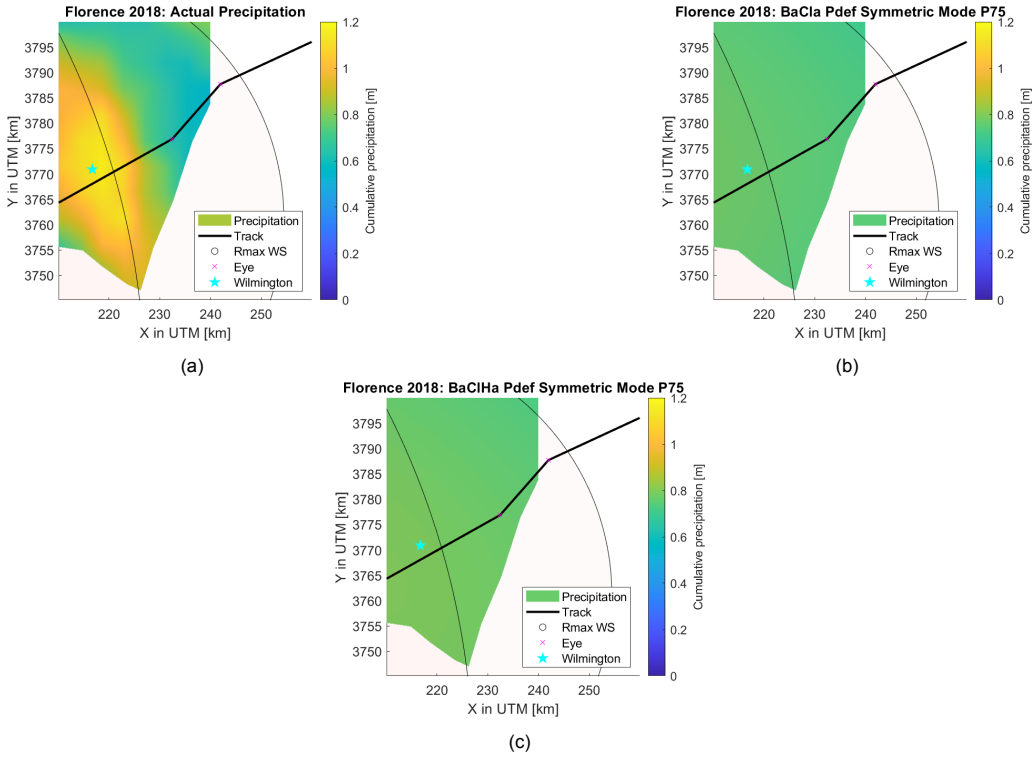


Figure 5.26: Florence 2018: Cumulative precipitation at Wilmington **(a)** Observed (Stage IV) cumulative precipitation **(b)** BaCla model cumulative precipitation for 75 percentile **(c)** Improved model (BaClHa) cumulative precipitation for 75 percentile

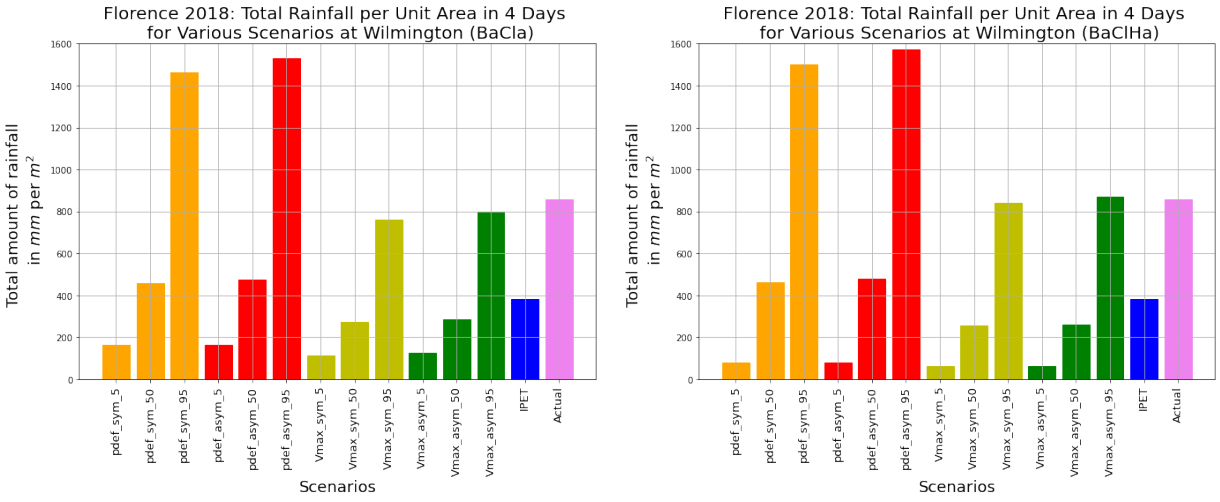


(a) (b)

Figure 5.27: Florence 2018: Cumulative precipitation for different model at Wilmington Carolina **(a)** BaCla model results **(b)** Improved model (BaClHa) results

## 5.3.2. Matthew 2016

### N-S Carolina

For Matthew 2016, contrary to BaCla model, the BaClHa model is almost able to capture cumulative precipitation (fig.5.28) and the spread of precipitation is better captured (fig.5.29). For N-S Carolina the BaCla $pdef$ symmetric mode model predicts 103.99 $mm/m^2$ of precipitation for $95^{th}$ percentile. The BaClHa $pdef$ symmetric mode model on the other hand predicts 182.64 $mm/m^2$ of precipitation for $95^{th}$ percentile (table:5.5). The actual amount of precipitation based on StageIV data is 197.34 $mm/m^2$. The BaClHa model is able to increase the spread of rainfall more inland but still is not effective in capturing actual spatial distribution. There is a region of less rainfall near Charleston based on StageIV data but the model is not able to capture that along with in-land rainfall to the west of Wilmington (fig.5.29). This is because the symmetrical model is considered and the BaClHa model is not effective in capturing the asymmetrical rainfall distribution.

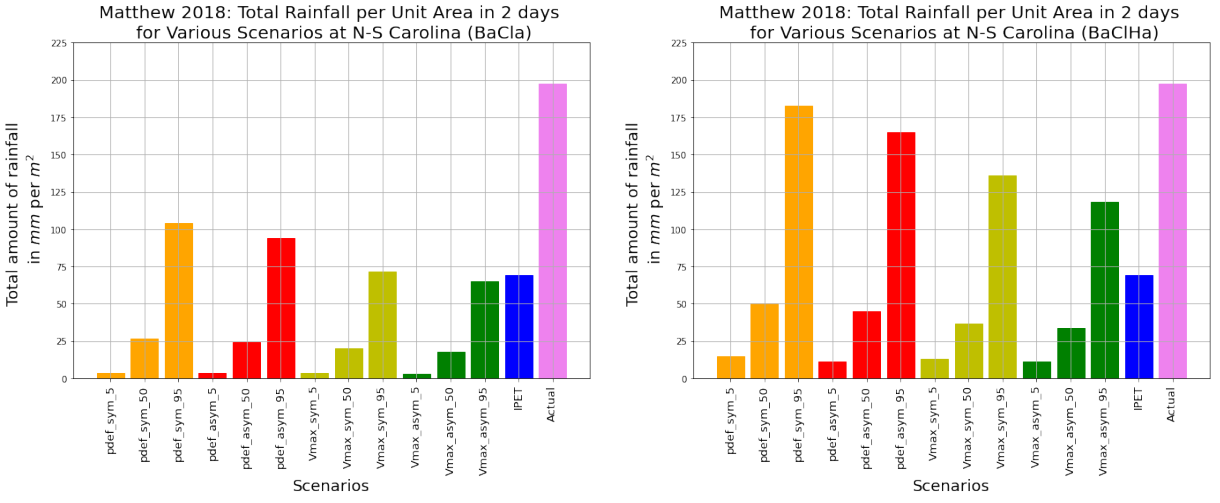


(a) (b)

Figure 5.28: Matthew 2016: Cumulative precipitation for different model at selected regions of N-S Carolina **(a)** BaCla model results **(b)** Improved model (BaClHa) results

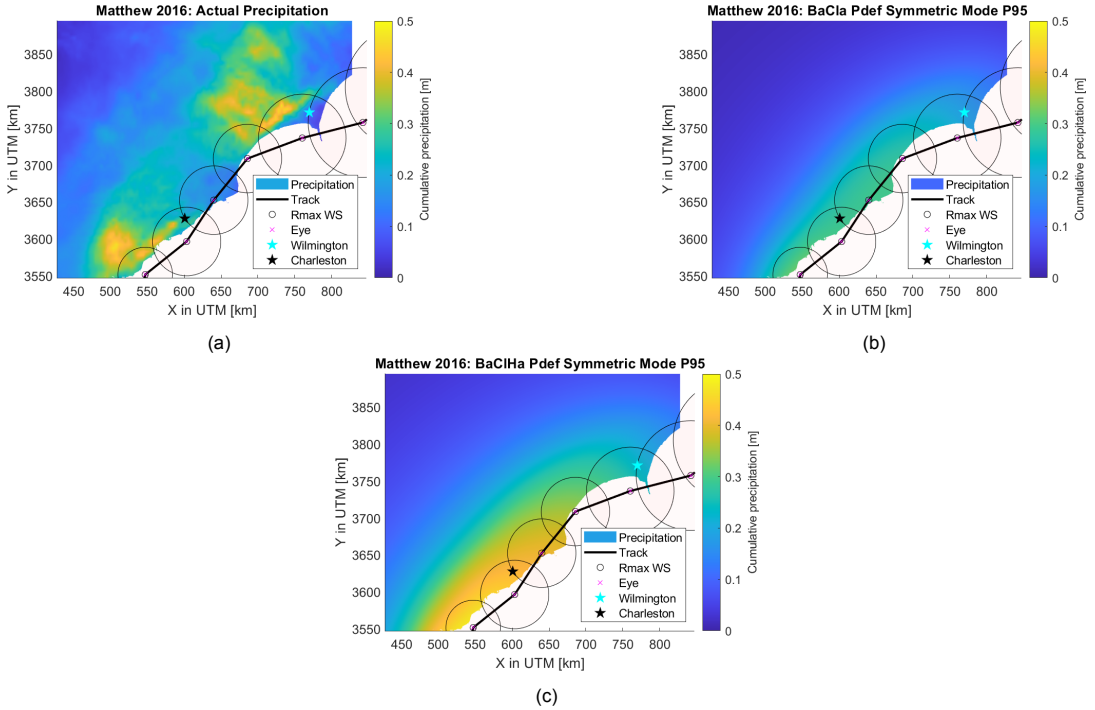


Figure 5.29: Matthew 2016: Cumulative precipitation at selected regions of North South Carolina **(a)** Observed (Stage IV) cumulative precipitation **(b)** BaCla model cumulative precipitation for $95^{th}$ percentile **(c)** Improved model (BaClHa) cumulative precipitation for $95^{th}$ percentile

## Charleston

Figure 5.31 shows the BaClHa model helps in capturing the spread of rainfall at a lower percentile but the reduction in rainfall pattern is gradual and not as sharp as it is in StageIV based observations. The BaClHa model is able to completely capture the cumulative amount of rainfall at Charleston (fig. 5.30). The BaCla $pdef$ symmetric mode model predicts 126.37 $mm/m^2$ and 253.32 $mm/m^2$ of precipitation whereas the BaClHa model suggest 190.94 $mm/m^2$ and 392.84 $mm/m^2$ of precipitation for 75 and $95^{th}$ percentile (table:5.2).The actual amount of precipitation based on StageIV data is 235.29 $mm/m^2$.

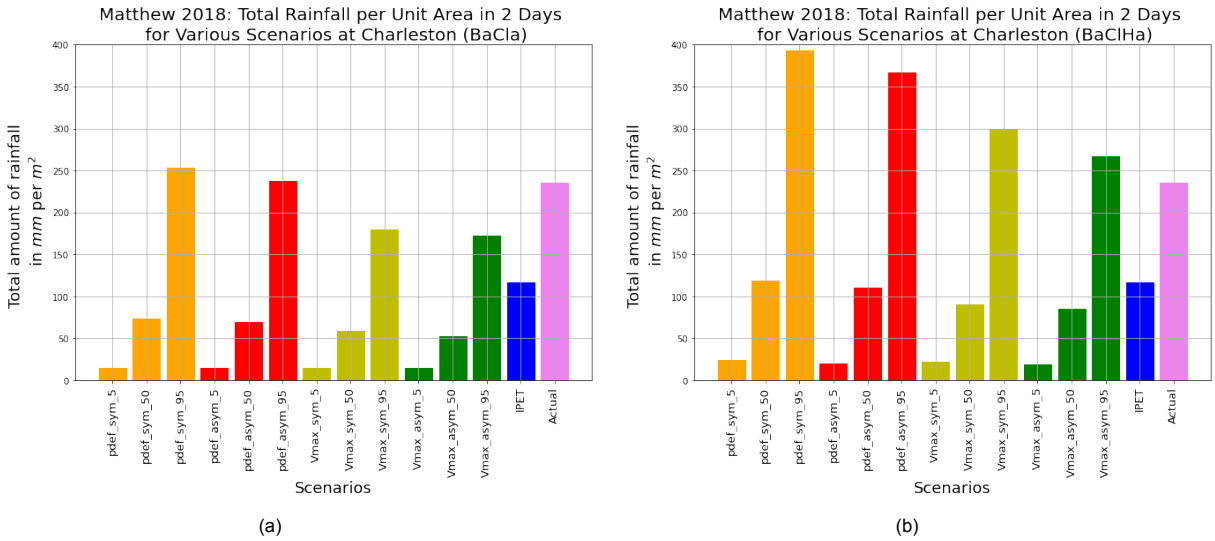


Figure 5.30: Matthew 2016: Cumulative precipitation for different model at Charleston **(a)** BaCla model results **(b)** Improved model (BaClHa) results

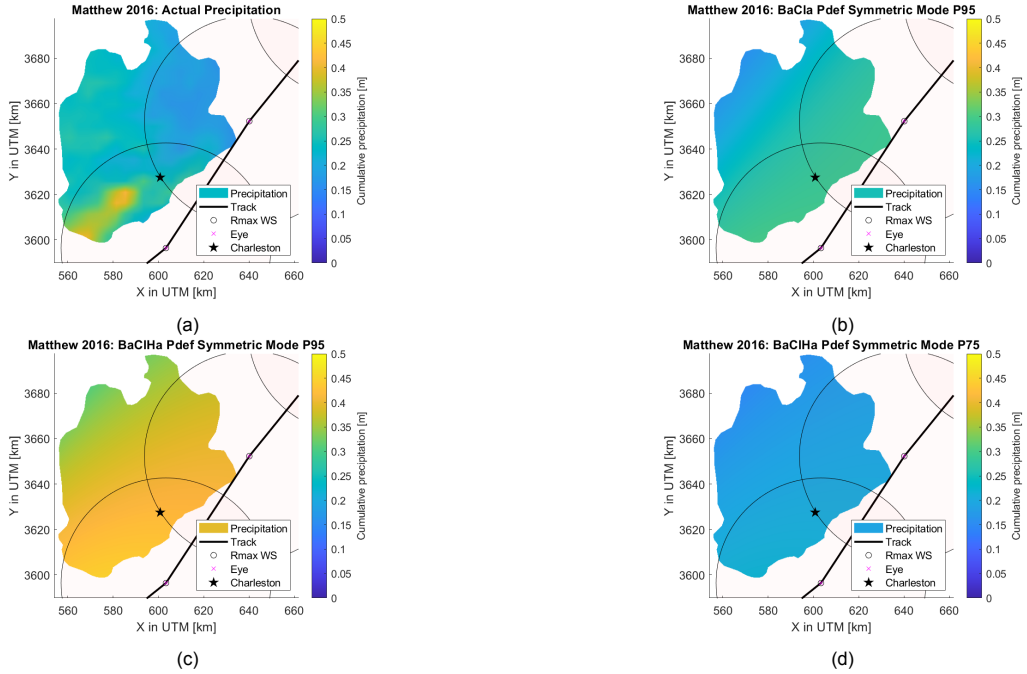


Figure 5.31: Matthew 2016: Cumulative precipitation for different model at Charleston **(a)** Observed (Stage IV) cumulative precipitation **(b)** BaCla model cumulative precipitation for $95^{th}$ percentile **(c)** Improved model (BaClHa) cumulative precipitation for $95^{th}$ percentile **(d)** Improved model (BaClHa) cumulative precipitation for 75 percentile

### 5.3.3. Bonnie 2016

#### N-S Carolina

For Bonnie 2016, contrary to BaCla model, the BaClHa model is able to capture cumulative precipitation (fig.5.32) and now the spread of precipitation is better captured (fig.5.33). For N-S Carolina the BaCla $pdef$ symmetric mode model predicts 140.26 $mm/m^2$ of precipitation for the $5^{th}$ percentile. The BaClHa $pdef$ symmetric mode model on the other hand predicts 33.28 $mm/m^2$ of precipitation for the $5^{th}$ percentile (table:5.4). The actual amount of precipitation based on StageIV data is 50.04 $mm/m^2$. The BaClHa model is not able to exactly show the consolidated patches of high cumulative rainfall per unit area but provides a good general overview (fig.5.33). This is because the symmetrical model is considered and the BaClHa model is not effective in capturing the asymmetrical rainfall distribution. The cumulative amount of rainfall per unit area has also reduced in BaClHa model as compared to BaCla as there is no over estimation of rainfall for low peak amount of rainfall.

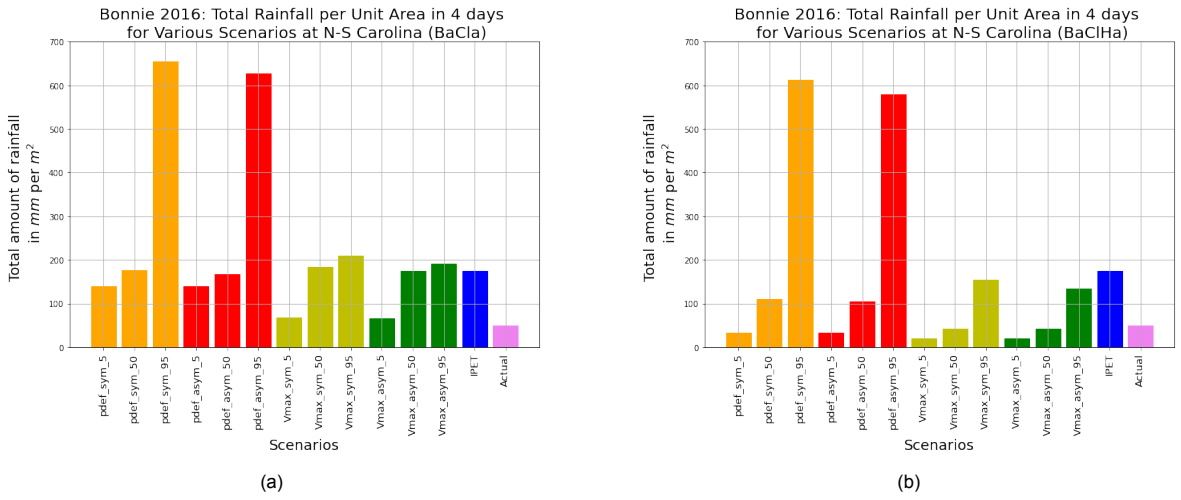


Figure 5.32: Bonnie 2016: Cumulative precipitation for different model at selected regions of N-S Carolina **(a)** BaCla model results **(b)** Improved model (BaClHa) results

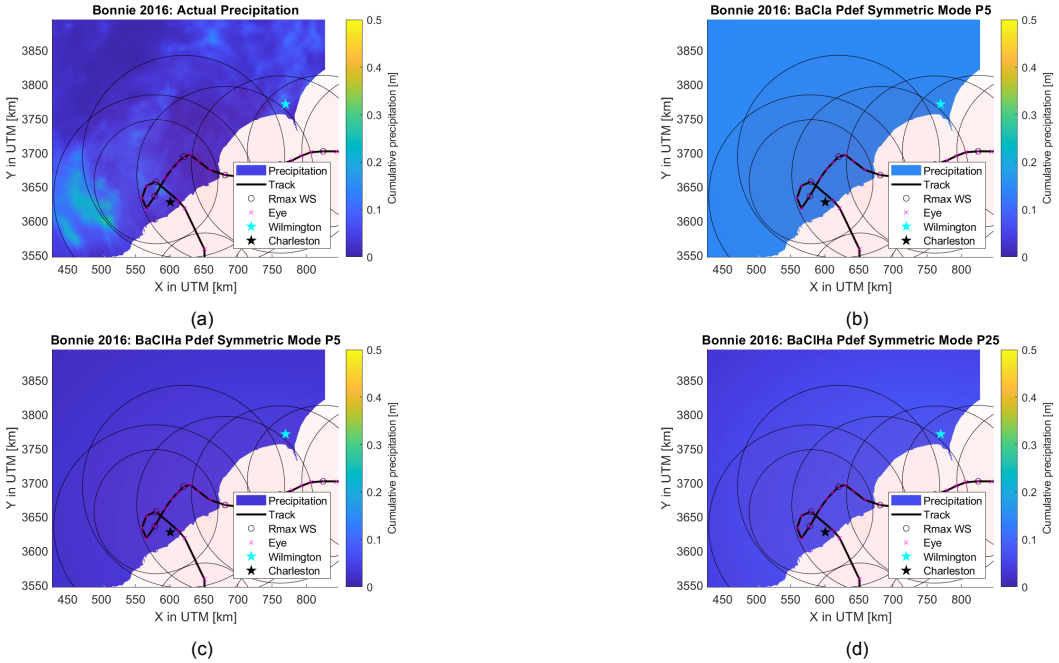


Figure 5.33: Bonnie 2016: Cumulative precipitation at selected regions of North South Carolina **(a)** Observed (Stage IV) cumulative precipitation **(b)** BaCla model cumulative precipitation for 5 percentile **(c)** Improved model (BaClHa) cumulative precipitation for 5 percentile **(d)** Improved model (BaClHa) cumulative precipitation for 25 percentile

## Charleston

The figure 5.35 shows that the BaClHa model is able to completely capture the cumulative amount of rainfall at Charleston (fig. 5.34) contrary to over-estimations by BaCla model. The BaClHa model is not able to exactly show the consolidated patches of high cumulative rainfall per unit area but provides a good general overview (fig.5.35). The BaCla $pdef$ symmetric mode model predicts 149.31 $mm/m^2$ of precipitation whereas the BaClHa model suggest 44.68 $mm/m^2$ of precipitation for 5 percentile (table:5.1).The actual amount of precipitation based on StageIV data is 56.26 $mm/m^2$.

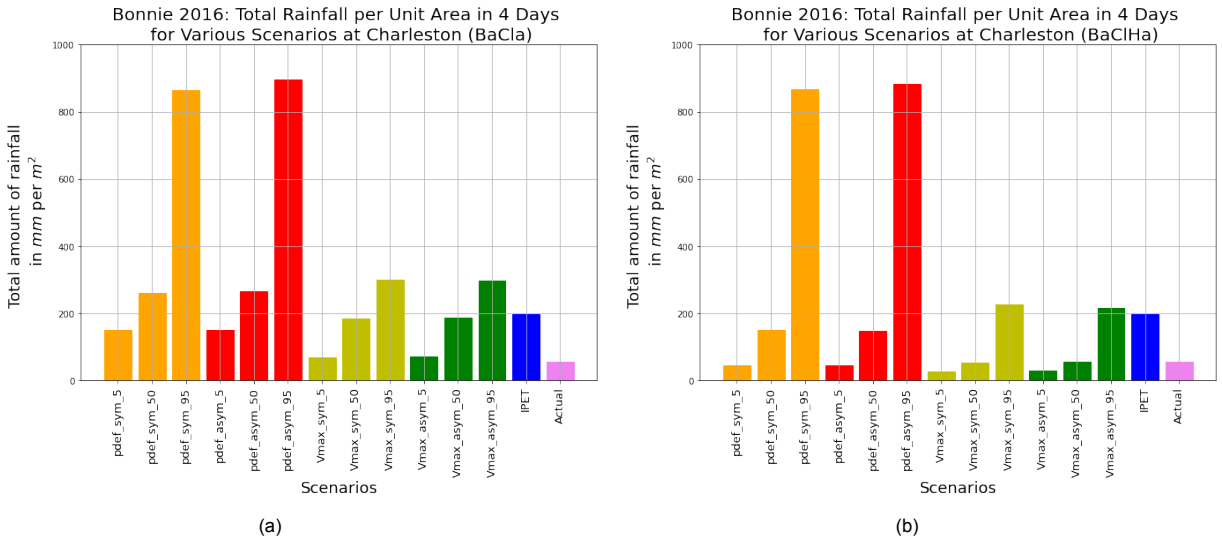


Figure 5.34: Bonnie 2016: Cumulative precipitation for different model at Charleston **(a)** BaCla model results **(b)** Improved model (BaClHa) results

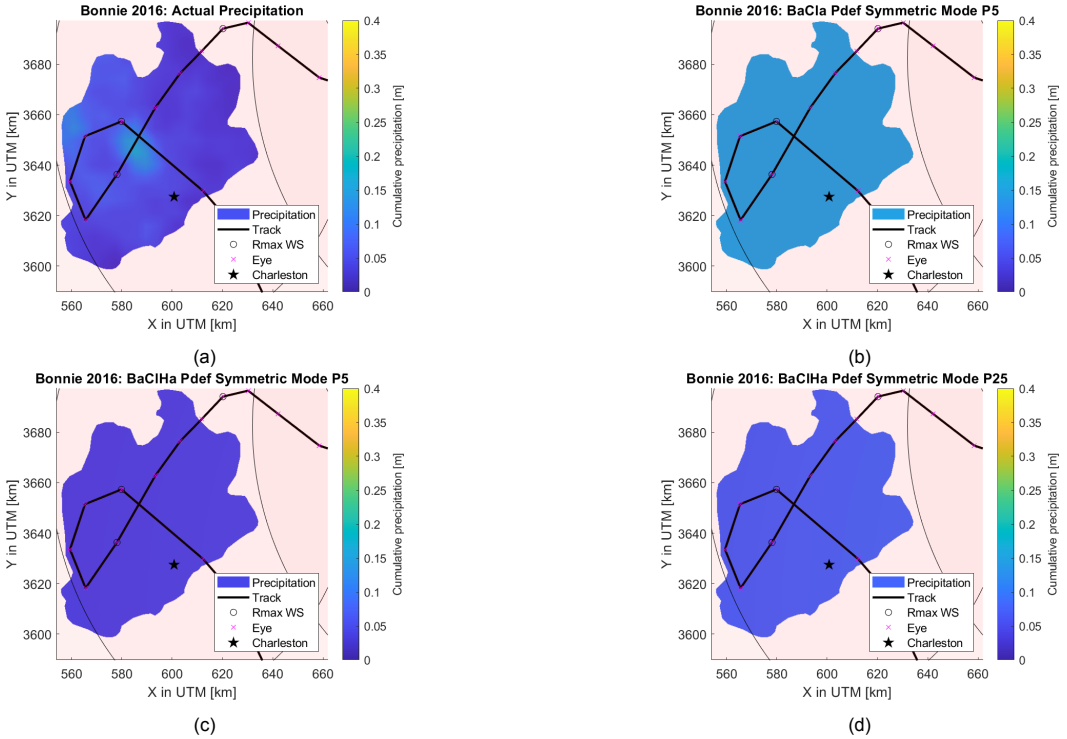


Figure 5.35: Bonnie 2016: Cumulative precipitation for different model at Charleston **(a)** Observed (Stage IV) cumulative precipitation **(b)** BaCla model cumulative precipitation for 5 percentile **(c)** Improved model (BaClHa) cumulative precipitation for 5 percentile **(d)** Improved model (BaClHa) cumulative precipitation for 25 percentile

It must be noted that the peak amount of rainfall is not captured as the model still considers the radial mean amount of rainfall while training as well as predicting the amount of rainfall.

## 5.4. Validation over other TC

To further evaluate the effectiveness of the improved model three other tropical cyclones Alberto 2006, Hermine 2016 and Charley 2004 are selected. They have different characteristics and pass through the same area of interest. The cumulative amount of rainfall and spread of rainfall are compared. In section both BaCla and BaClHa model is compared for $pdef$ symmetric mode.

### 5.4.1. Alberto 2006

#### N-S Carolina

Alberto 2006, had low wind speed and almost evenly distributed rainfall in major portions of N-S Carolina. For Alberto 2006, contrary to BaCla model, the BaClHa model is able to better capture cumulative precipitation for different percentiles (fig.5.36). The figure 5.37 shows that the BaCla $pdef$ symmetric mode model both $5^{th}$ and $50^{th}$ percentile are having almost the same cumulative rainfall per unit area. The BaCla $pdef$ asymmetric mode model for the $95^{th}$ percentile has lesser cumulative rainfall per unit area as compared to $5^{th}$ and $50^{th}$ percentile. All these parameter are improved in BaClHa model along with capturing the spread of rainfall. For N-S Carolina the BaCla $pdef$ symmetric mode model predicts around 80 $mm/m^2$ and 85 $mm/m^2$ of precipitation for $5^{th}$ and $50^{th}$ percentile. The BaClHa $pdef$ symmetric mode model on the other hand predicts around 20 $mm/m^2$ and 70 $mm/m^2$ of precipitation for $5^{th}$ and $50^{th}$ percentile (fig. 5.37). The actual amount of precipitation based on StageIV data is around 60 $mm/m^2$. The BaClHa model is not able to exactly show the consolidated patches of high cumulative rainfall per unit area but provides a good general overview (fig.5.36). The cumulative amount of rainfall per unit area is reduced in BaClHa model as compared to BaCla as there is no over estimation of rainfall for low peak amount of rainfall.

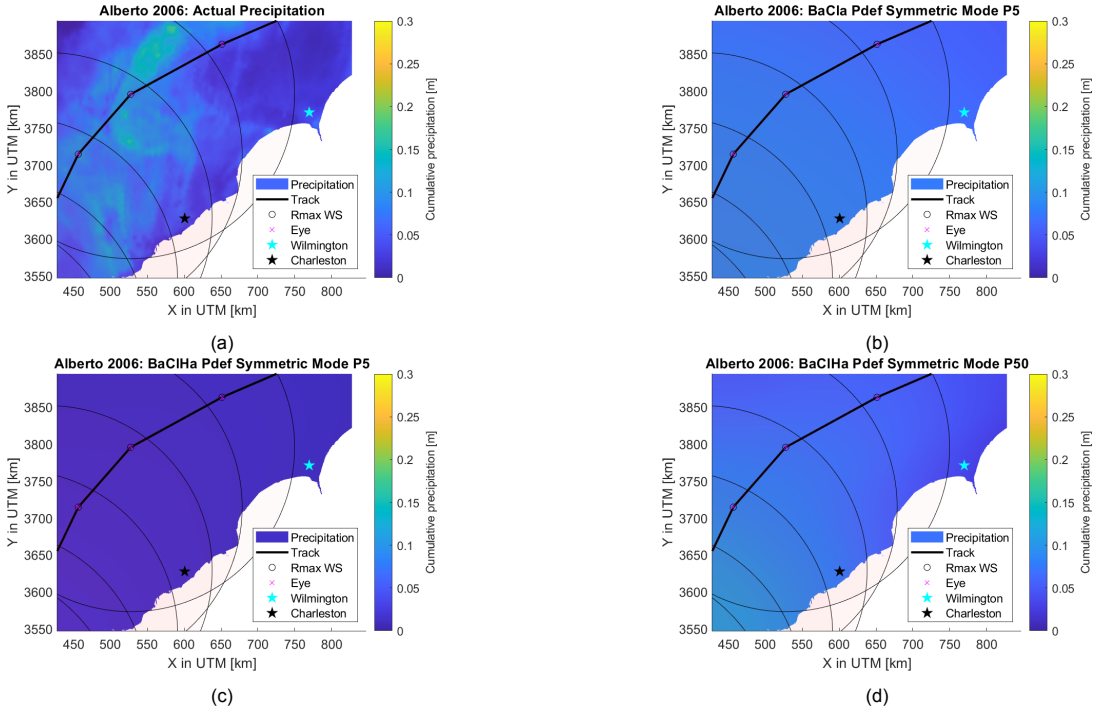


Figure 5.36: Alberto 2006: Cumulative precipitation at selected regions of North South Carolina **(a)** Observed (Stage IV) cumulative precipitation **(b)** BaCla model cumulative precipitation for $5^{th}$ percentile **(c)** Improved model (BaClHa) cumulative precipitation for 5 percentile **(d)** Improved model (BaClHa) cumulative precipitation for $50^{th}$ percentile

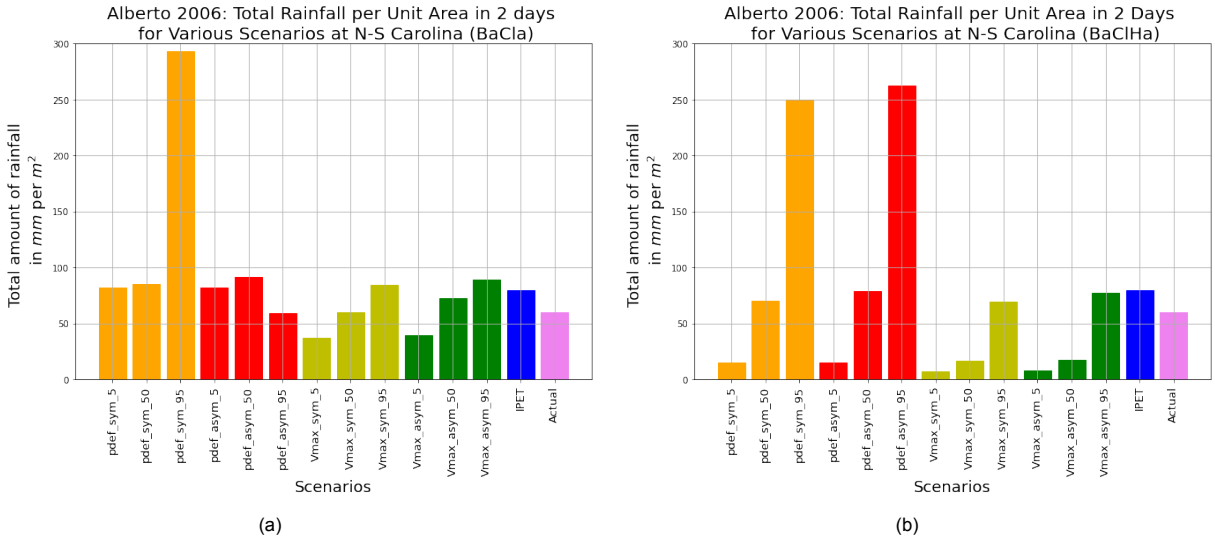


Figure 5.37: Alberto 2006: Cumulative precipitation for different model at selected regions of N-S Carolina **(a)** BaCla model results **(b)** Improved model (BaClHa) results

## Charleston

The figure 5.39 shows that the BaClHa model is able to completely capture the cumulative amount of rainfall at Charleston contrary to overestimation by BaCla model. The BaClHa model is not able to show the exact consolidated patches of high cumulative rainfall per unit area but provides a good general overview (fig.5.38). The inconsistencies in cumulative amount of rainfall per unit area is also improved. The BaCla $pdef$ symmetric mode model predicts around 100 $mm/m^2$ and 95 $mm/m^2$ of precipitation whereas the BaClHa model suggest 20 $mm/m^2$ and 80 $mm/m^2$ of precipitation for $5^{th}$ and $50^{th}$ percentile (fig. 5.39).The actual amount of precipitation based on StageIV data is around 45 $mm/m^2$.

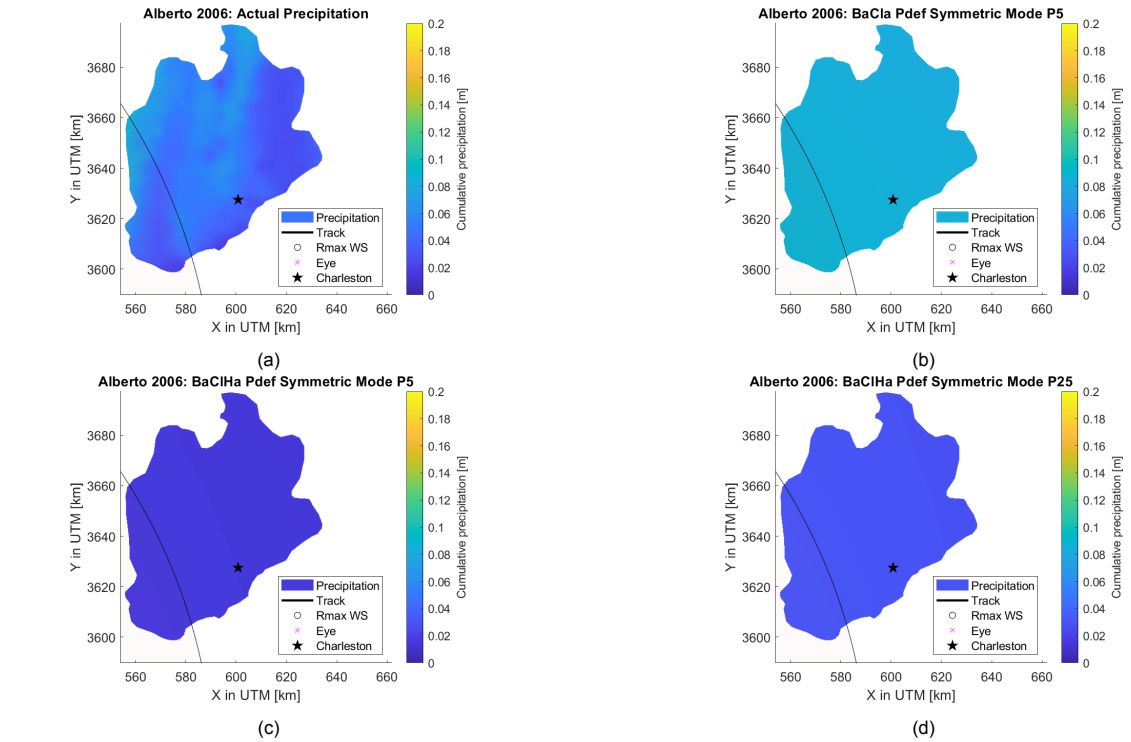


Figure 5.38: Alberto 2006: Cumulative precipitation for different model at Charleston **(a)** Observed (Stage IV) cumulative precipitation **(b)** BaCla model cumulative precipitation for 5 percentile **(c)** Improved model (BaClHa) cumulative precipitation for 5 percentile **(d)** Improved model (BaClHa) cumulative precipitation for 25 percentile

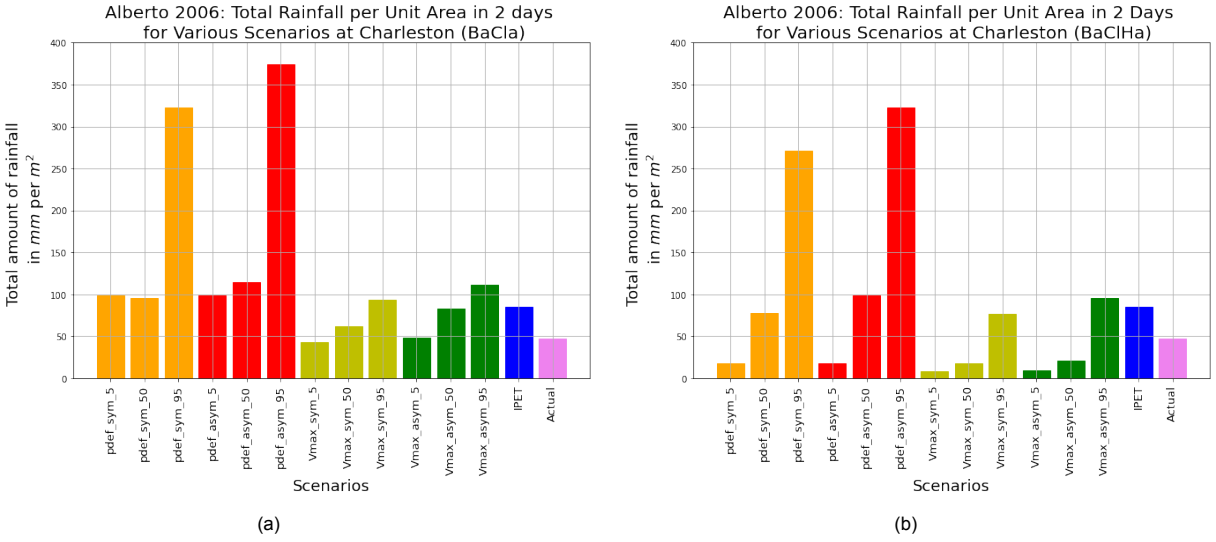


Figure 5.39: Alberto 2006: Cumulative precipitation for different model at Charleston **(a)** BaCla model results **(b)** Improved model (BaClHa) results

### 5.4.2. Charley 2004

N-S Carolina

Charley 2004, was a hurricane of category 1 before it made second landfall in South Carolina and gradually became Tropical Storm afterwards. It shows 2 bands of rainfall (fig. 5.40), one nearby its track and the other more inland. The rainfall near the track is well captured by $50^{th}$ percentile $pdef$ symmetric by both BaCla and BaClHa model but the second band of in-land rainfall is not captured at all. The reason for the same are as follows. Primarily our model is based on adapted Holland wind profile

that just captures 1 peak amount of rainfall and then gradually reduces and secondly these rainfall might be because of topographic effects (fig. 4.3) that our model does not takes into account [8],[28]. The effects of three changes introduced in BaClHa model can clearly be seen here. The fig. 5.40 and fig. 5.41 shows the BaCla model is over-estimates rainfall for $5^{th}$ percentile which is improved in BaClHa model. The BaClHa model shows higher amount of rainfall for $95^{th}$ percentile. This is because of the change in relation between radius of maximum wind-speed and radius of maximum precipitation.For N-S Carolina the BaCla $pdef$ symmetric mode model predicts around 42 $mm/m^2$ and 15 $mm/m^2$ of precipitation for $5^{th}$ and $50^{th}$ percentile respectively. The BaClHa $pdef$ symmetric mode model on the other hand predicts around 8 $mm/m^2$ and 20 $mm/m^2$ of precipitation for $5^{th}$ and $50^{th}$ percentile (fig. 5.41). The actual amount of precipitation based on StageIV data is around 17 $mm/m^2$.

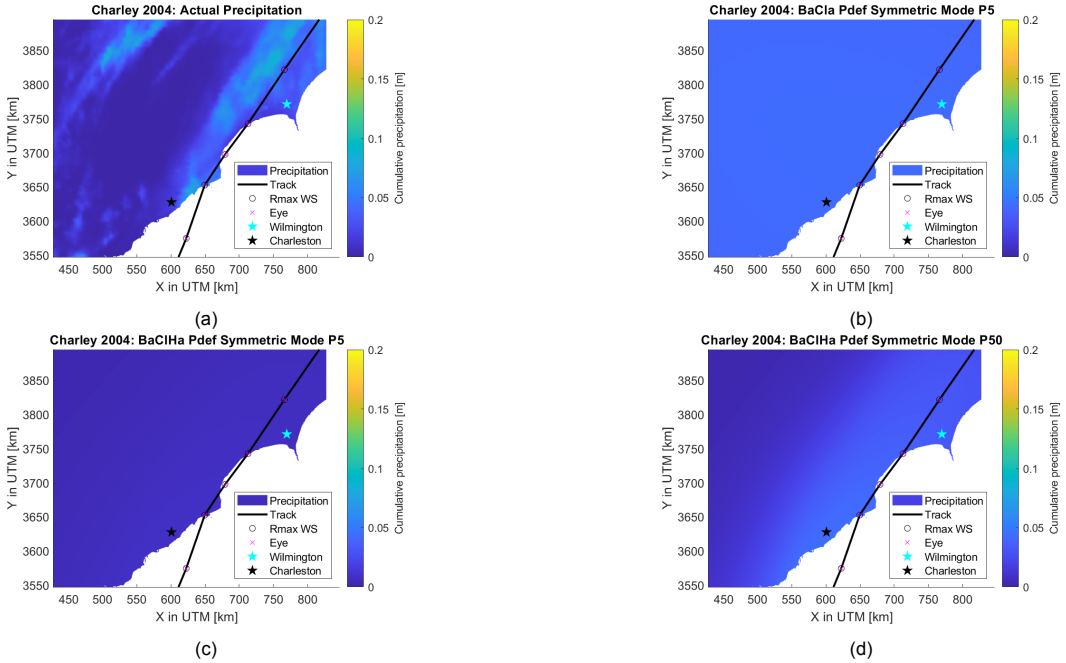


Figure 5.40: Charley 2004: Cumulative precipitation at selected regions of North South Carolina **(a)** Observed (Stage IV) cumulative precipitation **(b)** BaCla model cumulative precipitation for $5^{th}$ percentile **(c)** Improved model (BaClHa) cumulative precipitation for $5^{th}$ percentile **(d)** Improved model (BaClHa) cumulative precipitation for $50^{th}$ percentile

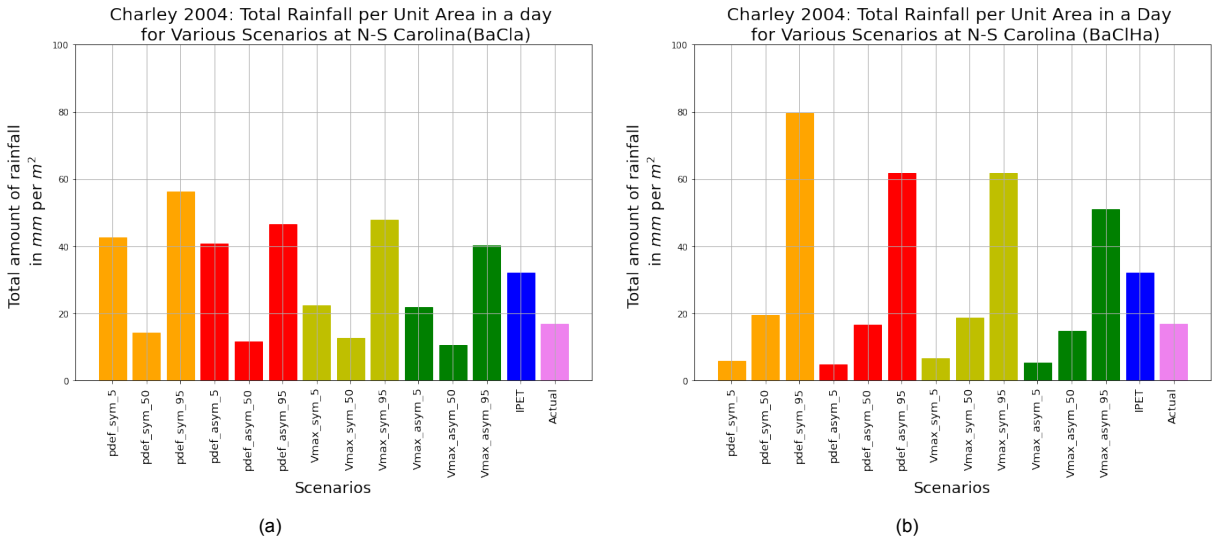


Figure 5.41: Charley 2004: Cumulative precipitation for different model at selected regions of N-S Carolina **(a)** BaCla model results **(b)** Improved model (BaClHa) results

### Charleston

The figure 5.42 shows that the BaClHa model is able to completely capture the cumulative amount of rainfall at Charleston contrary to overestimation by BaCla model. The BaClHa model is unable to show exactly the consolidated patches of high cumulative rainfall per unit area but provides a good general overview (fig.5.42). The inconsistencies in cumulative amount of rainfall per unit area is also improved. The BaCla $pdef$ symmetric mode model predicts around 42 $mm/m^2$ and 30 $mm/m^2$ of precipitation whereas the BaClHa model suggest 10 $mm/m^2$ and 40 $mm/m^2$ of precipitation for $5^{th}$ and $50^{th}$ percentile (fig. 5.43).The actual amount of precipitation based on StageIV data is around 16 $mm/m^2$.

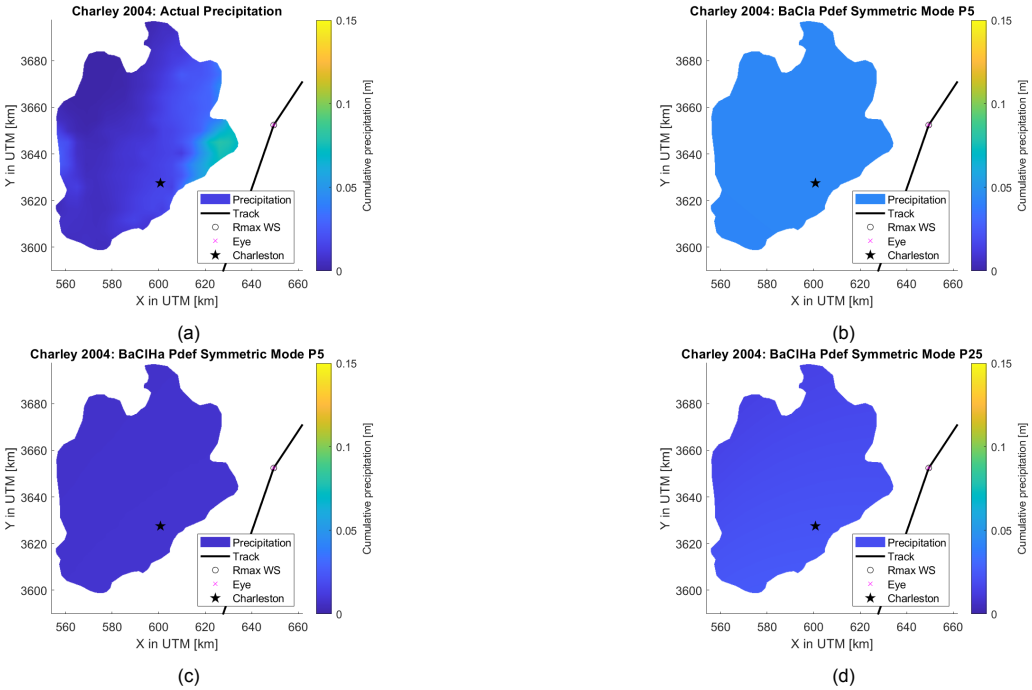


Figure 5.42: Charley 2004: Cumulative precipitation for different model at Charleston **(a)** Observed (Stage IV) cumulative precipitation **(b)** BaCla model cumulative precipitation for 5 percentile **(c)** Improved model (BaClHa) cumulative precipitation for 5 percentile **(d)** Improved model (BaClHa) cumulative precipitation for 25 percentile

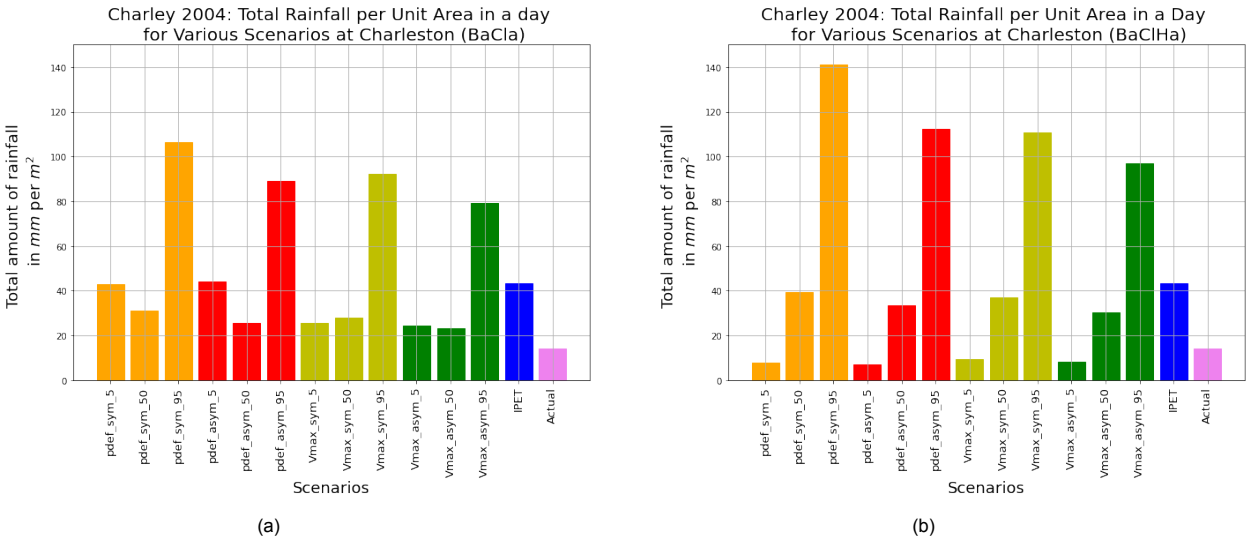


Figure 5.43: Charley 2004: Cumulative precipitation for different model at Charleston **(a)** BaCla model results **(b)** Improved model (BaClHa) results

### 5.4.3. Hermine 2016

N-S Carolina

Hermine 2016 crossed inland coastal region of N-S Carolina as a Tropical Storm. It resulted in almost evenly spread rainfall in most regions of our area of study. The fig. 5.45 shows that the rainfall near the track is well captured by around $75^{th}$ percentile $pdef$ symmetric mode for both BaCla and BaClHa model. The fig. 5.44 and fig. 5.45 shows the BaCla model is over-estimates rainfall for $5^{th}$ percentile which is improved in BaClHa model. For N-S Carolina both the BaCla and BaClHa $pdef$ symmetric mode model predicts around 65 $mm/m^2$ and 195 $mm/m^2$ of precipitation for $50^{th}$ and $95^{th}$ percentile respectively. The actual amount of precipitation based on StageIV data is around 120 $mm/m^2$(fig. 5.45).

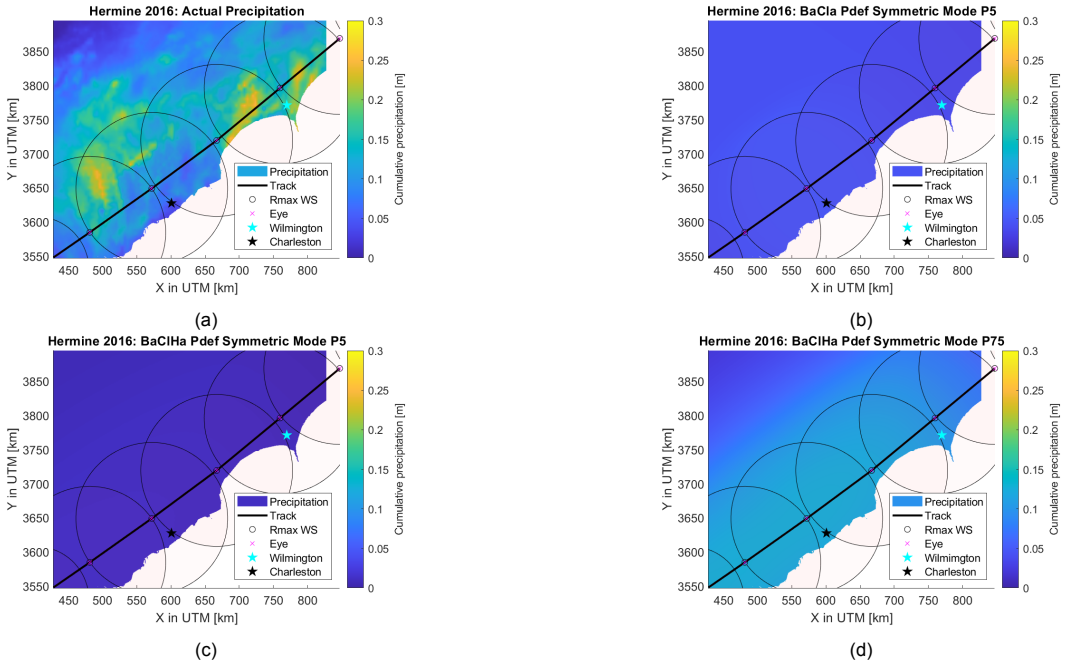


Figure 5.44: Hermine 2016: Cumulative precipitation at selected regions of North South Carolina **(a)** Observed (Stage IV) cumulative precipitation **(b)** BaCla model cumulative precipitation for 5 percentile **(c)** Improved model (BaClHa) cumulative precipitation for 5 percentile **(d)** Improved model (BaClHa) cumulative precipitation for 75 percentile

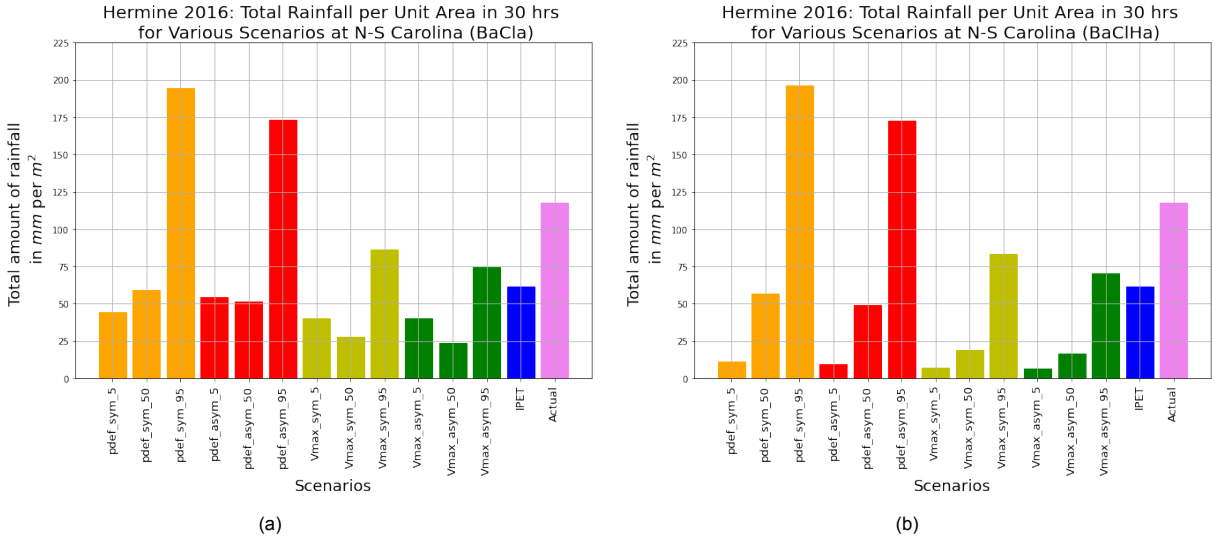


Figure 5.45: Hermine 2016: Cumulative precipitation for different model at selected regions of N-S Carolina **(a)** BaCla model results **(b)** Improved model (BaClHa) results

## Charleston

The figure 5.47 shows that both BaClHaand BaClHa model are able to completely capture the cumulative amount of rainfall at Charleston. The BaClHa model is unable to exactly show the consolidated patches of high cumulative rainfall per unit area but provides a good general overview (fig.5.46). The inconsistencies in cumulative amount of rainfall per unit area for $5^{th}$ percentile scenario is improved. Both the BaCla and BaClHa $pdef$ symmetric mode model predicts around 75 $mm/m^2$ of precipitation for $50^{th}$ percentile (fig. 5.47).The actual amount of precipitation based on StageIV data is around 80 $mm/m^2$.

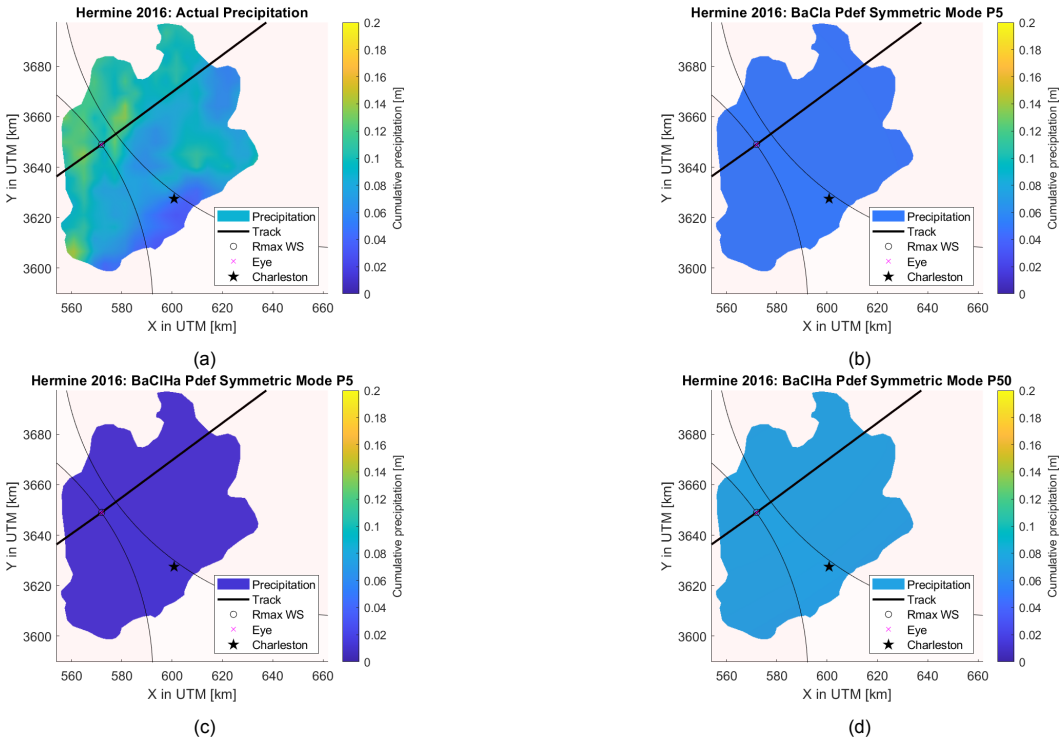


Figure 5.46: Hermine 2016: Cumulative precipitation for different model at Charleston **(a)** Observed (Stage IV) cumulative precipitation **(b)** BaCla model cumulative precipitation for $5^{th}$ percentile **(c)** Improved model (BaClHa) cumulative precipitation for $5^{th}$ percentile **(d)** Improved model (BaClHa) cumulative precipitation for $50^{th}$ percentile

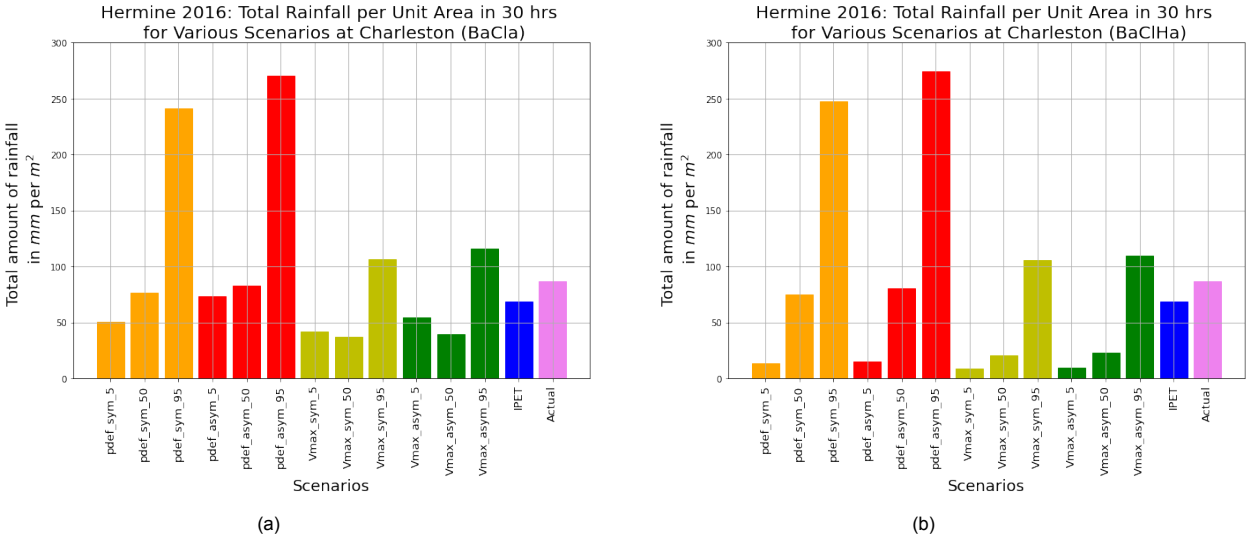


Figure 5.47: Hermine 2016: Cumulative precipitation for different model at Charleston **(a)** BaCla model results **(b)** Improved model (BaClHa) results

## 5.5. Flood hazard and damage

In this section the damage associated with flooding due to Florence 2018, Matthew 2016 and Bonnie 2016 are discussed.

### 5.5.1. Florence 2018

Based on the rainfall values estimated by the models (BaCla and IPET), and providing the results of SFINCS as an input in FIAT model, the damage associated with the cyclone is calculated in US dollar ($) as explained in section 4.5. For Wilmington as the higher percentile based results of models had nearby rainfall values to actual stageIV based observation (fig 5.5), so, the damage associated also lies in the range of damage associated with the stageIV based rainfall values. There are few strange observations as well. For few higher percentile conditions, with higher amount of rainfall the damage is less whereas for IPET where the rainfall is almost the half of the actual stageIV based rainfall the damage associated is higher. This might be because of high rainfall distribution in the area with houses and constructions that can get damaged or might be because the highest amount of damage that can happen, already happened in the region so extra rainfall does not add to the value fig 5.48. The higher damage might also be because of variation in surface water level between the different percentile. To verify that the damage is not variation is not because of tidal effects, the thick bar graph in fig. 5.48 shows the damage just associated with rainfall where as the thin bar graph shows damage associated with all factors. Based on the results no justifiable conclusions have been reached. Refer appendix C for more details. When the variation in rainfall between $5^{th}$ and $95^{th}$ percentile is compared with variation of damage it is observed that in case of Wilmington the variation in rainfall is around 700% where as variation is associated damage is just 16%.

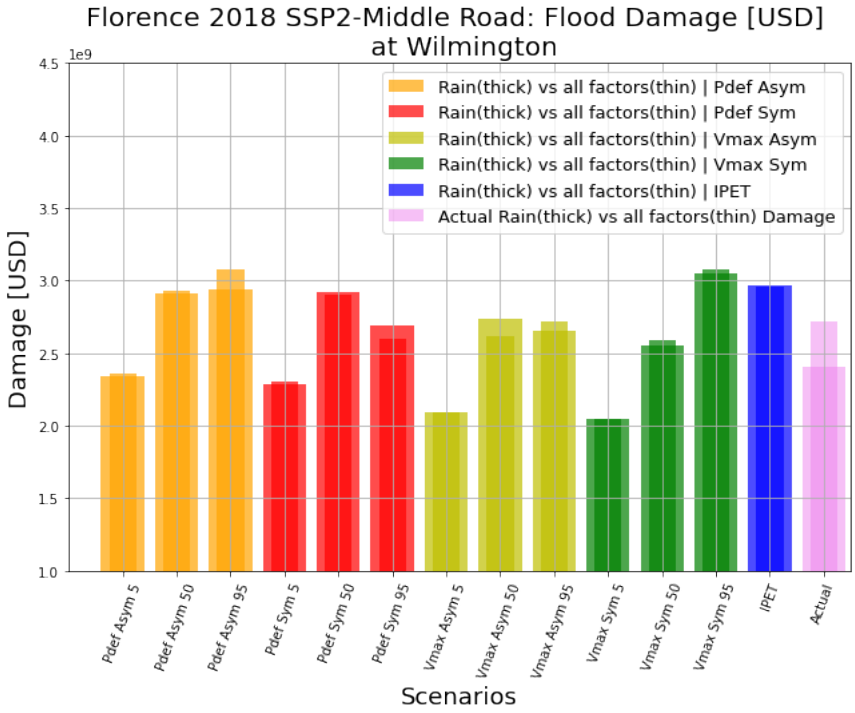


Figure 5.48: Florence 2018: Damage associated with Florence 2018 at Wilmington. The blue color stands for IPET model, pink for observed stage IV data, orange for $pdef$ symmetric, red for $pdef$ symmetric, light green for $vmax$ symmetric and dark green for $vmax$ asymmetric model. The black color is for $pdef$ symmetric random percentile model. The thin bar graph includes tidal effects whereas the thick represents constant offshore water level.

When we look for damage at Charleston, as all the models suggested higher amount of rainfall, (fig 5.8) so the damage associated is higher as well, when compared to damage that can happen because of stageIV based total rainfall. In case of Charleston as the percentile of rainfall increases, so is the damage associated fig (5.49). However, IPET demonstrates nearly identical damage to the $65^{th}$ percentile of the vmax-based model, despite having more rainfall. Again this can be associated

with the reasons discussed above. In case of Charleston damage just because of rainfall and those including all factors shows almost the same pattern. When the variation in rainfall between $5^{th}$ and $95^{th}$ percentile is compared with variation of damage it is observed that in case of Wilmington the variation in rainfall is around 900% where as variation is associated damage is just 120%.

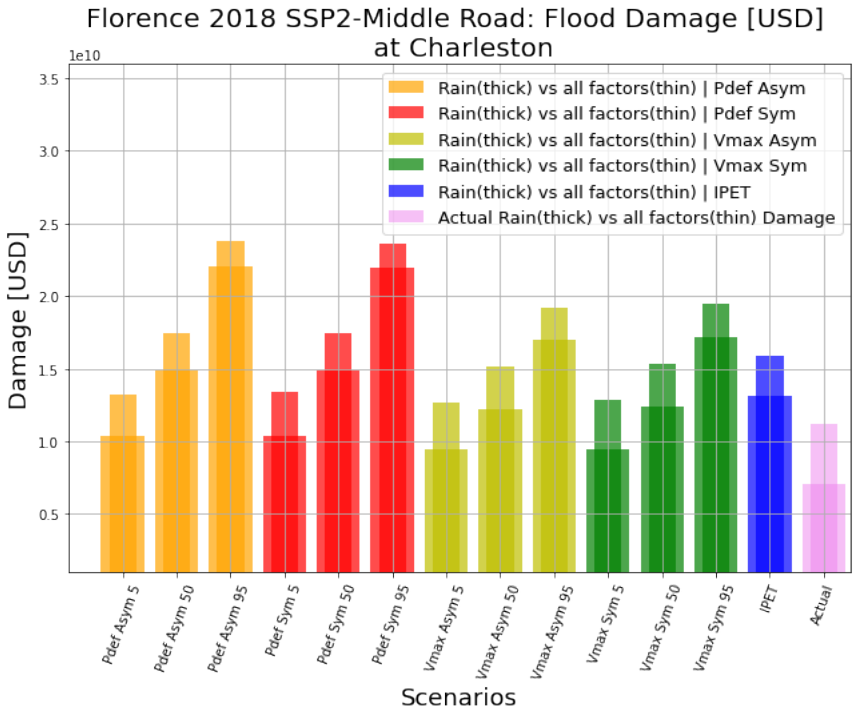


Figure 5.49: Florence 2018: Damage associated with Florence 2018 at Charleston

## 5.5.2. Matthew 2016 and Bonnie 2016

In case of Matthew 2016 when the actual amount of rainfall is near to $95^{th}$ percentile of BaCla model based results the damage associated also remains near the percentile but the damage associated with $5^{th}$ percentile is not as low as compared to the variation in amount of rainfall. When the variation in rainfall between $5^{th}$ and $95^{th}$ percentile is compared with variation of damage it is observed that in case of Wilmington the variation in rainfall is around 1650% where as variation is associated damage is just 100%.

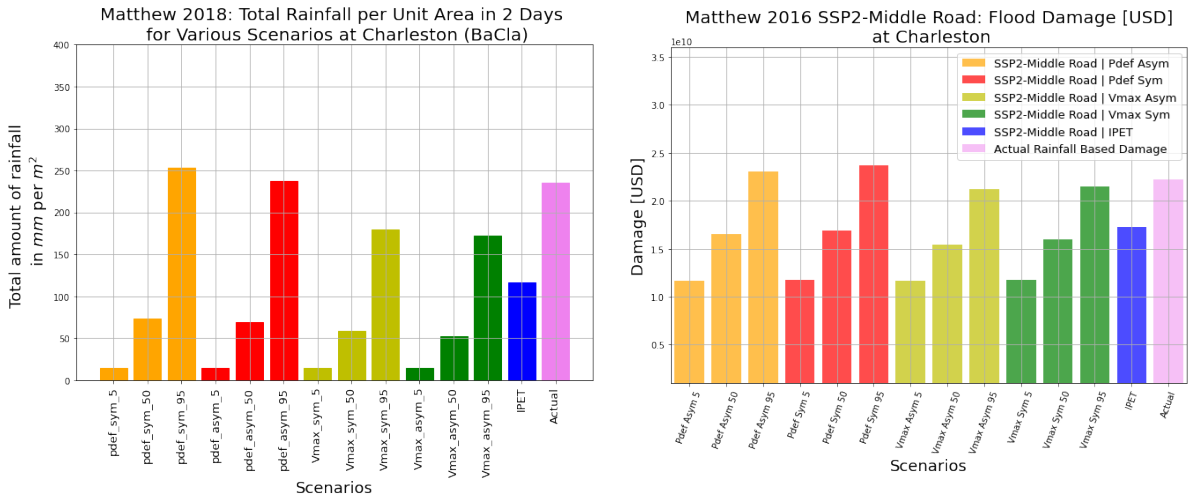


Figure 5.50: Matthew 2016: Charleston precipitation plot for different percentile along with damage associated

For Bonnie even though the model overestimates the amount of rainfall, the damage associated remains similar to the damage associated to stageIV based rainfall. For 5 percentile scenarios when the amount of rainfall is higher than the actual (stageIV) based rainfall, the damage associated is lower because of variation in the distribution of rainfall.When the variation in rainfall between 5 and $95^{th}$ percentile is compared with variation of damage it is observed that in case of Wilmington the variation in rainfall is around 475% where as variation is associated damage is just around 57%.

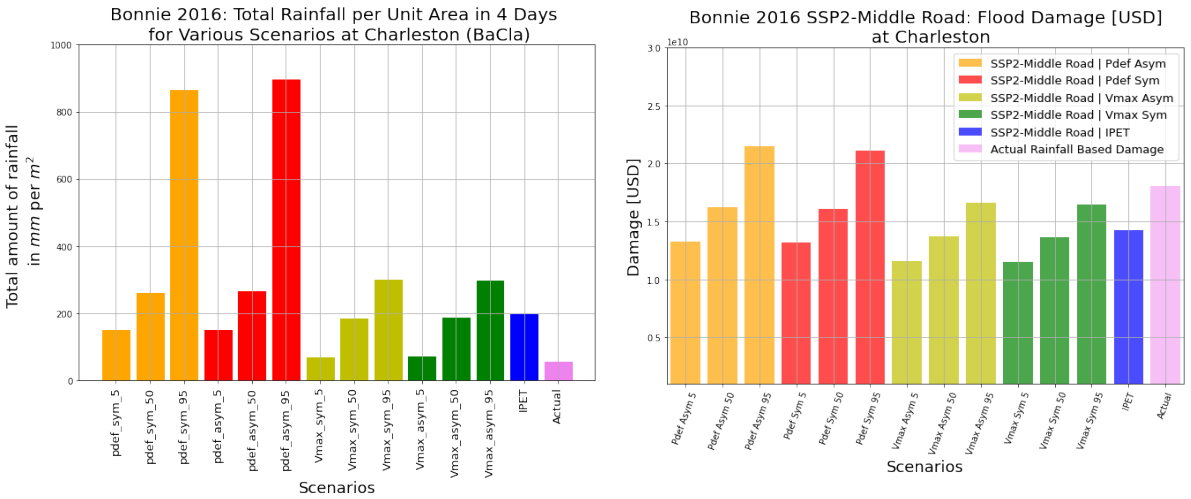


Figure 5.51: Bonnie 2016: Charleston precipitation plot for different percentile along with damage associated

### 5.5.3. Overall - flood hazard and damage

- Performance of rainfall prediction is not one to one transformable to damage prediction.
- Damage associated is less sensitive than rainfall prediction. For example the variation in rainfall at Wilmington due to Florence 2018 is around 700% where as the associated damage variation is just around 16%.
- For Wilmington there are cases when low amount of rainfall results in high damage.(appendix C)
- Location of rainfall plays an important role associated damage calculation. For instance, even though the associated IPET rainfall in Wilmington during Hurricane Florence in 2018 was about half as much as what was seen based on Stage IV, the IPET still predicts greater damage.
- Tidal effects generally result in more flooding-related damage.

# 6

# Conclusions and recommendations

## 6.1. Synthesis

In this thesis, an improvement of the existing parametric BaCla stochastic tropical cyclone precipitation model has been proposed and is compared with the standard practice IPET model in order to answer the research question:

**How can the spatio-temporal biases of the BaCla model be reduced, and how do they impact the parametric tropical cyclone precipitation model's ability to predict precipitation, associated flood hazards and damage?**

In this study the main biases of the BaCla model have been identified as follows:

- The model may over- or underestimate the total quantity of cumulative rainfall depending on the location and scenario.
- For tropical cyclones of category 1 or stronger, the model underestimates the cumulative amount of rainfall whereas for low wind-speed, Tropical storms and depressions it overestimates the amount of rainfall.
- The model may not always accurately predict the maximum quantity of precipitation because it takes into account the azimuthal average of the TC associated precipitation.
- Due to the uniform radial rainfall assumption, the BaCla model overestimates the quantity of rainfall in situations where the peak amount of rainfall is less than 2.8mm/hr.
- The appropriate threshold for using method D (best fit area under the total rainfall curve method) to get fitting coefficients may not be 2.8 mm/hr as it leads to over estimation of rainfall e.g. table 5.3
- The assumption of the radius that the maximum wind speed radius and radius of maximum precipitation are equal generally does not hold.

The main components that were of importance for the reduction of the aforementioned biases in the model were identified as the relation between radius of maximum wind speed ($Rv_{max}$) and radius of maximum precipitation ($Rp_{max}$) and the fitting coefficients of precipitation profile (adapted Holland wind profile, Section 2.2.2).

In order to determine a correlation between the radius of the maximum wind speed ($Rv_{max}$) and the radius of the maximum precipitation ($Rp_{max}$), 53 TCs were chosen for which blended data sets (including Stage IV data, TRMM, and GPM) were available. For the selected tropical cyclones there were 220 time steps for which the radius of maximum wind-speed ($Rv_{max}$) and correspondingly StageIV based radius of maximum precipitation ($Rp_{max}$) was available. Out of those observation 170 time steps were plotted for which the radius of maximum precipitation ($Rp_{max}$) was within 300 km from the eye of TC. This is the radius generally up to which the maximum precipitation because of a TC can occurs

based on the study by Lonfat, Marks Jr, and Chen [27], Jiang, Halverson, and Simpson [21] and Bader [2]. The relationship between the radius of the maximum wind speed ($Rv_{max}$) and the radius of the maximum precipitation ($Rp_{max}$) was then determined using a linear fit.

$$y = 0.6383x + 34.7867 \qquad 5.1$$

In equation 5.1, y and x represents the radius of maximum precipitation and radius of maximum wind-speed respectively. The linear relation was used to find the radius of maximum precipitation by the model, which helped to better capture the spread of rainfall. The least square fit (method A) was used to obtain fitting coefficients of adapted Holland wind profile for the cases where the maximum amount of rainfall was less than 2.8 mm/hr. This helped in reducing over-estimation of rainfall for the cases where the BaCla model was providing constant high value of rainfall (e.g. fig. 5.21c). Despite the improvement to the model, there were cases like fig. 5.21e, where the precipitation was over estimated because the peak amount of rainfall was just above 2.8 mm/hr. To overcome this problem, the threshold was increased to 5 mm/hr as proposed by Claassen [11] in method B (separate least square fitting for rainfall above and below 5 mm/hr). This threshold with method A is in turn used to determine the fitting coefficient for adapted Holland wind profile. Instead of only providing a continuous high value of rainfall, this improvement provided for a more realistic representation of the rainfall at larger distances from the eye of the TC. It also helped in capturing the rainfall when the wind speed was low or the radius of maximum wind speed was large.

The three improvements in the model were validated for calibration sets of TCs together with three other tropical cyclones that crossed the same area of interest. The results showed that the BaClHa (improved) model performed better at capturing the cumulative amount of rainfall that occurred during different tropical cyclonic event for smaller area of interest (e.g. Charleston) as well as a larger one (N-S Carolina). In this study, the $vmax$ based cumulative mean precipitation range lower than the $Pdef$ based cumulative mean precipitation. However, single-parameter models are rudimentary, unable to replicate the intricate spatio-temporal rainfall pattern that tropical cyclones create when they make landfall. For instance, there are situations where $Pdef$ and $vmax$ values are low yet the rainfall rates are high due to other physical phenomena, such as topographic effects [8],[28]. A model with only one parameter has this genuine limitation.

A comparison with the IPET model showed that the BaClHa model is competitive as generally the $40^{th} - 60^{th}$ percentile of the cumulative mean precipitation based on the $Pdef$ model is almost identical to that of IPET. However, the $Pdef$ based model performs best for the selected case studies, but it still needs to be tested for more tropical cyclones, preferably in some other geographical location to test the global applicability of the model and to comment on the efficiency of $Pdef$ and $vmax$ based model. The new model ensured better representation over land, the over and under estimation is reduced, and the model is expected to be applicable globally with more confidence.

Having a model calibrated by the incorporation of appropriate prepossessed data that highlights the risks associated with extreme occurrences, such as TC, may be extremely beneficial in the field of risk management for a better understanding of flood risk. The current study suggests that the performance of rainfall prediction is not a one-to-one transformable to damage prediction. Damage associated is less sensitive to the rainfall prediction. Therefore the range of damage estimation is narrower than the range of rainfall prediction. The improved model is better at predicting the actual amount of rainfall. As it is better at estimating rainfall, it can act as a better choice for creating flood scenario but might contribute less to risk assessment.

## 6.2. Limitations

Despite a major improvement over the original BaCla model, the new model still has a number of drawbacks.

1. The improved model fails to capture the peak amount of rainfall at a particular location and time. This is because the model considers the radial mean amount of precipitation which will always lower than the actual peak amount of rainfall.

2. The model does not takes into account the topographic effects, so it generally fails to capture the rainfall due to topographic effects.

3. The model only captures the highest peak of rainfall neglecting other peaks, like rain bands, since it is based on the adapted Holland wind-profile, even though they are sometimes only slightly lower in value.
4. The model is still unable to capture the asymmetrical rainfall distribution by following the asymmetry in wind profile.
5. For some high and very low wind speed storms the $95^{th}$ and $5^{th}$ percentile based results of the BaClHa model slightly underestimates and overestimates the cumulative amount of rainfall.
6. The model has not been tested for its applicability at other geographical locations. It might be the case that it does not perform well at other locations as the model is trained based on data from the North Atlantic basin only.

## 6.3. Recommendations for future research

The study could be advanced by concentrating on the points listed below.

1. Test the model at some other location outside the North Atlantic basin, preferably somewhere in the southern hemisphere. This is due to the fact that a different geographic position will be verified together with the clockwise rotation of the TCs.
2. The BaClHa model's asymmetrical rainfall distribution does not completely match with the actual rainfall distribution. Explore better ways to take into account the asymmetry in the rainfall (like making use of Golden spiral).
3. Re-verify the relation between radius of maximum wind-speed and radius of maximum precipitation by taking more data into account and subsequently check the effectiveness of the model.

# A

# Radius of maximum wind-speed vs radius of maximum precipitation

To understand if it is justifiable to assume radius of maximum wind-speed is same as radius of maximum precipitation, IBTrACs based radius of maximum wind-speed is plotted with radius of maximum precipitation based on TRMM or GPM data and StageIV blended data. The radius on maximum precipitation is capped at 300 km as Lonfat et al [27] fig 2.1 and Jiang et al. [21] fig. 2.2 suggested that maximum precipitation because of TCs occur at a distance of within 300 km from eye.

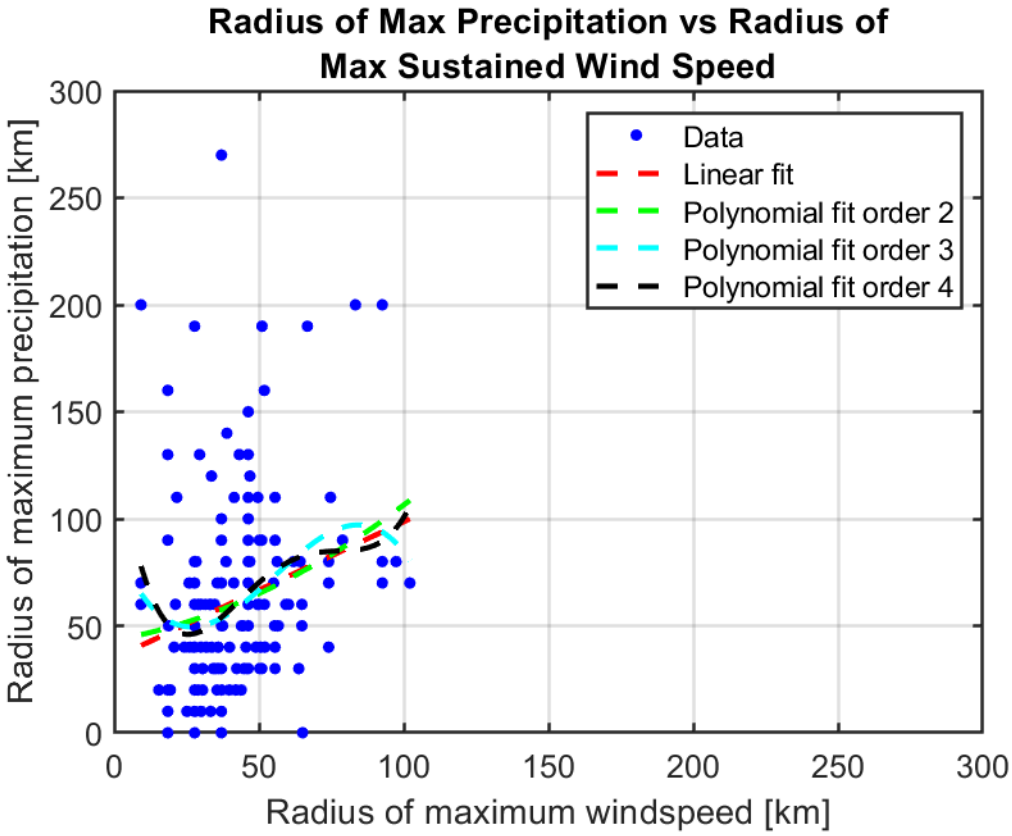


Figure A.1: Radius of maximum sustained wind-speed vs radius of maximum precipitation

Fig. A.1 shows the data based on 54 different TC cyclones (220 observations) data for the IBTrACS was having radius of maximum wind-speed available. Fig. A.1 depicts it is not always the case that

radius of maximum wind speed is equal to radius of maximum precipitation. Radius of maximum precipitation is almost twice or more for smaller values (e.g. 20km) of radius of maximum wind-speed but it reduces to almost equivalent or less than radius of maximum wind speed for values around 100 km. To better understand the relation box plot are plotted first at 20 km interval of maximum wind speed fig. A.2 and then at an interval of 40 km fig. A.3.

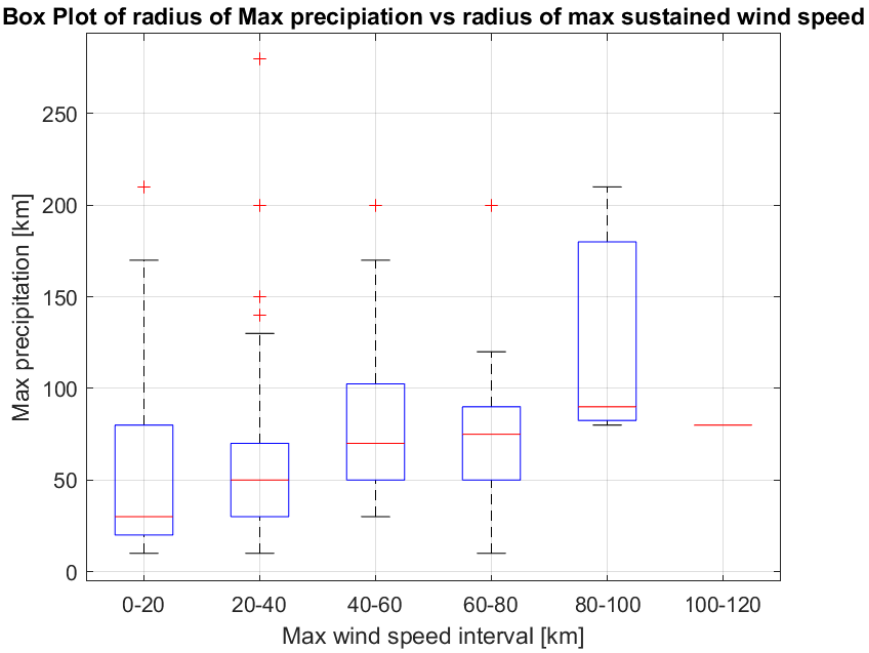


Figure A.2: Box plot of radius of maximum sustained wind-speed vs radius of maximum precipitation at 20 km interval

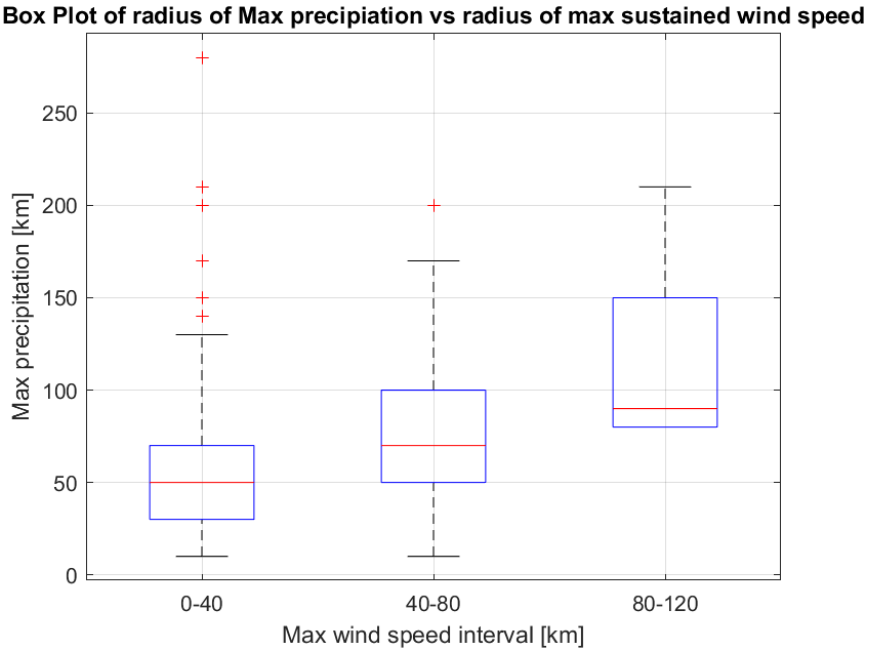


Figure A.3: Box plot of radius of maximum sustained wind-speed vs radius of maximum precipitation at 40 km interval

Box plots clearly suggested that the radius of maximum wind speed is not always equal to radius of maximum precipitation. Considering the median values for fig A.3 the relation between Rpmax = 2.5 Rvmax for radius of maximum wind speed up to 40 km. The relation changes to Rpmax = 1.67

Rvmax and Rpmax = 0.9 Rvmax for interval 40-80km and 80-120 km respectively. But the limitation of proceeding ahead with this interval method is that it might not hold true for all the case as the interval is quite large. This might lead to over estimation of rainfall or might show a larger spread of rainfall. So, it is decided to proceed further with the linear fit in the scatter plot as in the fig. A.1 not significantly better than the linear fit in terms of fit. For a polynomial of order 2, 3, and 4, the $R^2$ values are 0.067, 0.083, and 0.091, respectively. The $R^2$ value for a linear fit is 0.065.

The Gaussian Model probability PDF is presented for the given data since the $R2$ values are relatively low (fig. A.4). The Gaussian model is considered as that is the most common distribution in climatology (Central Limit Theorem).The linear fit is drawn in magenta, and each point for the radius of maximum wind-speed with the highest chance of occurrence for the radius of maximum precipitation is plotted in red. The graph A.4 suggest the linear fit, and the points of highest probability runs almost with constant slope and different Y intercept. The Y intercept value for linear fit it 34.7 km whereas for the Gaussian model it is 18.1 km. After the point where the radius of maximum wind-speed is greater than 60 km the probability curve behaves differently. This might be because of less availability of data for the extreme values. But this method appears to be a promising option with more data.

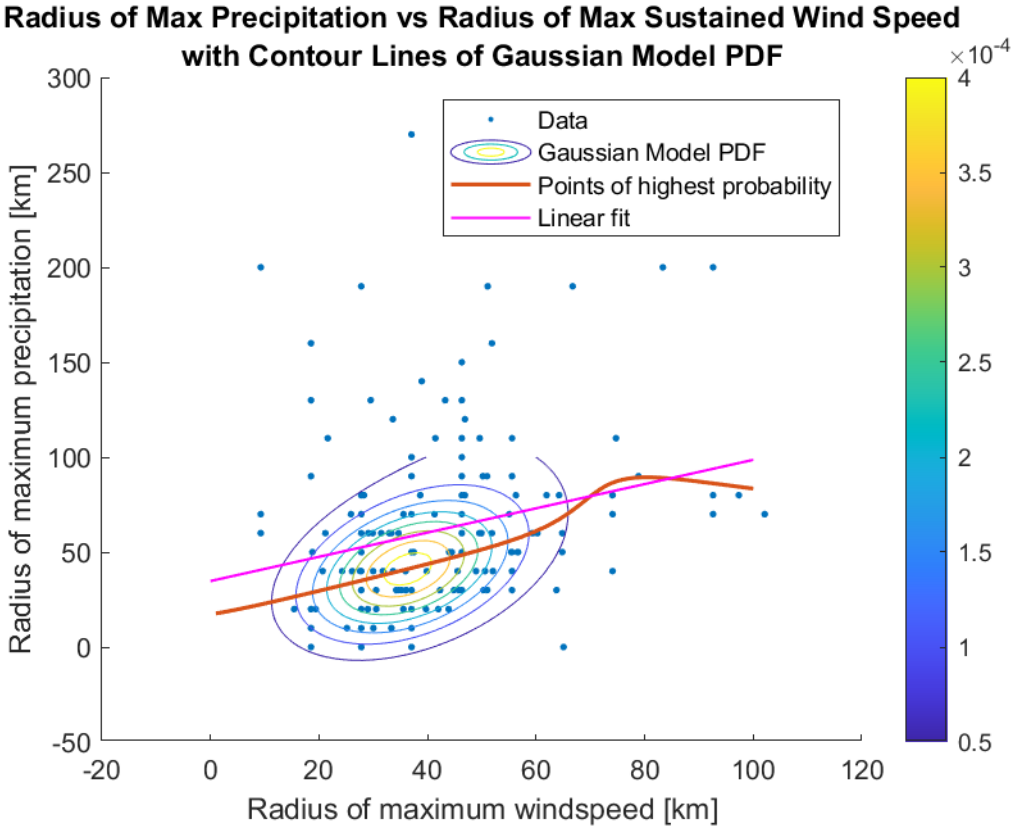


Figure A.4: Radius of maximum sustained wind-speed vs radius of maximum precipitation with contour lines of Gaussian model PDF

So, in this study linear fit is considered to keep model simple. The linear fit gives us a relation between radius of maximum wind speed and radius of maximum precipitation as :

$$y = 0.6383x + 34.7867 \tag{A.1}$$

where y is radius of maximum precipitation and x is the radius of maximum wind-speed.

# B

# Flood Risk assessment for different SSP scenario

In research long term scenarios on global environmental change plays an important role. The shared socioeconomic pathways (SSPs) is one of the characterisation that describes plausible alternative changes in social, economic, technological, demographic, governance and environmental factors of society. It is based on back-casting approach, where an end state is already in mind as the pathways are being developed. SSP outcomes helps in adaptation to socioeconomic challenges. Without explicitly considering climate change itself, it is intended to describe worlds in which societal trends results in making mitigation of, or adaptation to, climate change harder or easier [36]. A simple graphical representation has been attached in section 4.5.

It this study SSP2 (intermediate challenges) case has been considered for calculation of flood associated damage because of TCs. To have an idea how much the results vary for 10 years of return period, a graph showing the damage caused at Charleston for different parametric model in SSP1 and SSP2 scenario has been attached below. It is clear that there is not much of a difference.

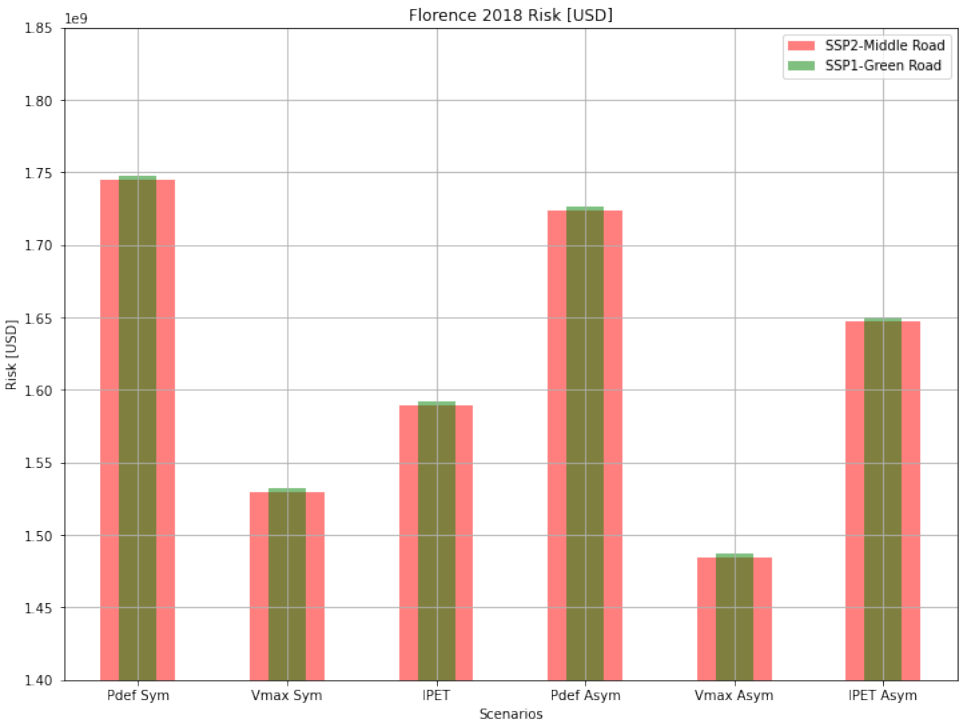


Figure B.1: Damage caused at Charleston for different parametric model in SSP1 and SSP2 scenario

# C

# Florence: Rainfall variation and associated damage at Wilmington

Based on the BaCla model, the rainfall variance at Wilmington for various percentiles were analyzed (fig C.1). Because the spiderwebs took a bigger quantity of rainfall into account in each time step, it was expected that the rainfall would grow with an increase in percentile. However, analysis of the accompanying damage (fig. C.2) reveals that the 65 percentile has less damage than the 50 percentile of rainfall. Due to SFINCS's consideration of tidal effects, it was initially thought that this was the reason.In certain circumstances, excluding tidal effects reduced damage, and in other cases, it increased damage (fig. C.2). However, damage caused by rainfall at the 65th percentile was less severe than damage from rainfall at the 50th percentile.

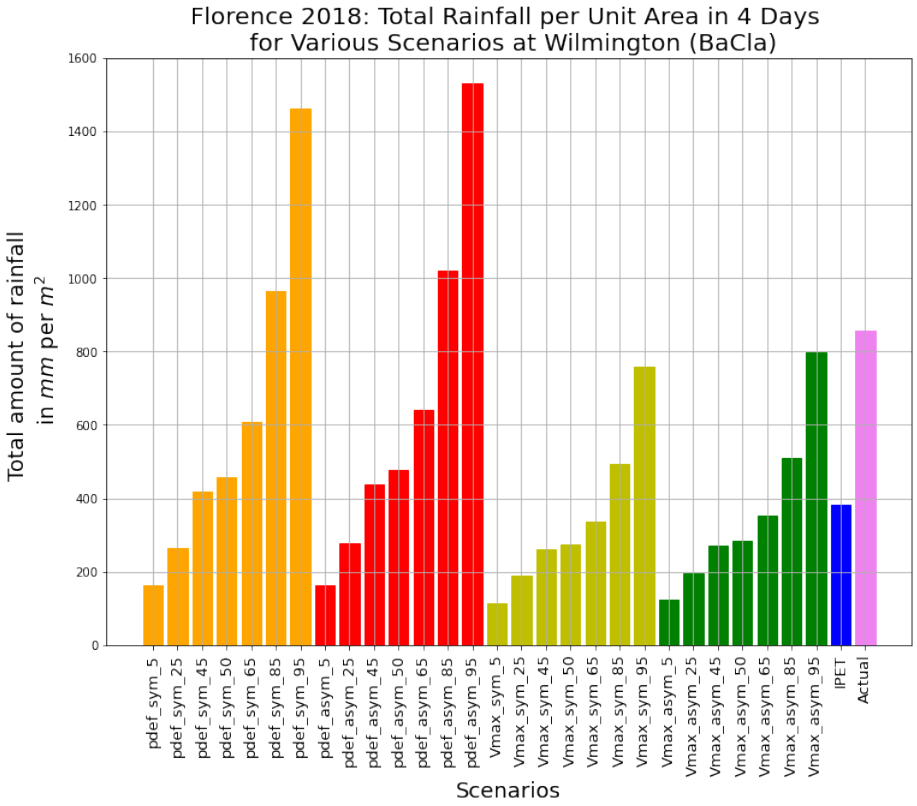


Figure C.1: Florence 2018: Total rainfall per unit area in 4 days for various scenarios at Wilmington (BaCla)

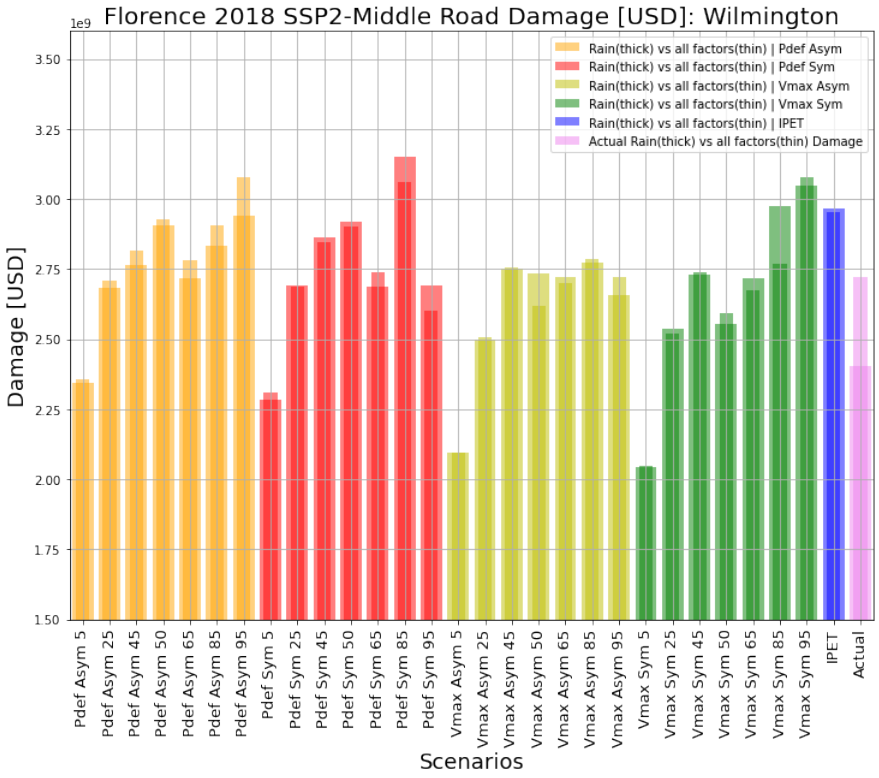


Figure C.2: Florence 2018 SSP2-Middle Road:Flood Damage [USD] at Wilmington

The variation in rainfall, difference in associated flooding, and associated damage are compared to better understand the cause (fig. C.3). The 65 percentile scenario results in an additional 14 to 15 cm of rainfall overall, although the region highlighted with a circle in the map experiences less flooding. Surprisingly, some areas in the circle have seen more damage even with less flooding.Perhaps how the houses are arranged or how much of a region is constructed is important. Further research is necessary to determine the cause of this, which is yet unknown.

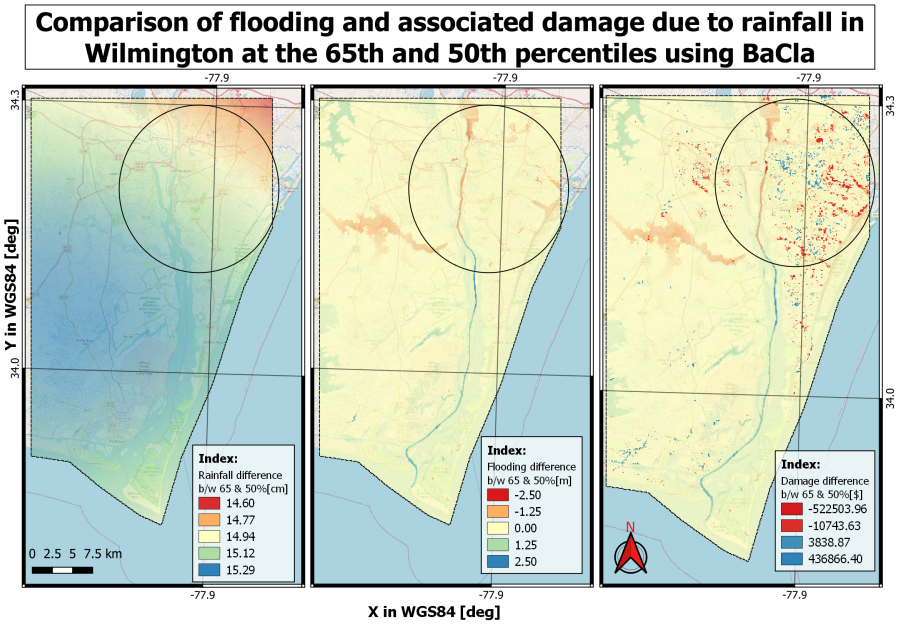


Figure C.3: Florence 2018: Comparison of 65 and 50 percentile of rainfall, flooding and associated damage

# D

# Tropical cyclone eye wall replacement

The rate of dissipation of the inner eye-wall in tropical cyclones determines the Eye-wall Replacement Cycle (ERC), this is an important indicator for forecasting changes in the intensity and structure of tropical cyclones. Li et al. [26] studied the eye-wall replacement cycle of typhoon Trami 2018. Trami 2018 simulations produced an ERC that matched the observation using a coupled atmospheric-ocean model based on Weather Research and Forecasting (WRF) Model. Fig. D.1 and D.2 clearly show high rain-bands inside the 50km circle for time step **(a)** and **(b)**. When we look at time step **(d)** and **(e)** it is clear that the high rain-bands are outside the 50 km circle.

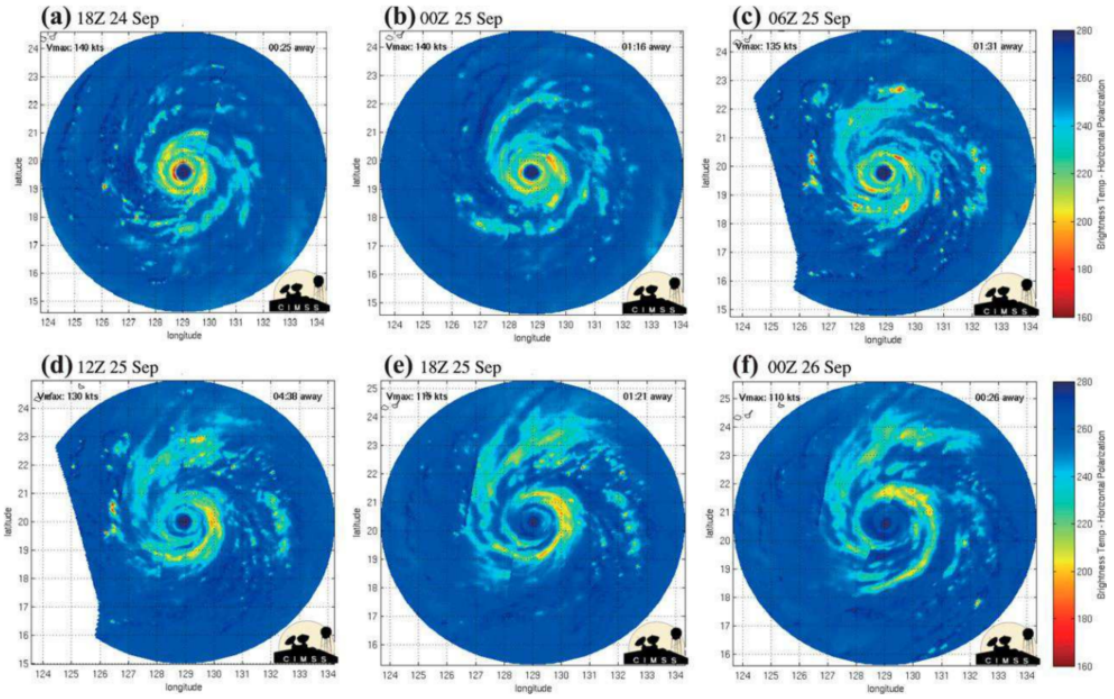


Figure D.1: Trami 2018: Satellite microwave images from Cooperative Institute for Meteorological Satellite Studies (CIMSS) at **(a)** 1800 UTC 24 Sept, **(b)** 0000 UTC 25 Sept, **(c)** 0600 UTC 25Sept, **(d)** 1200 UTC 25Sept, **(e)** 1800 UTC 25Sept, **(f)** 0000 UTC 26Sept.

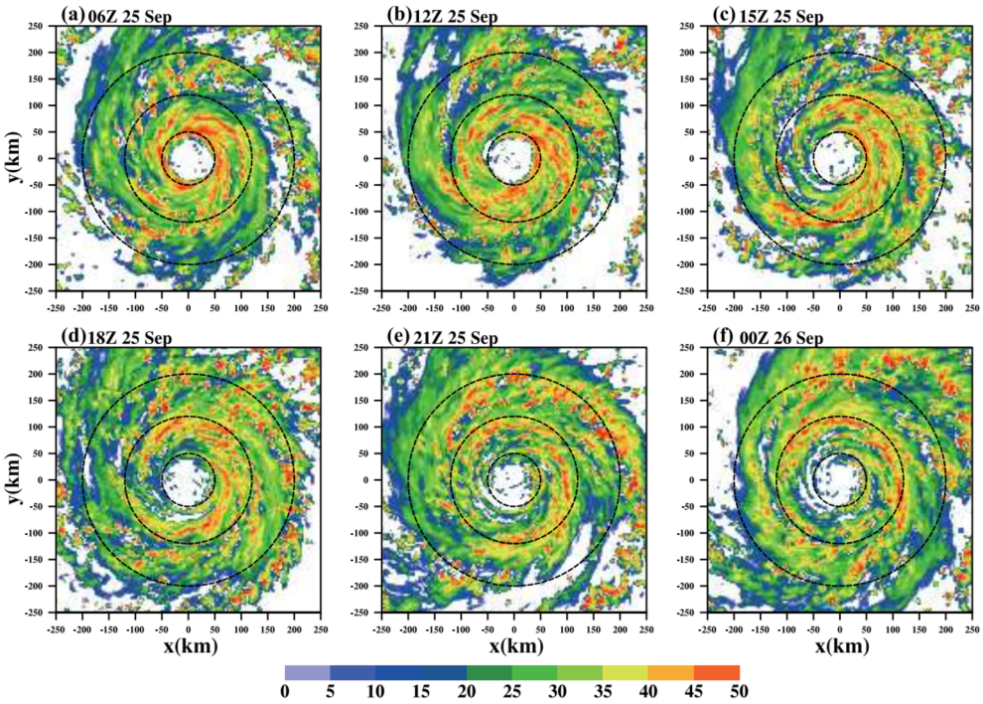


Figure D.2: Trami 2018: Plane view of the radar reflectivity (dBZ) at the height of 3 km in the coupled simulation. The model time is noted at the top left of each panel. The dashed circles located at the radii of 50, 120, and 200km. The annular regions between the dashed circles indicate the inner and outer rain-bands regions.

In another study by Rozoff et al. [42] to simulate secondary eyewall formation (SEF) in a tropical cyclone (TC) using WRF model similar kind of observations could be observed (fig. D.3).

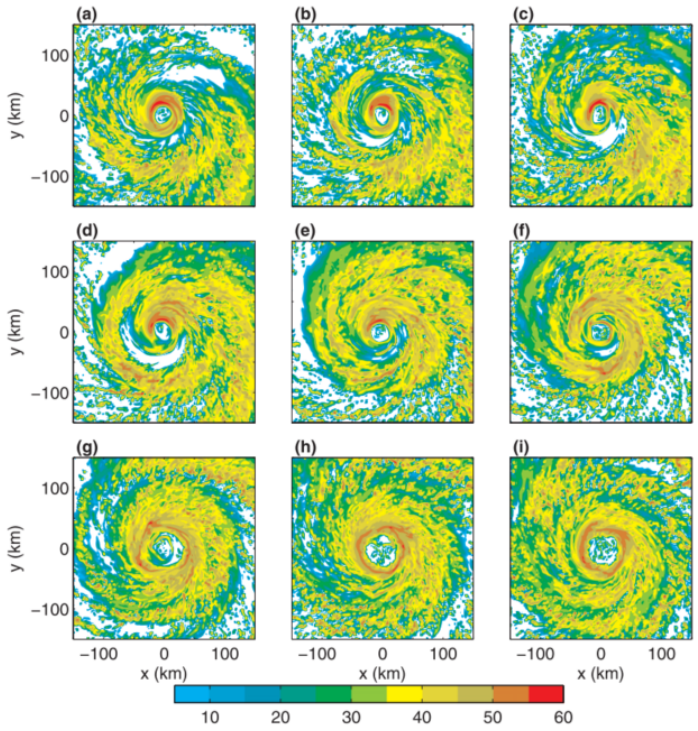


Figure D.3: Low level(z = 1km) synthetic radar reflectivity (dBZ) at (a) 102, (b) 107, (c) 112, (d) 117, (e) 122, (f) 127, (g) 132, (h) 137, and (i) 142 h.

# E

# Rainfall variation for different TC based on distance from coast

To understand how rainfall is affected when the eye of TC is near the coast and when it is farther away over land? A total of 143 TC are studied. TCs were divided into three parts, in the first type there were TC that were just Tropical storm or tropical depression near the coast or inland, Second type was TC upto category 2 and in third type there were TC that were of category 3 to category 5. For all three parts the rainfall suggested by stageIV data within the radii of 600 km of eye of TC over land is plotted with respect to distance from coast. Distance of eye from coast is made the color coded third axis.

Based on the plots it is observed that when the eye of TC is within 100-200 Km from coast the rainfall gets concentrated to a smaller region for higher wind speed TC as compared to low speed TC i.e. for type 1 the rainfall is spread quite in-land up to 600-700 km where as for part 3 it mainly gets concentrated within 200 km from the coast. This suggests that radius of maximum wind speed and radius of maximum precipitation is affected by the type of TC and its associated wind speed.

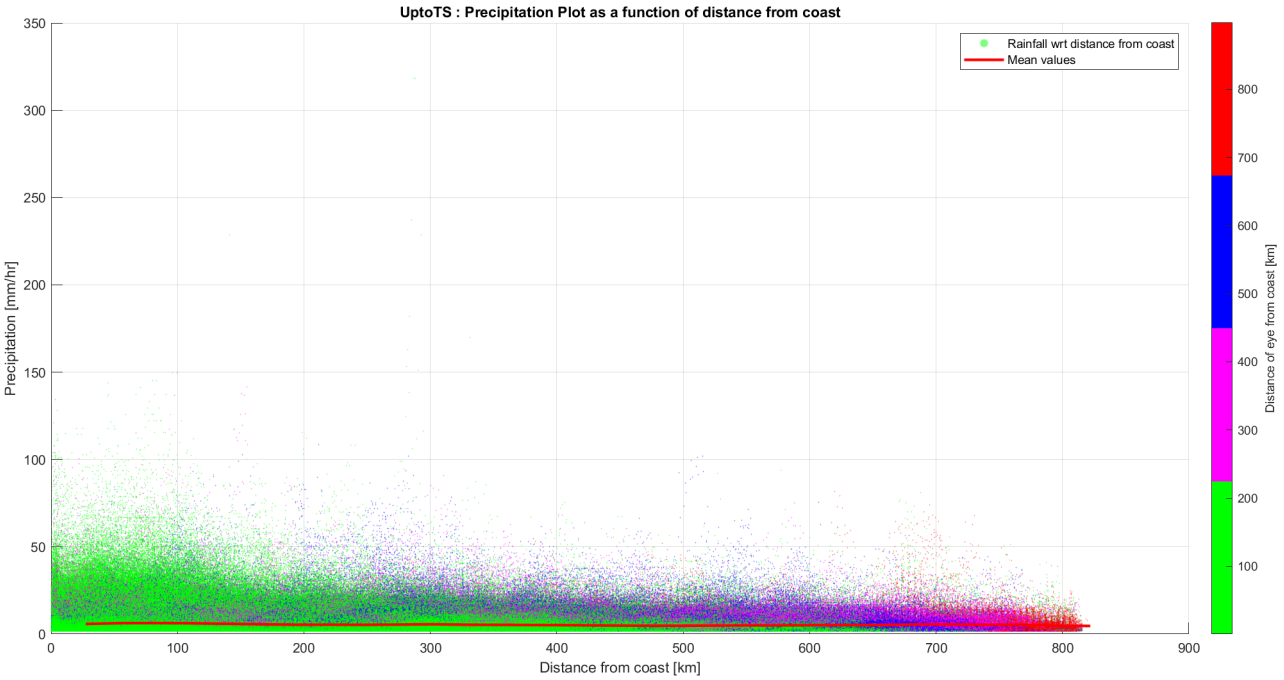


Figure E.1: Rainfall variation as a function of distance from coast for TC of type 1

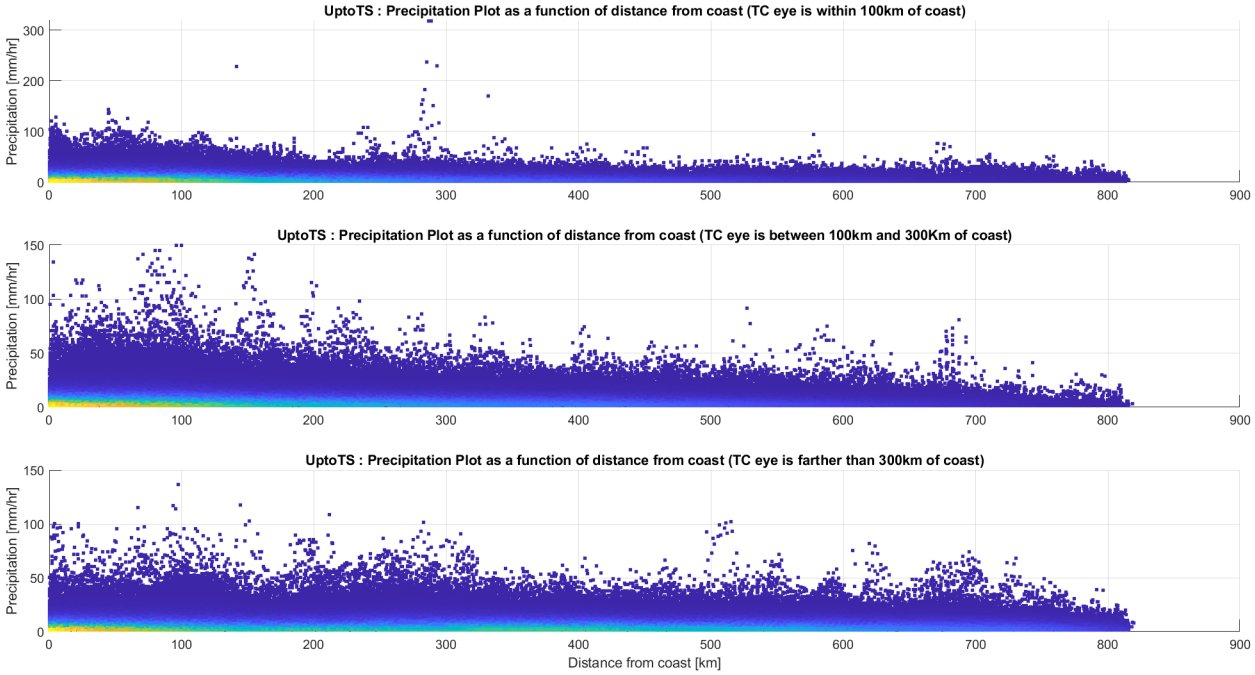


Figure E.2: Rainfall variation as a function of distance from coast for TC of type 1 based on location eye

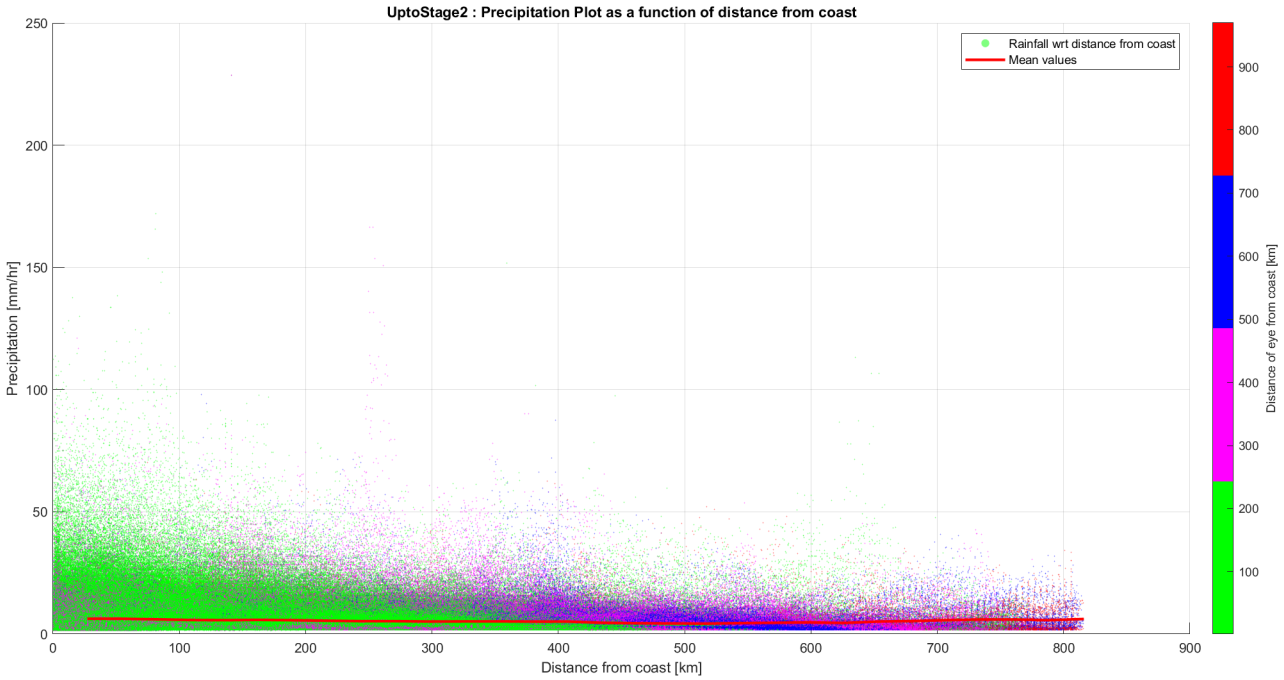


Figure E.3: Rainfall variation as a function of distance from coast for TC of type 2

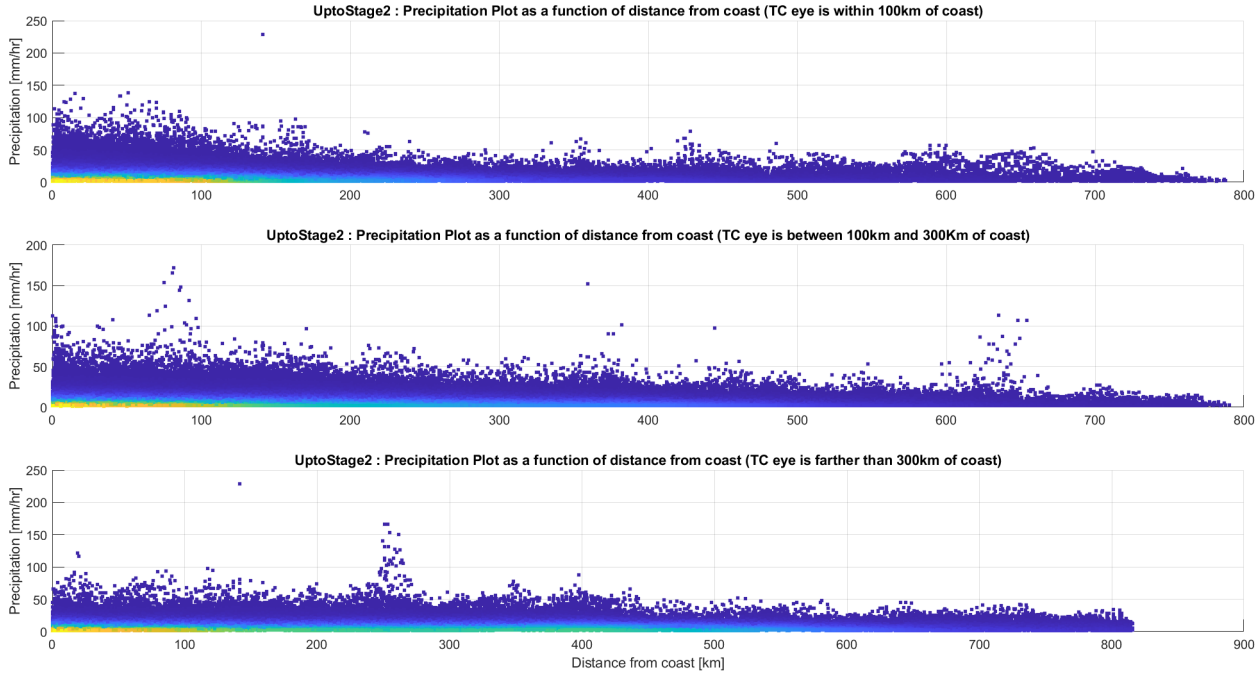


Figure E.4: Rainfall variation as a function of distance from coast for TC of type 2 based on location eye

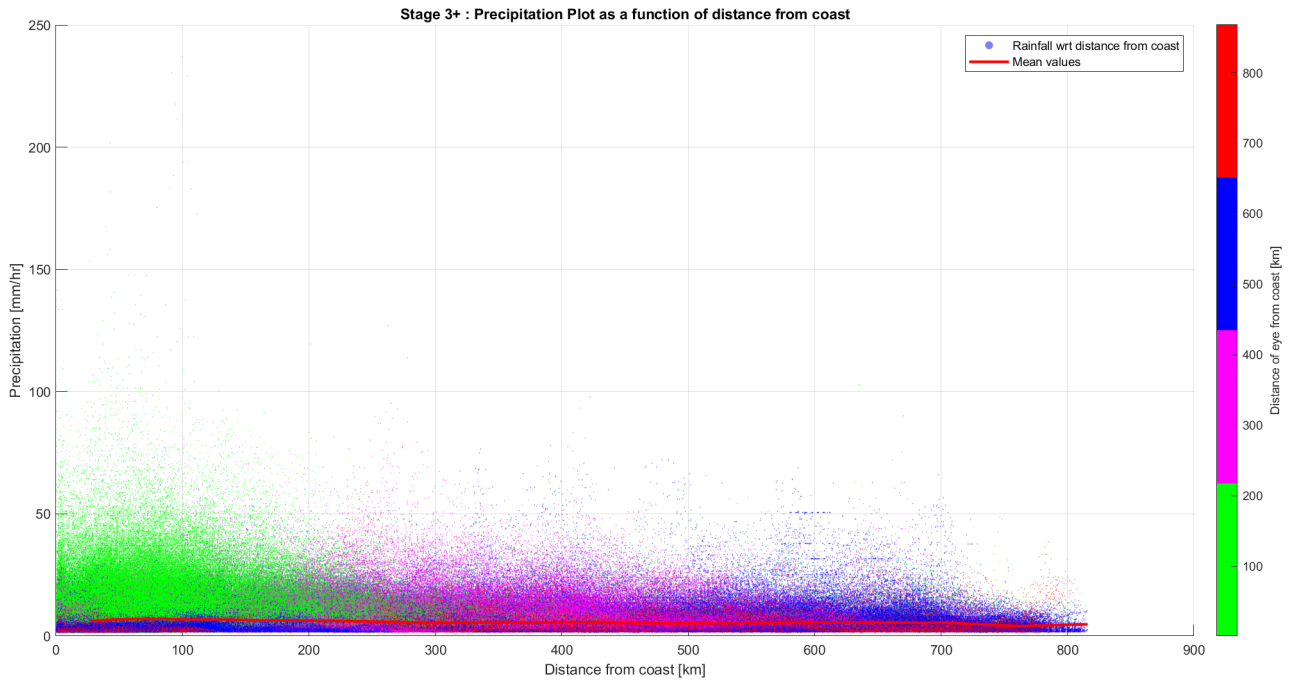


Figure E.5: Rainfall variation as a function of distance from coast for TC of type 3

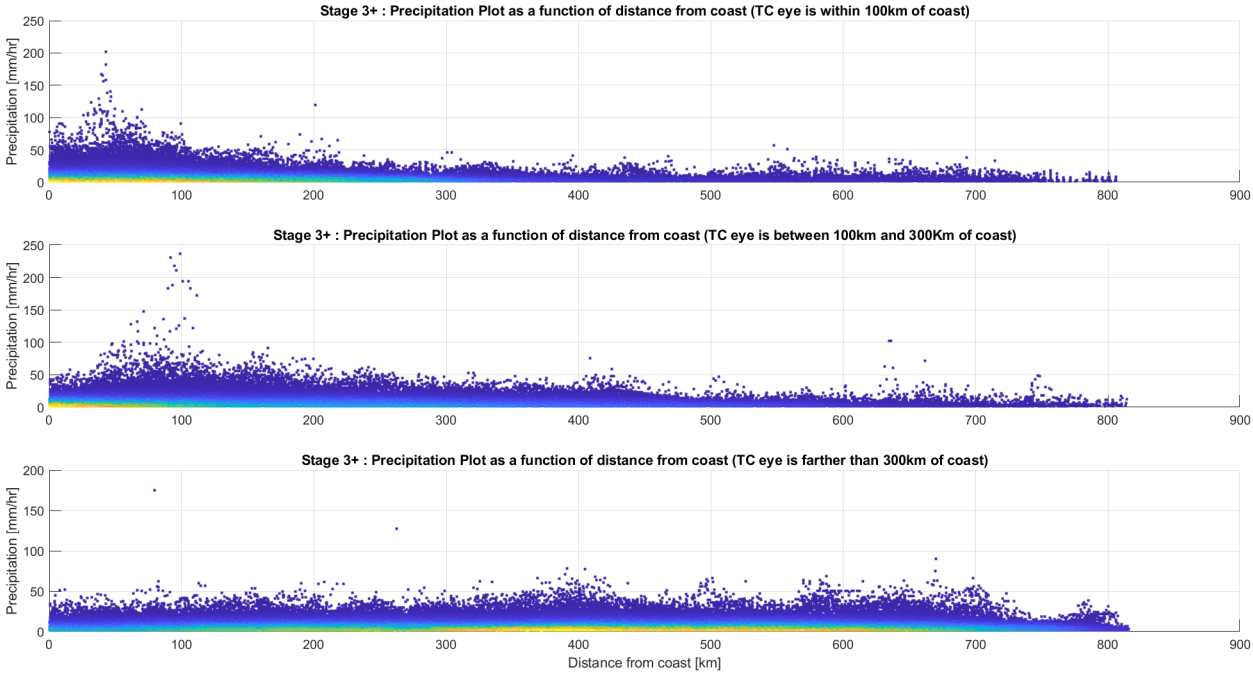


Figure E.6: Rainfall variation as a function of distance from coast for TC of type 3 based on location eye

# Bibliography


[1] LA Avila and DP Brown. “Tropical cyclone report: Tropical storm Alberto”. In: *NHC Rep. TCR-AL012006* (2006).

[2] Daan Bader. “Including stochastic rainfall distributions in a probabilistic modelling approach for compound flooding due to tropical cyclones: A case study for Houston, Texas”. In: (2019).

[3] Paul D Bates, Matthew S Horritt, and Timothy J Fewtrell. “A simple inertial formulation of the shallow water equations for efficient two-dimensional flood inundation modelling”. In: *Journal of Hydrology* 387.1-2 (2010), pp. 33–45.

[4] Hylke E Beck et al. “Daily evaluation of 26 precipitation datasets using Stage-IV gauge-radar data for the CONUS”. In: *Hydrology and Earth System Sciences* 23.1 (2019), pp. 207–224.

[5] R Berg. “National Hurricane Center Tropical Cyclone Report-Hurricane Hermine”. In: *National Hurricane Center, National Oceanic and Atmospheric Administration, National Weather Service, Miami, FL, Rep. AL092016* (2016).

[6] John T Brackins and Alfred J Kalyanapu. “Evaluation of parametric precipitation models in reproducing tropical cyclone rainfall patterns”. In: *Journal of Hydrology* 580 (2020), p. 124255.

[7] Sally Brown et al. “Land raising as a solution to sea-level rise: An analysis of coastal flooding on an artificial island in the Maldives”. In: *Journal of Flood Risk Management* 13 (2020), e12567.

[8] Chih-Pei Chang, Yi-Ting Yang, and Hung-Chi Kuo. “Large increasing trend of tropical cyclone rainfall in Taiwan and the roles of terrain”. In: *Journal of Climate* 26.12 (2013), pp. 4138–4147.

[9] Shuyi S Chen, John A Knaff, and Frank D Marks Jr. “Effects of vertical wind shear and storm motion on tropical cyclone rainfall asymmetries deduced from TRMM”. In: *Monthly Weather Review* 134.11 (2006), pp. 3190–3208.

[10] Young-Sun Choun and Min-Kyu Kim. “Logic tree approach for probabilistic typhoon wind hazard assessment”. In: *Nuclear Engineering and Technology* 51.2 (2019), pp. 607–617.

[11] Judith Claassen. “Parametric Precipitation Model for Tropical Cyclone Radial Rainfall Profiles: Reducing the biases in the Bader model for the North Atlantic”. In: (2021).

[12] Brian A Colle, James F Booth, and Edmund KM Chang. “A review of historical and future changes of extratropical cyclones and associated impacts along the US East Coast”. In: *Current Climate Change Reports* 1.3 (2015), pp. 125–143.

[13] Ruben Dahm, Ferdinand Diermanse, and Ho Long Phi. “On the flood and inundation management of Ho Chi Minh City, Vietnam”. In: *Proceeding of the International Conference on Flood Resilience: Experiences in Asia and Europe*. 2013, pp. 5–7.

[14] Deltares. “Delft-FIAT Home”. In: (2022). URL: https://publicwiki.deltares.nl/display/DFIAT/Delft-FIAT+Home.

[15] Deltares. “hydromt fiat”. In: (2021). URL: https://github.com/Deltares/hydromt_fiat.

[16] RL Elsberry, LE Carr, and MA Boothe. “Progress toward a generalized description of the environment structure contribution to tropical cyclone track types”. In: *Meteorology and Atmospheric Physics* 67.1 (1998), pp. 93–116.

[17] J Henry. “Tropical and equatorial climates”. In: *Encyclopedia of World Climatology* (2005), pp. 742–50.

[18] Greg J Holland, James I Belanger, and Angela Fritz. “A revised model for radial profiles of hurricane winds”. In: *Monthly weather review* 138.12 (2010), pp. 4393–4401.

[19] Miles Per Hour and Meters per Second. “Hurricane FAQ Hurricanes Frequently Asked Questions”. In: ().

[20] Pang-Chi Hsu, June-Yi Lee, and Kyung-Ja Ha. “Influence of boreal summer intraseasonal oscillation on rainfall extremes in southern China”. In: *International Journal of Climatology* 36.3 (2016), pp. 1403–1412.

[21] Haiyan Jiang, JB Halverson, and J Simpson. “Difference of Rainfall Distribution for Tropical Cyclones Over Land and Ocean and Rainfall Potential Derived From Satellite Observations and Its Implication on Hurricane”. In: *27th Conference on Hurricanes and Tropical Meteorology, Monterey, CA, American Meteorology Society*. 2006.

[22] William Kleiber et al. “Stochastic Tropical Cyclone Precipitation Field Generation”. In: *arXiv preprint arXiv:2011.09918* (2020).

[23] Kenneth R Knapp et al. “International best track archive for climate stewardship (IBTrACS) project, version 4”. In: *NOAA National Centers for Environmental Information* (2018).

[24] Tim Leijnse et al. “Modeling compound flooding in coastal systems using a computationally efficient reduced-physics solver: Including fluvial, pluvial, tidal, wind- and wave-driven processes”. In: *Coastal Engineering* 163 (2021), p. 103796. ISSN: 0378-3839. DOI: https://doi.org/10.1016/j.coastaleng.2020.103796. URL: https://www.sciencedirect.com/science/article/pii/S0378383920304828.

[25] Tim Willem Bart Leijnse et al. “Generating reliable estimates of tropical-cyclone-induced coastal hazards along the Bay of Bengal for current and future climates using synthetic tracks”. In: *Natural Hazards and Earth System Sciences* 22.6 (2022), pp. 1863–1891.

[26] Xiangcheng Li et al. “The modulation effect of sea surface cooling on the eyewall replacement cycle in Typhoon Trami (2018)”. In: *Monthly Weather Review* (2022).

[27] Manuel Lonfat, Frank D Marks Jr, and Shuyi S Chen. “Precipitation distribution in tropical cyclones using the Tropical Rainfall Measuring Mission (TRMM) Microwave Imager: A global perspective”. In: *Monthly Weather Review* 132.7 (2004), pp. 1645–1660.

[28] Manuel Lonfat et al. “A parametric model for predicting hurricane rainfall”. In: *Monthly Weather Review* 135.9 (2007), pp. 3086–3097.

[29] Daniel Lyons-Harrison. “Accounting for Social Vulnerability in Flood Risk Assessment in Colombo, Sri Lanka”. PhD thesis. Doctoral dissertation, Stichting Deltares, 2017.

[30] Kees Nederhoff et al. “Estimates of tropical cyclone geometry parameters based on best-track data”. In: *Natural Hazards and Earth System Sciences* 19.11 (2019), pp. 2359–2370.

[31] Kees Nederhoff et al. “Simulating synthetic tropical cyclone tracks for statistically reliable wind and pressure estimations”. In: *Natural Hazards and Earth System Sciences* 21.3 (2021), pp. 861–878.

[32] AOML NOAA. “Anatomy and Life Cycle of a Hurricane”. In: (2021). URL: https://www.aoml.noaa.gov/hrd-faq/#tc-components.

[33] NWS and NOAA. “2016 Climate Summary for Southeastern North Carolina & Northeastern South Carolina”. In: (2016). URL: https://www.weather.gov/ilm/2016ClimateSummary.

[34] NWS and NOAA. “Hurricane Florence: September 14, 2018.” In: (2018). URL: https://www.weather.gov/ilm/HurricaneFlorence.

[35] NWS and NOAA. “Tropical Cyclone Structure”. In: (2022). URL: https://www.weather.gov/jetstream/tc_structure.

[36] Brian C O’Neill et al. “The roads ahead: Narratives for shared socioeconomic pathways describing world futures in the 21st century”. In: *Global environmental change* 42 (2017), pp. 169–180.

[37] M. U. Parodi et al. “Uncertainties in coastal flood risk assessments in small island developing states”. In: *Natural Hazards and Earth System Sciences* 20.9 (2020), pp. 2397–2414. DOI: 10.5194/nhess-20-2397-2020. URL: https://nhess.copernicus.org/articles/20/2397/2020/.

[38] Matteo U Parodi et al. “Uncertainties in coastal flood risk assessments in small island developing states”. In: *Natural Hazards and Earth System Sciences* 20.9 (2020), pp. 2397–2414.

[39] RJ Pasch, Daniel P Brown, and ES Blake. “Tropical Cyclone Report, Hurricane Charley, 9-14 August 2004”. In: *Miami, Florida: National Oceanic and Atmospheric Administration, National Weather Service, National Hurricane Center, 23p* (2005).

[40] ZHANG Qinghong and GUO Chunrui. “Typhoon Winnie (1997) with a very large eye: High resolution numerical simulation”. In: *Journal of Meteorological Research* 21.1 (2007), pp. 114–120.

[41] R Rogers, F Marks, and T Marchok. *Tropical cyclone rainfall. Encyclopedia of hydrological sciences*. 2009.

[42] Christopher M Rozoff et al. “The roles of an expanding wind field and inertial stability in tropical cyclone secondary eyewall formation”. In: *Journal of the atmospheric sciences* 69.9 (2012), pp. 2621–2643.

[43] Richard W Schwerdt, Francis P Ho, and Roger R Watkins. “Meteorological criteria for standard project hurricane and probable maximum hurricane windfields, Gulf and East Coasts of the United States”. In: (1979).

[44] Gail Skofronick-Jackson et al. “The Global Precipitation Measurement (GPM) mission for science and society”. In: *Bulletin of the American Meteorological Society* 98.8 (2017), pp. 1679–1695.

[45] Roland B Stull, C Donald Ahrens, et al. *Meteorology for scientists and engineers*. Brooks/Cole, 2000.

[46] Anthony J. Gotvald Toby D. Feaster J. Curtis Weaver and Katharine Kolb. “Preliminary peak stage and streamflow data for selected U.S. Geological Survey streamgaging stations in North and South Carolina for flooding following Hurricane Florence, September 2018”. In: *USGS Publications Warehouse* (2018). ISSN: 2331-1258 (online). DOI: 10.3133/ofr20181172. URL: https://pubs.er.usgs.gov/publication/ofr20181172.

[47] Robert E Tuleya, Mark DeMaria, and Robert J Kuligowski. “Evaluation of GFDL and simple statistical model rainfall forecasts for US landfalling tropical storms”. In: *Weather and forecasting* 22.1 (2007), pp. 56–70.

[48] Thomas Wahl et al. “Increasing risk of compound flooding from storm surge and rainfall for major US cities”. In: *Nature Climate Change* 5.12 (2015), pp. 1093–1097.

[49] Dazhi Xi, Ning Lin, and James Smith. “Evaluation of a physics-based tropical cyclone rainfall model for risk assessment”. In: *Journal of Hydrometeorology* 21.9 (2020), pp. 2197–2218.

[50] Jun A Zhang and Eric W Uhlhorn. “Hurricane sea surface inflow angle and an observation-based parametric model”. In: *Monthly Weather Review* 140.11 (2012), pp. 3587–3605.

[51] Qiang Zhang, Liguang Wu, and Qiufeng Liu. “Tropical cyclone damages in China 1983–2006”. In: *Bulletin of the American Meteorological Society* 90.4 (2009), pp. 489–496.

[52] Xuebin Zhang et al. “Indices for monitoring changes in extremes based on daily temperature and precipitation data”. In: *Wiley Interdisciplinary Reviews: Climate Change* 2.6 (2011), pp. 851–870.